0008-7114

Caryologia

International Journal of Cytology, Cytosystematics and Cytogenetics

2019
Vol. 72 - n. 1

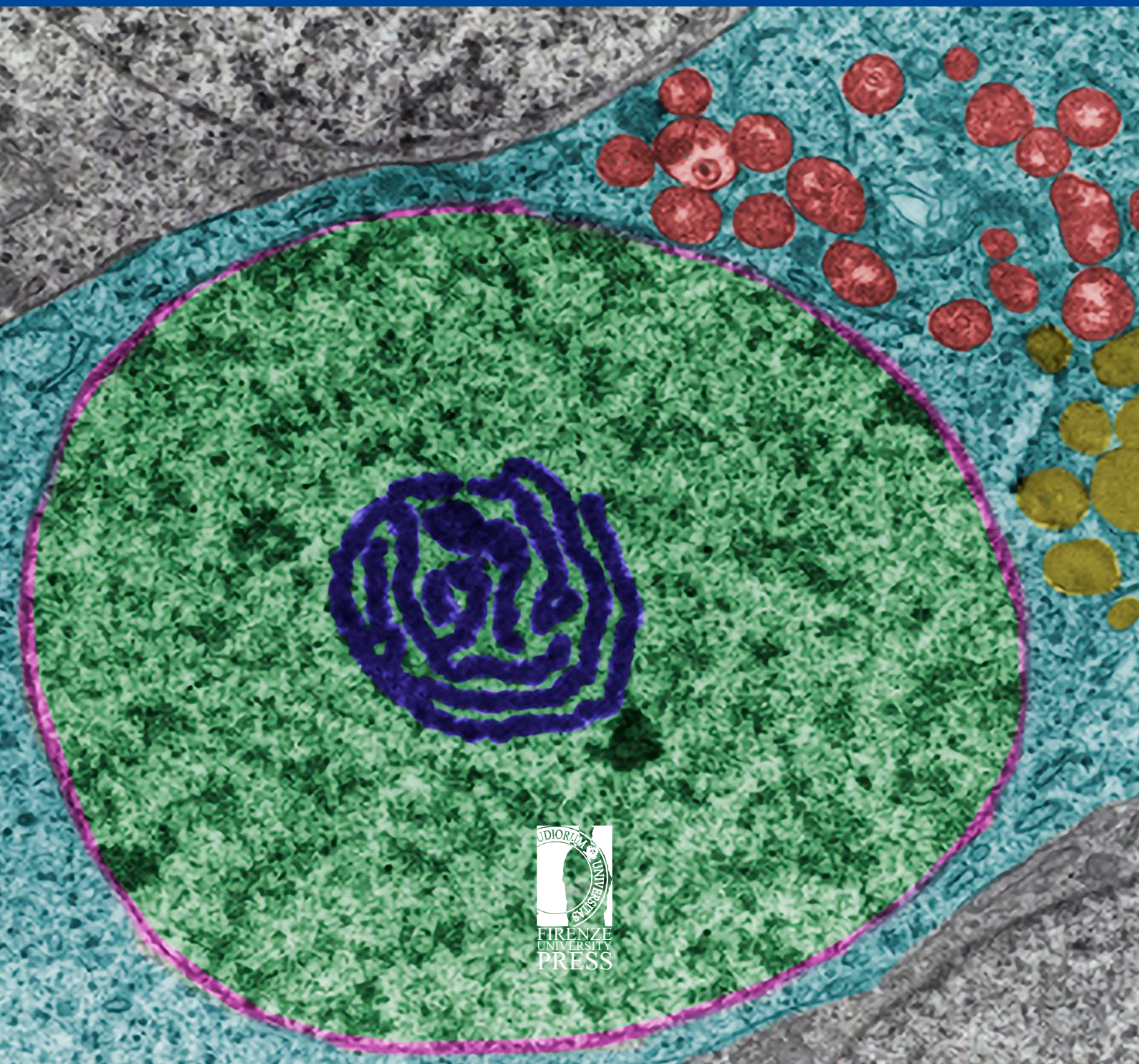

FIRENZE UNIVERSITY PRESS

Caryologia. International Journal of Cytology, Cytosystematics and Cytogenetics
Caryologia is devoted to the publication of original papers, and occasionally of reviews, about plant, animal and human karyological, cytological, cytogenetic, embryological and ultrastructural studies. Articles about the structure, the organization and the biological events relating to DNA and chromatin organization in eukaryotic cells are considered. Caryologia has a strong tradition in plant and animal cytosystematics and in cytotoxicology. Bioinformatics articles may be considered, but only if they have an emphasis on the relationship between the nucleus and cytoplasm and/or the structural organization of the eukaryotic cell.

Caryologia

International Journal of Cytology, Cytosystematics and Cytogenetics

Volume 72, Issue 1 - 2019

Firenze University Press

***Caryologia*. International Journal of Cytology, Cytosystematics and Cytogenetics**

Published by
Firenze University Press – University of Florence, Italy
Via Cittadella, 7 - 50144 Florence - Italy
http://www.fupress.com/caryologia

Caryologia
International Journal of Cytology, Cytosystematics and Cytogenetics

Firenze University Press
www.fupress.com/caryologia

OPEN ACCESS

Citation: M. Khajavi, M. Rahaie, A.Ebrahimi (2019) The effect of TiO_2 and SiO_2 nanoparticles and salinity stress on expression of genes involved in parthenolide biosynthesis in Feverfew (*Tanacetum parthenium* L.). *Caryologia* 72(1): 3-14. doi: 10.13128/cayologia-246

Received: 30th July 2018

Accepted: 24th December 2018

Published: 10th May 2019

Data Availability Statement: All relevant data are within the paper and its Supporting Information files.

Competing Interests: The Author(s) declare(s) no conflict of interest.

The effect of TiO_2 and SiO_2 nanoparticles and salinity stress on expression of genes involved in parthenolide biosynthesis in Feverfew (*Tanacetum parthenium* L.)

Mahshid Khajavi[1], Mahdi Rahaie[2,*], Asa Ebrahimi[1]

[1] *Department of Biotechnology and Plant Breeding, Faculty of Agriculture, Science and Research Branch of Islamic Azad university, Tehran, Iran*
[2] *Department of Life Science Engineering, Faculty of New Sciences and Technologies, University of Tehran, Tehran, Iran*
* Corresponding author: Tel: +98-21-86093408; Fax: +98-21-88497324; Email: mrahaie@ut.ac.ir

Abstract. Medicinal plants can produce various chemical compounds as secondary metabolites that have benefit to human. Feverfew (*Tanacetum parthenium* L.) is a medicinal plant belongs to the Asteraceae family. This plant due to have parthenolide compounds has attracted much attention for medicinal value and pharmacological activity. Due to the economic importance of the plant metabolite in cancer and migraine treatment, application of approaches for increasing the metabolite was the objective of this study. For this purpose, after cultivation in greenhouse, plants were treated with TiO_2 and SiO_2 nanoparticles and salinity stress at different times and concentrations. Real Time PCR used to evaluate the expression of *TpGAS,* COST and *TpCarS* genes which involved in secondary metabolites biosynthesis pathway (parthenolide and β-caryophyllen). It was found, SiO_2 NPs can increase the expression of *TpCarS*, COST and *TpGAS* in the concentration of 25mM with increasing time from 6 to 24h. In this concentration (25mM), TiO_2 treatment, up-regulated the *COST* and *TpGAS* in contrast, down-regulated the *TpCarS* with increasing time from 6 to 24h. Salinity treatment affected the expression of all three genes, so that with increasing time, the expression of all three genes was elevated. In conclusion, according to above and HPLC results, it was shown the nanoparticles and salinity treatments can increase parthenolide synthesis in whole plant of Feverfew and then they can be used as elicitor for more production of the metabolite.

Keywords. *Tanacetum parthenium* L., Nanoparticle, SiO_2, TiO_2, Salinity stress, Gene expression analysis.

Abbreviations: *GAS*, Germacrene A Synthase; *COST*, Costunolide Synthase; *CarS*, Cariophyllene Synthase; PTL, Parthenolide; NP, Nanoparticle.

INTRODUCTION

Medicinal plants have a specific role in treatment and prevention of many human diseases. These plants are attracting more attention for produc-

ing safer medicine because it is believed that they rarely have side effects compared to chemical drugs. Feverfew (*Tanacetum parthenium* L.) (Asteraceae), is a diploid (2n=2x=18) and perennial medicinal plant. This plant has medical applications on a wide range of disease such as migraine headaches, stomach aches, toothaches, insect bites, rheumatoid arthritis and infertility (Pareek et al. 2011). These medicinal properties are due to the existence of chemical compounds which called secondary metabolites. Terpenoids are the largest class of plant secondary metabolites (Croteau et al. 2000). Sesquiterpene lactones are the main group of terpenoids and frequently are derived from Mevalonic acid (MVA) pathway (Van Klink et al. 2003). *T. parthenium* (L.), contains many sesquiterpene lactones and parthenolide has the most concentration (comprises up to 85%) among the total sesquiterpenes (Pareek et al. 2011).

Parthenolide is used for the treatment of migraine and shows specifically anticancer and anti-inflammatory activity, as well (Tassorelli et al. 2005; Walsh et al. 2011; Mathema et al. 2012; Al-Fatlawi et al. 2015; Wang and Li, 2015). β-caryophyllene is another sesquiterpene lactone distributed in the essential oil of various plants. This compound has represented several biological activities, such as anti-inflammatory, antibiotic, antioxidant (Legault and Pichette, 2007), anticancer (Tundis et al. 2009) and antiproliferative activity (Amiel et al. 2012).

Sesquiterpenes, like parthenolide and β-caryophyllene are synthesized via farnesyl diphosphate (FPP) in Mevalonate pathway. TpGAS and COST are two genes involved in parthenolide production. At the first step, *TpGAS* converts farnesyl diphosphate to germacrene A, COST converts germacrene A acid to costunolide, and parthenolide is one of the deratives of costunolide. It has been revealed that costunolide synthase is a cytochrom P450 enzyme. *TpCars* is another sesquiterpene synthase in Feverfew which is responsible for the production of β-caryophyllene. This enzyme converts farnesyl diphosphate to β-caryophyllene directly. (Majdi et al. 2011; Liu et al. 2011; Menin et al. 2012; Basha et al. 2016).

Several factors affect the production of secondary metabolites, and elicitors are one of the most efficient ones (Zhao et al. 2005). Plants and plant cells (*in vitro* culture) show the morphological, biochemical and physiological reactions to biological, chemical or physical factors, which is considered as "elicitors." In fact, Elicitation is an induced or enhanced synthesis process of secondary metabolites by the plants and it is a way to ensure their survival, persistence, and competitiveness (Karuppusamy, 2009; Kiong et al. 2005). Elicitors are biological or nonbiological agents that cause biosynthesis and accumulation of secondary metabolites in plants through induction of defense responses (Ramirez-Estrada et al. 2016). The components of microbial cells and poly and oligosaccharides, chemicals such pesticides, heavy metals, and the signaling compounds in plant defense responses (growth factors, e.g. jasmonate) and physical factors such as hyperosmotic stress, UV, cold shock, ultrasound, and pulsed electric field can act as stimulators for hyperproduction of secondary metabolites (Zhao et al. 2010; Gueven and Knorr, 2011; Lin and Wu, 2002).

Nanoparticles (NPs) are new materials which show unique properties related to their physical size. The nanoparticles used in present work are SiO_2 and TiO_2 which are among the most used nanomaterials (Servin et al. 2012; Siddiqui and Al-Whaibi 2014). Titania (TiO_2) has a wide range of applications such as cosmetics (Anselmann, 2001), cancer treatment (Kalbacova et al. 2008), sunscreens or food (Lan et al. 2013). Silica (SiO_2) is another popular metal oxide NPs used in multiple varieties of applications such as disease labeling, drug delivery, photodynamic therapy (Ohulchanskyy et al. 2007), cancer therapy (Cheng et al. 2010; Rosenholm et al. 2010), fertilizer and pest control (Sakr, 2017; Tripathi et al. 2014; Laing et al. 2006).

The effects of TiO_2 NPs on different biological characters of the plant have been done in several studies. Among them, it could be pointed out to the effect of TiO_2 on the growth and microRNA expression profile of tobacco (Frazier et al. 2014), effects of nano-TiO_2 on seed germination (Castiglione et al. 2011), development and mitosis of root tip cells of *Vicia narbonensis* L. and *Zea mays* L. (Castiglione et al. 2011), The effect of SiO_2 and TiO_2 nanoparticles on the expression of GPPS gene (involved in thymoquinone biosynthetic pathway) in *Nigella sativa* L. (Kahila et al. 2017) and finally, Mandeh et al. (2012) which studied *in vitro* influences of TiO_2 nanoparticles on barley tissue culture and quantitative and qualitative characteristics of calli were analyzed after each subculture. In the field of agriculture, SiO_2 has an inhibition effect on the pest (HongShu et al. 2009), Carriers in drug delivery and absorption and transport of nutrients in plants (Liu et al. 2006). The role of nano-SiO_2 in the characteristics of seed germination of tomato has also investigated (Siddiqui and Al-Whaibi, 2014).

Salinity stress is a high concentration of soluble salts in soil and water. Most common soil salinity is caused by high sodium (Na+) and chloride (Cl^-) (Tavakkoli et al. 2010). Salt stress as an environmental factor is another factor that influences on gene expression (Siddiqui and Al-Whaibi 2014).

The effect of salinity on secondary metabolites in plants is various. There are different examples in this case. For example, during NaCl stress in *Swertia chirata,* significant increases ($p \leq 0.05$) was occurred in secondary metabolites at 50mM and initial increase in 100mM NaCl, which falls back to normal levels at the seventh day (Abrol et al. 2012).

In the present work, to evaluate the elicitation role of nanoparticles and abiotic stress on hyperproduction of parthenolide, it was investigated the effect of two NPs (TiO_2 and SiO_2) and salinity stress on the expression of three related genes, *TpGAS*, *COST* and *TpCarS* that are involved in the biosynthetic pathway of PTL and β-caryophyllene in Feverfew.

MATERIALS AND METHODS

Plant material and growth conditions

The seeds of Feverfew were provided by the medicinal plant institute of Shahid Beheshti University, Tehran, Iran. Germinated seeds in pots were grown under controlled circumstances with a 16:8h photoperiod light/dark, 25/18 °C for day/night and supplied with a photosynthetic photon flux density of 3000 lux (Fig. 1).

Fig. 1. The grown plants in pots in green house under controlled condition.

Nanoparticles characterization

The SiO_2 nanoparticles were purchased from TECNAN Inc. (Tecnología Navarra de Nanoproductos S.L., Spain). A size of 10–15 nm for NPs was estimated (Fig. 2). The XRD measurement clearly showed that the SiO_2 NPs were amorphous. The elemental analysis of the nano-powder by ICP-MS technique (Thermo Elemental VG PQ-ExCell) showed a purity of 99.999%.

The TiO_2 nanoparticles were provided from Degussa Inc., Germany. The analyzed data from XRD showed ~25nm diameter and specific area equal to 55 $m^2g^{-1}$for the nanoparticles (Ave. of 24.5 nm in diameter, a mixture of anatase and rutile with more proportion of anatase (89.2 %),).

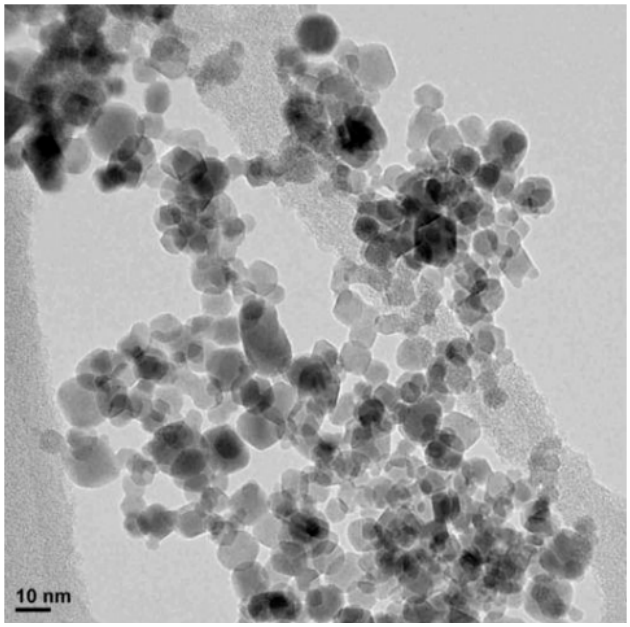

Fig. 2. The TEM micrograph of SiO_2 Nanoparticles.

Plant treatment with NPs and Salt

The SiO_2 and TiO_2 NPs, were separately prepared in two concentrations (25 and 50 mg/l) and the solution was used for watering of each pot. For each pot, 80 ml of 0.3M NaCl solution was applied for doing salinity stress treatment. All tissues were collected at the certain times (6, 24 and 48h after irrigation) for gene expression analysis and phytochemical studies and were instantly flash frozen in liquid nitrogen then stored at -80°C until RNA extraction.

HPLC analysis

The chromatography assay was performed on a 25 cm×4.6 mm with pre-column, Eurospher 100-5 C18 ana-

lytical column provided by KNAUER (Berline, Germany) reversed phase matrix (5µm) (Waters) and elution was carried out in a gradient system with acetonitrile as the organic phase (solvent A) and distilled water (solvent B) with the flow-rate of 1 mL min-1. The Peaks were monitored at 220 nm wavelength. Injection volume was 20 µL and the temperature was maintained at 25°C. All injections were repeated three times (n=3). Calibration graphs were plotted subsequently for linear regression analysis of the peak area with concentration 1, 10, 25, 50, 80, 120, 150 and 200 mg L^{-1}.

RNA extraction

Total RNA was isolated from the leaf tissue by using the Isolation total RNA Kit (Denazist Asia Inc., Mashhad, Iran), according to the manufacturer's instructions. The quantity and quality of extracted RNA were determined respectively by using a spectrophotometer instrument (NanoDrop2000c, Thermo scientific, USA) and Agarose gel electrophoresis. RNA samples were stored at −80 °C until further analysis.

Gene selection and primer designing

In the present work, *TpGAS* and Cost genes that involved in biosynthesis of PTL and *TpCarS* as mediator in biosynthesis of β-caryophyllen at Mevalonate pathway in Feverfew (Majdi et al. 2011), plus β-Actin as a house keeping gene were selected and their sequences retrieved from the gene bank, NCBI (http://www.ncbi.nih.gov). Four pairs of primers including β-Actin (-5'- AGCATGGTATTGTGAGCAACT-3', R-5'- TGGGTCATCTTCTCTCTGTTAGC-3'), *TpGAS* (F-5'-TACCAGTTTGAGCGTGAAAGA- 3', R- 5'-CAATCATGATCTTGAGCTCGT- 3'),*TpCarS* (F-5'-GAGCATGTCCACAAAGTATTTCAC-3', R-5'- GCATCGGAATATCTTTACACACAG-3') and Cost (F- 5'- GAGACACAAGAAGAAGTGAGATCAG-3', R- 5'- AAAGGTGTAGGAGCATGTAACCTC-3') were designed using primer 3 free software (http://biotools.umassmed.edu/bioapps/primer3_www.cgi).

Primers confirmation was performed by three criteria, including BLAST search in Gene Bank, single peak in qPCR and single band on gel electrophoresis.

cDNA synthesis

cDNA synthesis was performed by Revert Aid First strand cDNA synthesis Kit (Thermo Scientific, USA) with 200 U of M-MLV RT enzyme, oligo-dT and random Hexamer primers according to manufacturer's instruction.

Quantitative PCR

Quantification of *COST*, *TpGAS* and *TpCarS* genes expression levels in the samples were measured by qPCR using Hot Firepol EvaGreen qPCR master mix (solis BioDyne, Estonia). qPCR was performed according to manufacturer's instruction in Qiagen Real-time PCR System (Rotor-Gene Q, Germany) using above primers. It should be mentioned that before qPCR, the specificity of all primers and optimization of PCR reactions was done with conventional PCR. The relative expression levels were calculated according to Pfaffl method (Pfaffl 2001).

Data Statistics

Expression levels were calculated from the Ct values obtained from triplicate biological samples. Statistical significance analysis of relative gene expression level compared with the reference gene (β-*Actin*) was performed with completely randomized design (CRD). Mean values of relative expression levels were compared with LSD test (P=0.05) using SPSS ver. 21.0 software.

RESULTS

In this study, the effects of TiO2 and SiO2 nanoparticles and salinity stress on expression of *TpGAS*, and *COST* genes that are involved in the biosynthetic pathway of PTL in Feverfew (Fig. 3) were investigated. Also change of *TpCarS* gene expression which produces β-caryophyllen was analyzed. The present study focuses on elicitation effects of nanoparticles and salinity on parthenolide and β-caryophyllen productions in Feverfew.

Gene Expression Analysis

COST Gene

Two concentrations (25 and 50mM) of SiO_2 NP, in two periods of time (6 and 24h) were used. The results showed that, in both 25 and 50mM concentrations, the expression of *COST* gene was enhanced with increasing of time. While in both times, the gene expression in 25mM, was more than 50mM treatment; furthermore, the

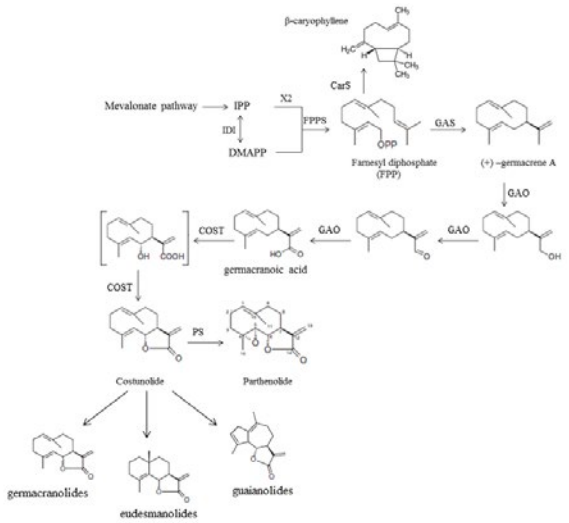

Fig. 3. The suggested biosynthetic pathway for parthenolide and β-caryophyllen synthesis in feverfew (Majdi et al., 2011). CarS: caryophyllen sybthase; GAS: germacrene A synthase; GAO: germacrene A oxidase; COST: costunolide synthase; PS: Parthenolide synthase.

expression of the gene in 25mM and after 24h was very high and more than 7-folds in comparison to 6h (Fig. 4a).

The result of TiO_2 NP was similar to SiO_2 treatment at 25mM concentration and increased the expression of COST gene. In 25mM Concentration of TiO_2 NP with increasing time from 6h to 24h, elevation of the gene expression by more than 6-fold (Fig.4b) was observed. In opposite, the gene expression in 50mM of TiO_2 NP was decreased by rising time until close to zero.

As Fig. 4 (a and b) shows, Although the ratio of expression level for SiO2 and TiO_2 nanoparticles in 6h/24h is nearly the same, but the absolute expression of the *COST* gene in TiO_2 treated samples (133.8 fold) is significantly more than SiO_2 treated plants (20.2 fold).

The effect of salinity treatment on expression of *COST* gene were also measured; after 6h and 48h at

0.3 M concentration A gradual increasing trend (2-folds) in gene expression was observed (Fig. 4c).

TpGAS Gene

TpGAS is a gene involved in the parthenolide biosynthesis pathway. The expression analysis of the gene transcript pointed that, it is affected by SiO_2 and TiO_2 NPs and salt stress treatment. The results represented that SiO_2 NPs in 25mM concentration at 24h, significantly increased the expression of GAS compared to 6h treatment (24.5 fold). In opposite, the TiO_2 NPs treatment didn't have a significant effect on the expression of

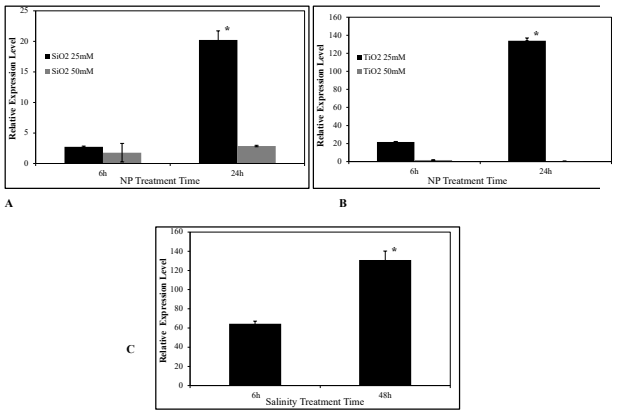

Fig. 4. The effect of elicitors on expression of *COST* gene in feverfew: A) SiO_2 NP treatment; B) TiO_2 NP treatment; C) salinity stress.

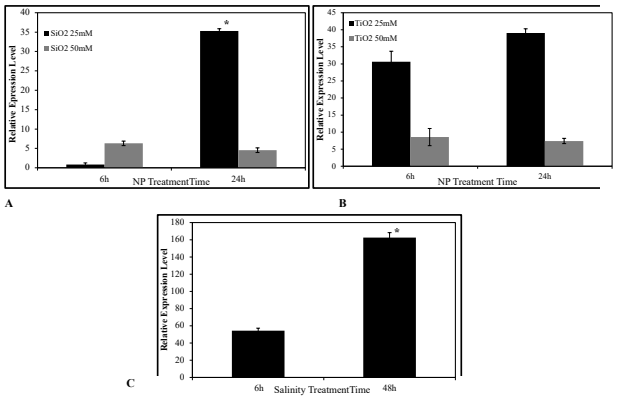

Fig. 5. The effect of elicitors on expression of *TpGAS* gene in feverfew. A: SiO_2 NP treatment; B: TiO_2 NP treatment; C: Salinity stress.

the gene in both time and concentrations (Fig. 5a and b).

The effect of salinity stress was investigated with the same concentration used above. As shown in the Fig.5c, the Expression of *TpGAS*, was statistically enhanced in 48h in comparison to 6h treatment, (~3 fold).

TpCarS Gene

TpCarS is another gene which was analyzed in our experiment. The results of expression analysis showed that the gene was affected by SiO_2 and TiO_2 NPs and salinity treatment, as well. As it can be seen in the Fig. 6a and b, an increase (1.4 fold) and decrease (6 fold) in expression of *TpCarS* in 25mM of SiO_2 and TiO_2 NPs treatment were observed respectively, from 6h to 24h. In contrast, in the 50mM concentration of NPs, no significant changes were detected during the time period.

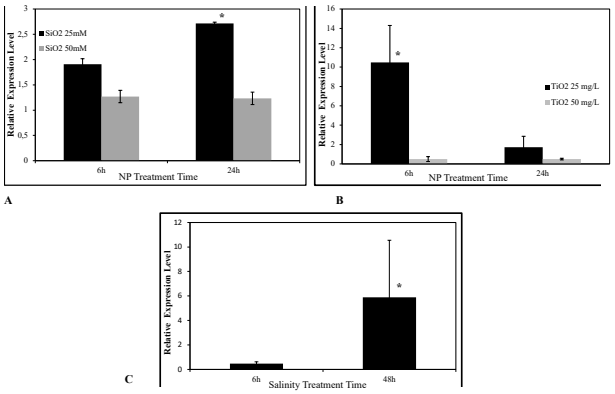

Fig. 6. The effect of elicitors on expression of *TpCarS* gene in feverfew. A: SiO_2 NP treatment; B: TiO_2 NP treatment; C: Salinity stress.

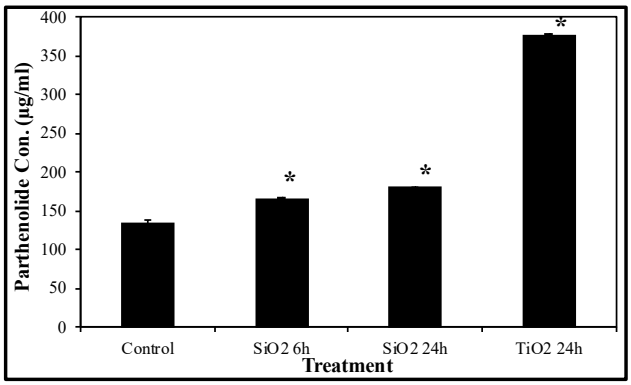

Fig. 8. Parthenolide concentration in *Tanacetum parthenium* leaves at different treatments.

The effect of salinity stress as an environmental elicitor with 300mM of NaCl in two times, including 6h and 48h was investigated. As shown in Fig. 6c, the 48h salt stress elevated the expression of *TpCarS* gene significantly (~12 fold) compared to 6h and 24h treatments.

Parthenolide concentrations in feverfew under different treatments

To assay the parthenolide concentration in different treatments, leaves tissue were analyzed by HPLC (Fig. 7). There were significant differences between parthenolide concentrations ($P< 0.05$) in different treatments (Fig. 8).

The highest and least amount of parthenolide was observed in 25mM of TiO_2 after 24h and control plants with 378.61µg/mg and 136.02µg/mg, respectively. All treatments increased the concentration of parthenolide in Feverfew leaves compared to control plants ($P<0.05$). The SiO_2 (25mM) after 6 and 24h treatments increased the leaves parthenolide content by 1.23 and 1.37 fold compared to control. The TiO_2 (25mM, 24h) raised the parthenolide amount in leaves far more than SiO_2 NPs with 2.78 fold.

DISCUSSION

Nanoparticles are a new class of men made materials which are emerging in these years. In hence, a new trend in biological sciences is toward investigation of interaction of the synthetic agents to organisms including plants. There are many reports which study the effect of them (TiO_2 and SiO_2) on plants in different kinds of morphological and molecular levels (Siddiqui and Al-Whaibi 2014; Castiglione et al. 2011; Frazier et al. 2014; Kahila et al. 2017), as well *in vivo* culture (Mandeh et al. 2012). A number of studies also prove the key role of different elicitors, including chemical compounds (Van Fürden et al. 2005; Esmaeilzadeh Bahabadi et al. 2011; Esmaeilzadeh Bahabadi et al. 2014;

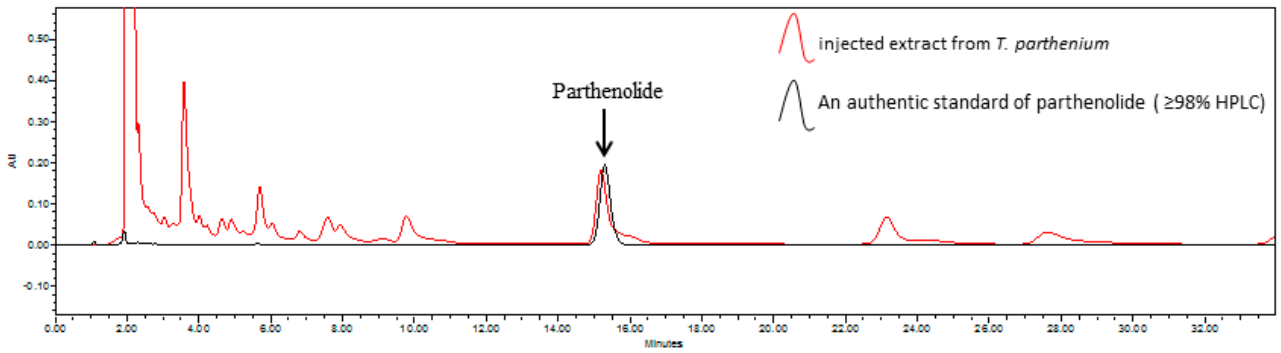

Fig. 7. The HPLC analysis of extract from *T. parthenium* and 110 ppm of standard partenolide from Sigma-Aldrich company (USA). Minutes: Run time, AU: Absobtion intensity.

Wang et al. 2007; Marsh et al. 2014), biotic (Kim et al. 2001; Jeong et al. 2005; Savitha et al. 2006; Wu et al. 2007; Kang et al. 2009; Gao et al. 2011; Swaroopa et al. 2013; Ahmed and Baig. 2014) and abiotic (Akula and Ravishankar 2011; Chan et al. 2010; Szakiel et al. 2011) on metabolite production in different plants. However, nearly most of studies have been conducted on cell or hairy root culture and investigation on *in vivo* whole plant elicitation is limit. The aim of the present work was to determine the elicitation role of nanoparticles and salt stress on metabolite hyperproduction through gene expression in whole plant.

NPs and salinity treatments affect the parthenolide biosynthesis genes

The effect of different kind of elicitors was investigated to find a clear view about the impact of elicitors on the expression of genes involved in the secondary metabolites biosynthesis pathway in *T. parthenium*. It seems that SiO_2 NPs in low concentration can have a positive effect on parthenolide production in Feverfew. In opposite to SiO_2, TiO_2 NPs treatment created a different expression pattern of the *TpGAS*, *COST* and *TpCarS* genes.

Dimkpa et al. (2012) demonstrated the beneficial effects of CuO and ZnO NPs on IAA production *in vitro* in the soil isolate *P. chlororaphis* O6. An increased IAA production with exposure to sublethal levels CuO NPs was observed in their study. They explained an ion release and nonspecific mechanism for increased level of IAA due to CuO and ZnO NPs treatment, respectively.

The salt stress up-regulated all the mentioned genes in our study. It seems, this is an evolutionary mechanism in medicinal plant to tolerance abiotic stress with producing of metabolites including PTL compound in Feverfew.

A comparison between the salts stress and the nanoparticles effect on the genes and hyperproduction of parthenolide, mentioned that, the NPs are more effective than salt stress, because they affected two key genes, including *TpGAS* and *COST* which catalyzes two steps of parthenolide biosynthesis pathway compared to salt stress which affect only on *TpCarS* gene.

The drought and salt stresses cause common reactions in plants. Cellular dehydration then osmotic stress and transfer of water from the cytoplasm to vacuoles are a result of both stresses (Akula and Ravishankar, 2011).

Salinity stress often causes both ionic and osmotic stress in plants, which increases or decreases specific secondary metabolites in plants (Mahajan and Tuteja, 2005). For example, Parida and Das (2005) found that anthocyanins are increased in response to salt stress. Oppositely, Daneshmand et al. (2010) demonstrated that salinity stress decreases the anthocyanin level in the salt-sensitive species. As the Plant polyamines are involved in plant response to salinity, changes of free and bound polyamines levels has been reported in sunflower (*Helianthus annuus* L.) roots under salinity stress (Mutlu and Bozcuk, 2007). The endogenous JA (Jasmonic acid) under salt stress in tomato cultivars has been found (Pedranzani et al. 2003). Polyphenols are another group of metabolites which their synthesis and accumulation is usually is stimulated as a reaction to biotic or abiotic stresses (Dixon and Paiva, 1995; Muthukumarasamy et al. 2000). In some of plants such red peppers (Navarro et al. 2006); a raise in polyphenol content with increasing level of salt in different tissues has also been reported (Parida and Das, 2005).

Positive correlation between TpGAS and COST expression and parthenolide concentration under NPs Treatments

A positive correlation between *TpGAS* and *COST* expression and parthenolide concentration was observed in SiO2 and TiO_2 treatments (25mM and 24h) compared to control plants, in contrast to *TpCarS* of which its expression had a negative correlation with increasing treatment time. Although few studies have revealed the genotoxic potential of TiO_2 nanoparticles in the plant systems (*A. cepa* and *N. tabacum*) with DNA damaging effect (Ghosh et al. 2010), in this work, TiO_2 nanoparticles had a positive effect on parthenolide production. *TpGAS* encodes the enzyme that highly likely catalyzes the first step in parthenolide biosynthesis, germacrene A synthase (Fig.3) (Majdi et al. 2011). Then, it seems that the Feverfew plant responds to the NPs by up-regulation of the responsive genes and then metabolite production.

TpCarS (β-Caryophyllene synthase) encodes β -Caryophyllene which is an anti-inflammatory (Martin et al. 1993; Tambe et al. 1996) and anti-carcinogenic (Kubo et al. 1996; Zheng et al. 1992) compound and a common and quite widely distributed sesquiterpene in plants (Knudsen et al. 1993; Kubo et al. 1996).

Similar to *Artemisia annua* plant (Chen et al. 2011), in *Tanacetum parthenium* (Bouwmeester et al. 2002) farnesyl diphosphate (FPP) (Fig.3) is an initial point and serves as a basic precursor to synthesize the various classes of sesquiterpenes with divergent structures and functions by different synthases such *TpCarS* through competitive pathways. Therefore, depending on their competition with the available FPP pool, the critical step catalyzed by different sesquiterpene synthases shows a metabolic regulating to direct the cellular carbon flux

towards parthenolide or other sesquiterpenes. Therefore, it seems, the nanoparticles directly and exclusively induce the genes toward more production of parthenolide compared to β-Caryophyllene.

Different studies have proved hyperproduction of secondary metabolite related to use of elicitors, including Jasmonate (Walker et al. 2002; Zhao et al. 2010; Tocci et al. 2012; Tocci et al. 2011; Gadzovska et al. 2013; Cui et al. 2014). It has been found that Jasmonic acid (JA) and its methyl esters, methyl jasmonate (MeJA), are important signaling compounds in the process of elicitation leading to the hyper production of various secondary metabolites (Walker et al. 2002). This compound plays a key role in signal transduction processes involved in defense responses in plant and has shown that is effective to induce the production of secondary metabolites in cell cultures (Walker et al. 2002; Zhao et al. 2010; Tocci et al. 2012; Tocci et al. 2011; Gadzovska et al. 2013; Cui et al. 2014).

The effect of the elicitors on flavonoid production was reported by Wang et al. (2015). They showed that the Flavonoid content is promoted by MeJA and SA induction, which were 2.1 and 1.5 times higher in comparison to control cultures, respectively.

A list of reports on different plant species have demonstrated a positive and strong correlation between terpene content and the level of the related mRNA transcripts, which proves the terpenoid biosynthesis is majorly regulated at the transcript level (Nagegowda, 2010).

CONCLUSION

The results of our work, showed a significant effect of nanoparticles in low concentration and salinity stress on the expression of two genes involved in partheonlide biosynthesis pathway, also *TpCarS* as a caryophyllen synthase in Feverfew. It seems due to the positive effect of SiO_2 NP compared to TiO_2, on the expression of all key genes for parthenolide and β-caryophyllen productions in Feverfew, these nanoparticles can be used as efficient elicitors and useful additives to soil for increasing of secondary metabolite production in the whole plant, practically. As it was mentioned above, the metabolites are used as medicinal compounds for patients with migraine disease and different type of cancers; in hence, our results can suggest a simple and cost effective technique for mass production of them. However, due to a dominant view among researchers about the destructive role of nanoparticles in the environment, it is necessary for more research for investigation about side effect of the nanoparticles on plant growth and development in future. In conclusion, in this work, it was tried to explain the role of nanoparticle by this point of view which the nanomaterial, can also be valuable for more providing of human medicinal necessities from herbs and then, it opened a new window toward nanoparticle application for medicinal plants studies. it should be mentioned that, in this project the short-term effects of elicitors on secondary metabolite production were investigated and further studies are needed to determine the long-term impact of these elicitors on plants gene expression.

ACKNOWLEDGEMENTS

We would to thank the University of Tehran for instrumental supports and all people who help us in this work.

AUTHOR CONTRIBUTION STATEMENT

MR conceived and designed research. MK conducted experiments. MR contributed new reagents or analytical tools. MR analyzed data. MK, MR and AE wrote the manuscript. All authors read and approved the manuscript.

AVAILABILITY OF DATA AND MATERIALS

The datasets during and/or analyzed during the current study available from the corresponding author on reasonable request.

REFERENCES

Abrol E, Vyas D, Koul S. 2012. Metabolic shift from secondary metabolite production to induction of anti-oxidative enzymes during NaCl stress in Swertia chirata Buch.-Ham. Acta Physiol Plant. 34(2):541-546.

Ahmed SA, Baig MM.2014. Biotic elicitor enhanced production of psoralen in suspension cultures of *Psoralea corylifolia* L. Saudi J Biol Sci. 21(5):499-504.

Akula R, Ravishankar GA.2011. Influence of abiotic stress signals on secondary metabolites in plants. Plant Signal Behav. 6(11):1720-1731.

Al-Fatlawi AA, Al-Fatlawi AA, Irshad M, Rahisuddin, Ahmad A. 2015. Effect of parthenolide on growth and apoptosis regulatory genes of human cancer cell lines. Pharm Biol. 53(1):104-109.

Amiel E, Ofir R, Dudai N, Soloway E, Rabinsky T, Rachmilevitch S. 2012. β-Caryophyllene, a compound isolated from the biblical balm of gilead (Commiphora gileadensis), is a selective apoptosis inducer for tumor cell lines. Evid Based complement alternat med. 2012: 1-8.

Anselmann R. 2001. Nanoparticles and nanolayers in commercial applications. J Nanopart Res. 3(4): 329-336.

Basha RH, Sankaranarayanan C. 2016. β-Caryophyllene, a natural sesquiterpene lactone attenuates hyperglycemia mediated oxidative and inflammatory stress in experimental diabetic rats. Chem Biol Interac. 245: 50-58.

Bouwmeester HJ, Kodde J, Verstappen FWA, Altug IG, de Kraker JW, Wallaart TE. 2002. Isolation and characterization of two germacrene A synthase cDNA clones from chicory. Plant Physiol. 129(1):134-144.

Castiglione MR, Giorgetti L, Geri C, Cremonini R. 2011. The effects of nano-TiO2 on seed germination, development and mitosis of root tip cells of *Vicia narbonensis* L. and *Zea mays* L. J. Nanopart Res. 13(6):2443-2449.

Chan LK, Koay SS, Boey PL, Bhatt A. 2010. Effects of abiotic stress on biomass and anthocyanin production in cell cultures of Melastoma malabathricum. Biol Res. 43:127-135.

Chen JL, Fang HM, Ji YP, Pu GB, Guo YW, Huang LL, Du ZG, Liu BY, Ye HC, Li GF, Wang H. 2011. Artemisinin biosynthesis enhancement in transgenic *Artemisia annua* plants by downregulation of the β-caryophyllene synthase gene. Planta medica. 77(15):1759-1765.

Cheng SH, Lee CH, Chen MC, Souris JS, Tseng FG, Yang CS, ... & Lo LW. 2010. Tri-functionalization of mesoporous silica nanoparticles for comprehensive cancer theranostics—the trio of imaging, targeting and therapy. J. Mater. Chem. 20: 6149-6157

Croteau R, Kutchan TM, Lewis NG. 2000. Natural products (secondary metabolites). Biochem Mol Biol Plants. 24: 1250-1319.

Cui XH, Murthy HN, Paek KY. 2014. Pilot-scale culture of *Hypericum Perforatum* L. adventitious roots in airlift bioreactors for the production of bioactive compounds. Appl Biochem Biotechnol. 174(2):784-792.

Daneshmand F, Arvin MJ, Kalantari KM. 2010. Physiological responses to NaCl stress in three wild species of potato in vitro. Acta Physiol Plant. 32(1):91-101.

Dimkpa CO, Zeng J, McLean JE, Britt DW, Zhan J, Anderson AJ. 2012. Production of indole-3-acetic acid via the indole-3-acetamide pathway in the plant-beneficial bacterium Pseudomonas chlororaphis O6 is inhibited by ZnO nanoparticles but enhanced by CuO nanoparticles. Appl Environ Microbiol. 78(5):1404-1410.

Dixon RA, Paiva NL. 1995. Stress-induced phenylpropanoid metabolism. The plant cell. 7(7):1085-1097.

Esmaeilzadeh Bahabadi S, Sharifi M, Murata J, Satake H. 2014. The effect of chitosan and chitin oligomers on gene expression and lignans production in *Linum album* cell cultures. J Med Plants. 1(49):46-53.

Esmaeilzadeh Bahabadi S, Sharifi M, Safaie N, Murata J, Yamagaki T, Satake H. 2011. Increased lignan biosynthesis in the suspension cultures of *Linum album* by fungal extracts. Plant Biotechnol Rep. 5(4):367-373.

Frazier TP, Burklew CE, Zhang B. 2014. Titanium dioxide nanoparticles affect the growth and microRNA expression of tobacco (*Nicotiana tabacum*). Funct Integr Genomic. 14(1):75-83.

Gadzovska S, Maury S, Delaunay A, Spasenoski M, Hagège D, Courtois D, Joseph C. 2013. The influence of salicylic acid elicitation of shoots, callus, and cell suspension cultures on production of naphtodianthrones and phenylpropanoids in *Hypericum perforatum* L. Plant Cell Tiss Organ Cult. 113(1):25-39.

Gao FK, Yong YH, Dai CC. 2011. Effects of endophytic fungal elicitor on two kinds of terpenoids production and physiological indexes in *Euphorbia pekinensis* suspension cells. J Med Plants Res. 5(18):4418-4425.

Ghosh M, Bandyopadhyay M, Mukherjee A. 2010. Genotoxicity of titanium dioxide (TiO 2) nanoparticles at two trophic levels: plant and human lymphocytes. Chemosphere. 81(10):1253-1262.

Gueven A, Knorr D. 2011. Isoflavonoid production by soy plant callus suspension culture. J Food Eng. 103(3):237-243.

HongShu X, HaiBo C, JunBo L, JingHua L, Chen G. 2009. Inhibition effect of SiO2 hydrosol against leaf mold of tomato. J Jilin Agric Uni. 31(3):252-254.

Jeong GT, Park DH, Ryu HW, Hwang B, Woo JC, Kim D, Kim SW. 2005. Production of antioxidant compounds by culture of *Panax ginseng* CA Meyer hairy roots. In: Twenty-Sixth Symposium on Biotechnology for Fuels and Chemicals pp 1147-1157. Humana Press.

Kahila MMH, Najy AM, Rahaie M, Mir-Derikvand M. 2017. Effect of Nanoparticle Treatment on Expression of a key gene involved in Thymoquinone biosynthetic pathway in *Nigella sativa* L. Nat Prod Res. 28: 1-5.

Kang SM, Min JY, Kim YD, Karigar CS, Kim SW, Goo GH, Choi MS. 2009. Effect of biotic elicitors on the

accumulation of bilobalide and ginkgolides in *Ginkgo biloba* cell cultures. J Biotechnol. 139(1):84-88.

Kalbacova M, Macak JM, Schmidt-Stein F, Mierke CT, Schmuki P. 2008. TiO2 nanotubes: photocatalyst for cancer cell killing. Phys Status Solidi R. 2(4): 194-196

Karuppusamy S. 2009. A review on trends in production of secondary metabolites from higher plants by in vitro tissue, organ and cell cultures. J Med Plants Res. 3(13):1222-1239.

Kim CY, Im HW, Kim HK, Huh H. 2001. Accumulation of 2, 5-dimethoxy-1, 4-benzoquinone in suspension cultures of *Panax ginseng* by a fungal elicitor preparation and a yeast elicitor preparation. Appl Microbiol Biotechnol. 56(1):239-242.

Kiong AL, Mahmood M, Fadzillah NM, Daud SK. 2005. Effects of precursor supplementation on the production of triterpenes by Centella asiatica callus culture. Pak J Biol Sci. 8(8):1160-1169.

Knudsen JT, Tollsten L, Bergstrom LG. 1993. Floral scents-a checklist of volatile compounds isolated by head-space techniques. Phytochemistry. 33(2):253-280.

Kubo I, Chaudhuri SK, Kubo Y, Sanchez Y, Ogura T, Saito T, Ishikawa H, Haraguchi H. 1996. Cytotoxic andantioxidative sesquiterpenoids fromHeterotheca inuloides. Planta Med. 62(5):427-430.

Laing MD, Gatarayiha MC, Adandonon A. 2006. Silicon use for pest control in agriculture: a review. Proceedings of the South African Sugar Technologists' Association. 80: 278-286.

Lan Y, Lu Y and Ren Z. 2013. Mini review on photocatalysis of titanium dioxide nanoparticles and their solar applications. Nano Energy. 2(5): 1031-1045.

Legault J, Pichette A. 2007. Potentiating effect of β-caryophyllene on anticancer activity of α-humulene, isocaryophyllene and paclitaxel. J Pharm Pharmacol. 59(12): 1643-1647.

Lin L, Wu J. 2002. Enhancement of shikonin production in single-and two-phase suspension cultures of *Lithospermum erythrorhizon* cells using low-energy ultrasound. Biotechnol Bioeng. 78(1):81-88.

Liu F, Wen LX, Li ZZ, Yu W, Sun HY, Chen JF. 2006. Porous hollow silica nanoparticles as controlled delivery system for water-soluble pesticide. Mater Res Bull. 41(12):2268-2275.

Mahajan S, Tuteja N. 2005. Cold, salinity and drought stresses: An overview. Arch Biochem Biophys. 444:139-158.

Majdi M, Liu Q, Karimzadeh G, Malboobi MA, Beekwilder J, Cankar K, de Vos R, Todorović S, Simonović A, Bouwmeester H. 2011. Biosynthesis and localization of parthenolide in glandular trichomes of feverfew (Tanacetum parthenium L. Schulz Bip.). Phytochemistry. 72(14):1739-1750.

Mandeh M, Omidi M, Rahaie M. 2012. In vitro influences of TiO2 nanoparticles on barley (Hordeum vulgare L.) tissue culture. Biol Trace Elem Res. 150(1-3):376-380.

Marsh Z, Yang T, Nopo-Olazabal L, Wu S, Ingle T, Joshee N, Medina-Bolivar F. 2014. Effect of light, methyl jasmonate and cyclodextrin on production of phenolic compounds in hairy root cultures of *Scutellaria lateriflora*. Phytochemistry. 107:50-60.

Martin S, Padilla E, Icete MA, Galvez J, Jimenez J, Zarznelo Z. 1993. Anti-inflammatory activity of the essential oil of *Bupleurum fruiticescens*. Planta Med. 59:533-536.

Mathema VB, Koh YS, Thakuri BC, Sillanpää M. 2012. Parthenolide, a sesquiterpene lactone, expresses multiple anti-cancer and anti-inflammatory activities. Inflammation. 35(2):560-565.

Menin B, Comino C, Portis E, Moglia A, Cankar K., Bouwmeester HJ, Lanteri S, Beekwilder J. 2012. Genetic mapping and characterization of the globe artichoke (+)-germacrene A synthase gene, encoding the first dedicated enzyme for biosynthesis of the bitter sesquiterpene lactone cynaropicrin. Plant Sci. 190: 1-8.

Muthukumarasamy M, Gupta SD, Panneerselvam R. 2000. Enhancement of peroxidase, polyphenol oxidase and superoxide dismutase activities by triadimefon in NaCl stressed Raphanus sativus L. Biol Plant. 43(2):317-320.

Mutlu F, Bozcuk S. 2007. Salinity-induced changes of free and bound polyamine levels in sunflower (*Helianthus annuus* L.) roots differing in salt tolerance. Pak J Bot. 39(4):1097-1102.

Nagegowda DA. 2010 Plant volatile terpenoid metabolism: biosynthetic genes, transcriptional regulation and subcellular compartmentation. FEBS let. 584(14):2965-2973.

Navarro JM, Flores P, Garrido C, Martinez V. 2006 Changes in the contents of antioxidant compounds in pepper fruits at different ripening stages, as affected by salinity. Food Chem. 96(1):66-73.

Ohulchanskyy TY, Roy I, Goswami LN, Chen Y, Bergey EJ, Pandey RK., Oseroff AR, Prasad PN. 2007. Organically modified silica nanoparticles with covalently incorporated photosensitizer for photodynamic therapy of cancer. Nano lett. 7(9): 2835-2842.

Pareek A, Suthar M, Rathore GS, Bansal V. 2011. Feverfew (*Tanacetum parthenium* L.): A systematic review. Pharmacogn Rev. 5(9):103-110.

Parida AK, Das AB. 2005. Salt tolerance and salinity effects on plants: a review. Ecotoxicol Environ Saf. 60(3):324-349.

Pedranzani H, Racagni G, Alemano S, Miersch O, Ramírez I, Peña-Cortés H, Taleisnik E, Machado-Domenech E, Abdala G. 2003. Salt tolerant tomato plants show increased levels of jasmonic acid. Plant Growth Regul. 41(2):149-58.

Pfaffl, MW. 2001. A new mathematical model for relative quantification in real-time RT–PCR. Nucleic acids res. 29(9): 45-45.

Ramirez-Estrada K, Vidal-Limon H, Hidalgo D, Moyano E, Golenioswki M, Cusidó RM, Palazon J. 2016. Elicitation, an effective strategy for the biotechnological production of bioactive high-added value compounds in plant cell factories. Molecules. 21(2):182.

Rosenholm JM, Sahlgren C, Linden M. 2010. Towards multifunctional, targeted drug delivery systems using mesoporous silica nanoparticles – opportunities & challenges'. Nanoscale. 2: 1870-1883

Sakr N, 2017. The role of silicon (Si) in increasing plant resistance against insect pests review article. Acta Phytopathol Entomol Hung. 52(2): 185-204.

Savitha BC, Thimmaraju R, Bhagyalakshmi N, Ravishankar GA. 2006. Different biotic and abiotic elicitors influence betalain production in hairy root cultures of Beta vulgaris in shake-flask and bioreactor. Process Biochem. 41(1):50-60.

Servin AD, Castillo-Michel H, Hernandez-Viezcas JA, Diaz BC, Peralta-Videa JR, Gardea-Torresdey JL. 2012. Synchrotron micro-XRF and micro-XANES confirmation of the uptake and translocation of TiO2 nanoparticles in cucumber (*Cucumis sativus*) plants. Environ Sci Technol. 46(14):7637-7643.

Siddiqui MH, Al-Whaibi MH. 2014. Role of nano-SiO2 in germination of tomato (*Lycopersicum esculentum* seeds Mill.). Saudi J Biol Sci. 21(1):13-17.

Swaroopa G, Anuradha M, Pullaiah T. 2013. Elicitation of forskolin in suspension cultures of Coleus forskohlii (willd.) Briq. using elicitors of fungal origin. Curr Trends Biotechnol Pharm. 7(3):755-762.

Szakiel A, Paczkowski C, Henry M. 2011. Influence of environmental abiotic factors on the content of saponins in plants. Phytochem Rev. 10(4): 471-91.

Tambe Y, Tsujiuchi H, Honda G, Ikeshiro Y, Tanaka S. 1996. Gastric cytoprotection of the non-steroidal anti-inflammatory sesquiterpene, b-caryophyllene. Planta Med. (62):469-470.

Tassorelli C, Greco R, Morazzoni P, Riva A, Sandrini G, Nappi G. 2005. Parthenolide is the component of *tanacetum parthenium* that inhibits nitroglycerin-induced Fos activation: studies in an animal model of migraine. Cephalalgia. 25(8):612-621.

Tavakkoli E, Rengasamy P, McDonald GK. 2010. High concentrations of Na+ and Cl–ions in soil solution have simultaneous detrimental effects on growth of faba bean under salinity stress. J Experimental botany. 61(15): 4449-4459.

Tocci N, D'Auria FD, Simonetti G, Panella S, Palamara AT, Pasqua G. 2012. A three-step culture system to increase the xanthone production and antifungal activity of Hypericum perforatum subsp. angustifolium in vitro roots. Plant Physiol Biochem. 57:54-58.

Tocci N, Simonetti G, D'Auria FD, Panella S, Palamara AT, Valletta A, Pasqua G. 2011. Root cultures of Hypericum perforatum subsp. angustifolium elicited with chitosan and production of xanthone-rich extracts with antifungal activity. Appl Microbiol Biotechnol. 91(4):977-987.

Tripathi DK, Singh VP, Gangwar S, Prasad SM, Maurya JN, Chauhan DK. 2014. Role of silicon in enrichment of plant nutrients and protection from biotic and abiotic stresses, in: In Improvement of crops in the era of climatic changes. New York, pp. 39-56.

Tundis R, Loizzo MR, Bonesi M, Menichini F, Dodaro D, Passalacqua NG, Statti G, Menichini F. 2009. In vitro cytotoxic effects of Senecio stabianus Lacaita (Asteraceae) on human cancer cell lines. Nat Prod Res. 23(18): 1707-1718.

Van Fürden B, Humburg A, Fuss E. 2005. Influence of methyl jasmonate on podophyllotoxin and 6-methoxypodophyllotoxin accumulation in *Linum album* cell suspension cultures. Plant Cell Rep. 24(5):312-317.

Van Klink J, Becker H, Andersson S, Boland W. 2003. Biosynthesis of anthecotuloide, an irregular sesquiterpene lactone from Anthemis cotula L.(Asteraceae) via a non-farnesyl diphosphate route. Org Biomol Chem. 1(9): 1503-1508.

Walker TS, Bais HP, Vivanco JM. 2002. Jasmonic acid-induced hypericin production in cell suspension cultures of *Hypericum perforatum* L. (St. John's wort). Phytochemistry. 60(3):289-293.

Walsh EL, Ashe S, Walsh JJ. 2011. Nature's Migraine Treatment: Isolation and Structure Elucidation of Parthenolide from *Tanacetum parthenium*. J Chem Educ. 89(1):134-137.

Walsh EL, Ashe S, Walsh JJ. 2011. Nature's Migraine Treatment: Isolation and Structure Elucidation of Parthenolide from *Tanacetum parthenium*. J Chem Educ. 89: 134-137.

Wang J, Qian J, Yao L, Lu Y. 2015. Enhanced production of flavonoids by methyl jasmonate elicitation in cell

suspension culture of *Hypericum perforatum*. Bioresour Bioprocess. 18;2(1):5.

Wang M, Li Q. 2015. Parthenolide could become a promising and stable drug with anti-inflammatory effects. Nat Prod Res. 29(12):1092-1101.

Wang YD, Wu JC, Yuan YJ. 2007. Salicylic acid-induced taxol production and isopentenyl pyrophosphate biosynthesis in suspension cultures of *Taxus chinensis* var. mairei. Cell Biol In. 31(10):1179-1183.

Wu JY, Ng J, Shi M, Wu SJ. 2007. Enhanced secondary metabolite (tanshinone) production of *Salvia miltiorrhiza* hairy roots in a novel root–bacteria coculture process. Appl Microbiol Biotechnol. 77(3):543-550.

Zhao J, Davis LC, Verpoorte R. 2005. Elicitor signal transduction leading to production of plant secondary metabolites. Biotechnol Adv. 23(4):283-333.

Zhao JL, Zhou LG, Wu JY. 2010. Effects of biotic and abiotic elicitors on cell growth and tanshinone accumulation in Salvia miltiorrhiza cell cultures. Appl Microbiol Biotechnol. 87(1):137-144.

Zheng GQ, Kenney PM, Lam LK. 1992. Sesquiterpenes from clove (*Eugenia caryophyllata*) as potential anticarcinogenic agents. J Nat Prod. 55(7):999-1003.

Caryologia
International Journal of Cytology, Cytosystematics and Cytogenetics

Firenze University Press
www.fupress.com/caryologia

OPEN ACCESS

Citation: Ramanpreet, R. Chand Gupta (2019) Meiotic studies in genus *Withania* Pauquy, from Indian Thar Desert. *Caryologia* 72(1): 15-21. doi: 10.13128/cayologia-247

Received: 19th July 2018

Accepted: 20th December 2018

Published: 10th May 2019

Data Availability Statement: All relevant data are within the paper and its Supporting Information files.

Competing Interests: The Author(s) declare(s) no conflict of interest.

Meiotic studies in genus *Withania* Pauquy, from Indian Thar Desert

Ramanpreet*, Raghbir Chand Gupta

Department of Botany Punjabi University, Patiala, 147002, Punjab, India
* Corresponding author: ramanbrar247@gmail.com

Abstract. Detailed male meiosis has been made in two species of genus *Withania* collected from desert regions of Rajasthan, India. The study revealed 2*n*=48 for both the species. The meiotic analysis of *W. somnifera* is reported to be normal whereas, *W. coagulans* showed abnormal meiosis with the presence of abnormalities like spindle irregularities, chromatin transfer, laggards and irregular microsporogensis with the presence of monads, dyads, triads, polyads and tetrads with micronuclei which further lowered the pollen fertility and giving rise to varying size pollen grains. Both the species are widely used for various medicinal purposes by local/tribal people of the state.

Keywords. *Withania*, Medicinal plant, Abnormal meiotic behavior, Indian Thar desert.

INTRODUCTION

The genus *Withania* belongs to the family Solanaceae. The family comprises of 100 genera and about 2500 species (Hunziker 2001, Olmstead *et al.* 2008). The genus is distributed throughout the tropical and sub-tropical regions of the world with 26 species (Ahmad 2014). *W. somnifera* is well distributed in India with and is growing well in dry parts of tropical and subtropical regions extending to the elevation of 1500 m. But *W. coagulans* is rare and endangered plant species found only in few localities in Rajasthan. Both the species are well distributed in East of Mediterranean regions extending to South Asia.

Regarding the medicinal properties of the species, a composite Ayurvedic medicine "Liv 52" commonly used as intestinal infections is a hepatoprotective herbal preparation and contains extracts from *W. coagulans* and *W. somnifera* (Mishra *et al.* 2013). *W. coagulans* is commonly known as "Indian cheese maker" since fruits and leaves of the plants are used as coagulant, as it contain an enzyme called Withanin, having milk coagulating activity (Naz *et. al.* 2010). In some parts of India and Pakistan, both the species are used as blood purifier, for cleaning teeth and plant smoke is inhaled for relief in toothache (Dymock *et al.* 1972, Krishnamurthi 1969). The plant possesses

antitumor, antimicrobial and anti-inflammatory properties. Since the plant is toxic in nature so it should be used with caution (Purohit and Yyas 2004). Flowers of its species are used to treat nervous exhaustion, insomnia and impotence. The meiotic course of the species reveals the presence of 2*n*=48 from West Pakistan (Baquar 1967) as well as outside India.

W. somnifera commonly known as "Ashwangandha" or "Indian ginseng" is extensively studied from India by Bir *et al.* (1978) Bir and Sidhu (1979 and 1980) from Punjab plains, Koul *et al.* (1976) from Jammu and Kashmir, Madhavadian (1968) from Tamil Nadu, Bhaduri (1933), Datta *et al.* (2005), Iqbal and Datta (2007) from West Bengal. It is also extensively worked out from Pakistan by Baquar (1967) and Khatton and Ali (1982) and from Saudi Arabia by Al-Turki *et al.* (2000). Earlier meiotic studies reveals the presence of intraspecific diploid cytotype (2*n*=24), tetraploid cytotype (2*n*=48) and hexaploid cytotypes (2*n*=72). The karyotype analysis of the species shows seven groups of the chromosomes with occurrence of metacentric and sub-metacentric types (Samaddar *et al.* 2012). The species also shows polysomatomy (2*n*=12, 18, 24, 36, 48, 72) with predominance of 2*n*=48.Whereas cytologically, *W. coagulans* is not as much explored. There is no cytological report of it from the studied area. Present research work is undertaken by keeping in view the existence of cytological diversity.

MATERIALS AND METHODS

Floral buds were fixed in freshly prepared Carnoy's fixative (6 parts of absolute alcohol: 3 parts of chloroform: 1 part of glacial acetic acid) for 24-48 hours. Afterwards, these were transferred to 70% ethyl alcohol and stored in refrigerator at 4˚C until use. For chromosomal preparations, anthers were crushed and tapped to prepare a smear of pollen mother cells (PMCs) in 1% acetocarmine (Belling 1921). A number of PMCs were observed and chromosome counts were confirmed. In case of species with meiotic abnormalities, large numbers of PMCs are observed to confirm frequency of various abnormalities. Pollen fertility was observed by mounting the pollen grains in 50% glycerol-aceto carmine (1:1) solution (Marks 1954). Pollen grains with stained nuclei were taken as fertile and viable, whereas, unstained pollen grains marked as sterile ones. Pollen grain size was measured using an occulometer. The photomicrographs of the PMCs and pollen grains were taken from the temporary slides by using, Nikon 80i digital imaging system.

The species are collected from different localities of district Churu and Jodhpur. *W. somnifera* is more frequent in its appearance as compared to *W. coagulans*, which is a rare medicinal plant and is collected only from single locality of the studied area. The plant specimens were identified with the help of various floras such as Flora of North East Rajasthan (Sharma and Tiagi 1979), Flora of the Indian Desert (Bhandari 1978), Flora of Rajasthan (Shetty and Singh 1993) and by comparing the plant specimens with the samples lying in of Herbaria of Department of Botany, Punjabi University, Patiala (PUP) and Botanical Survey of India, Jodhpur (BSI). The identified voucher specimens of plants have been deposited in the Herbarium, Department of Botany, Punjabi University Patiala (PUN), India.

RESULTS

Detailed cytological investigation is carried out in two species of genus *Withania* i.e., *W. somnifera* and *W. coagulans*. Meiotic studies of *W. somnifera* reveals the presence of 24 bivalents at metaphase-I (Fig. 1). PMCs also show the presence of equal segregation of 24:24 chromosomes at anaphase-I (Fig. 2). The meiotic course is normal with high pollen fertility (97.66%). The meiosis of *W. coagulans* depicts the presence 24 bivalents at metaphase-I (Fig. 3). These chromosomes are unable to segregate on the spindle and are scattered all over the cytoplasm (Fig. 4). A very few the cells also shows equal segregation of 24:24 chromosomes at anaphase-I (Fig. 5). The meiotic course reveals spindle irregularities in the PMCs as the chromosomes are unable to move towards the poles (Figs. 6, 7) and several chromosomes remain in the cytoplasm to the form of laggards (Fig. 8) at anaphase-I. The spindle abnormalities (Figs. 9, 10) and laggard formation is also observed at anaphase-II stages of meiosis (Fig. 10). Further the formation of bridges (Fig. 11) is also observed at telophase-II. All these abnormalities lead to the formation of multipolarity (Fig. 12) as chromosomes are not able to move towards their respective poles and remain in the cytoplasm. Microsporogenesis is highly abnormal with the presence of monad (Fig. 13), dyad (Fig. 14) and triad (Fig. 15). Chromatin transfer within tetrads (Fig. 16), polyad (Fig. 17) and polyads with micronuclei (Fig. 18) is also observed. Pollen grains with unequal size (Fig. 19) and fertile and sterile pollen are also observed (Fig. 20) which leads to low pollen fertility. The majority of the PMCs depicted abnormal spindle formation which resulted in irregular arrangement of bivalents at the spindle plate during metaphase-I and segregation of chromosomes during anaphase-I/teolophase-I and anaphase-II/telophase-II. Chromosomes also lack the ability of congregation at a single pole and

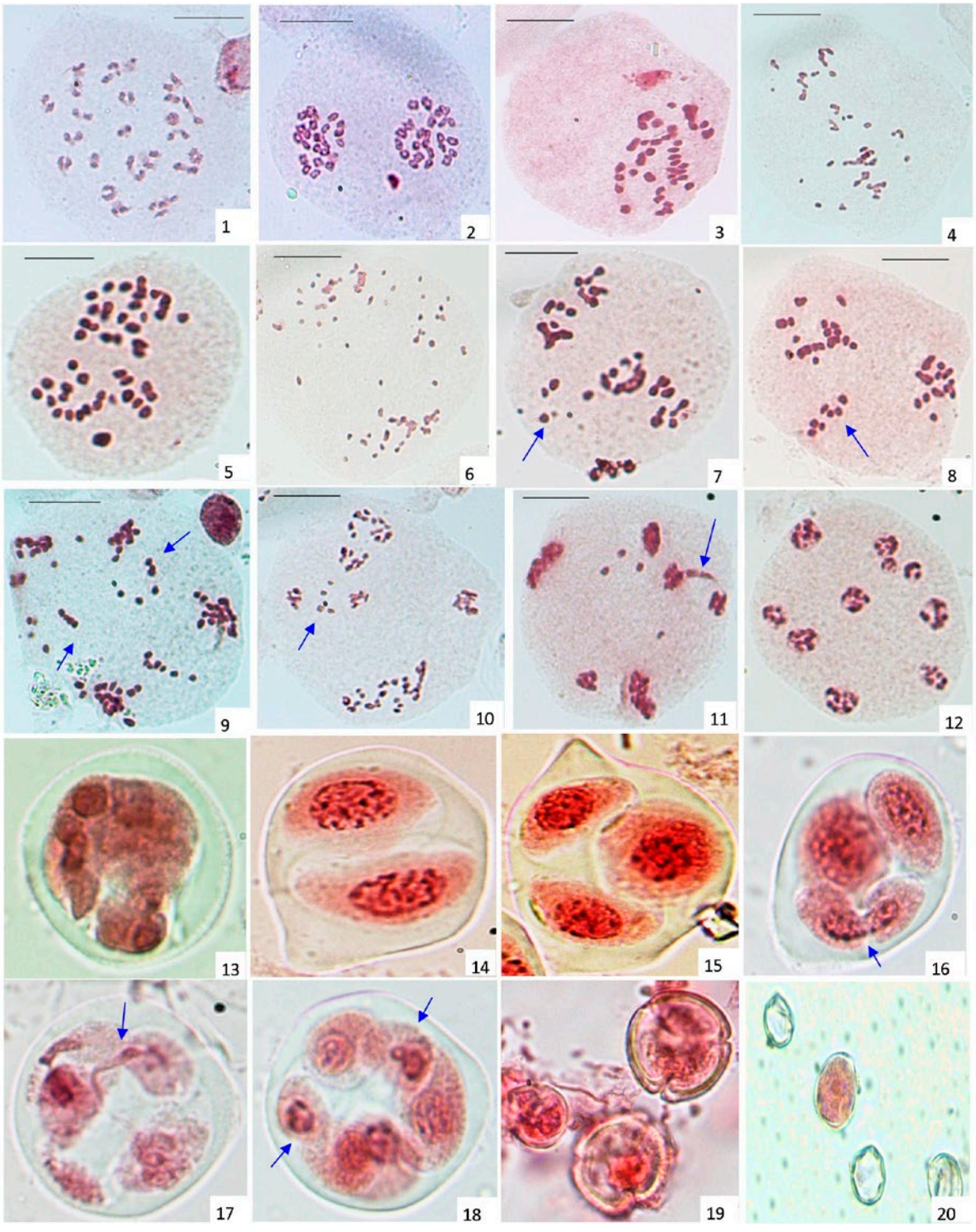

Figs. 1-20. *Withania somnifera* 1) PMC at metaphase-I showing 24 bivalents; 2) PMC at anaphase-I showing 24:24 chromosomes; *W. coagulans* 3-4) PMC at metaphase-I showing 24 bivalents; 5) PMC at anaphase-I showing 24:24 chromosomes; 6-7) PMC showing spindle irregularities with scattered chromosomes (scattered chromosomes arrowed); 8) PMC at anaphase-I showing laggards (laggards arrowed); 9, 10) PMCs at anaphase-II showing spindle irregularities in form of laggards (laggards arrowed); 11) PMC at telophase-II showing laggards and bridges (bridge arrowed); 12) PMC showing multipolarity; 13) Monad; 14) Dyad; 15) Triad; 16) Chromatin transfer within tetrad (chromatin transfer arrowed); 17) Chromatin transfer within polyad (chromatin transfer arrowed); 18) Polyad with micronuclei (micronuclei arrowed); 19) Unequal sized pollen grains; 20) Sterile and fertile pollen grains. Scale bar=10µm.

Map A) Map showing the geographical location of Rajasthan in India, B) Map depicting various localities in Rajasthan, C) Map depicting the boundary of Thar Desert and the amount of rainfall received by the State.

remained scattered in the cytoplasm or in small groups. Chromosomes in these PMCs failed to reach their respective poles and constitute micronuclei during late telophase stages and sporad formation. Irregular spindles in these plants are also depicted in the meiocytes, which showed multipolar presence of chromosomes.

DISCUSSION AND CONCLUSIONS

Meiosis is most sensitive stage in the life cycle for all sexual species and has direct relevance to natural selection; it leads to the formation of gametes, contributes to genome stability and generates genetic diversity. The process of meiosis depends upon interrelated events of homologous chromosome recognition, intimate association, synapsis and recombination (Hamant *et al.* 2006, de Muyt *et al.* 2009). In plants, it is affected by various genetic and environmental factors (Ahmad *et al.* 1984, Viccini and Carvalho, 2002, Sun *et al.* 2004, Bajpai and Singh 2006, Rezaei *et al.* 2010). There are various meiotic abnormalities which hinder the path of normal meiosis and are the cause of changes in the morphology and genetic constitutions of the plant. The evolution of vascular plants is dependent upon the variation in chromosome numbers which may be caused due to genomic mutations especially polyploidy (auto or allopolyploidy) (Soltis *et al.* 2009, Bedini *et al.* 2012). There are number of research papers on the phenomena of polyploidy, emphasizing its origin, impact and role in speciation (Stebbins 1985, Ramsey and Schemske 1998, Otto and Whitton 2000, Cifuentes *et al.* 2010, Jiao *et al.* 2011). The autotetraploids are generally characterized by the presence of quadrivalents due to homology of 4 sets of chromosomes, whereas, in allopolyploids there is normal pairing because of existence of two separate sets of chromosomes. On the other hand in segmental allotetraploids due to the partial homology of two genomes there is low frequency of quadrivalent formation. In the present study *W. somnifera* shows normal bivalent formation in all the PMCs, without any quadrivalent formation which indicates its allotetraploid behavior. However, the absence of quadrivalents does not confirm that it is an allotetraploid because there are many artificially produced autotetraploids where there is only bivalent formation because the formation of quadrivalents depends upon many other factors such as localization of chiasmata, small size of chromosomes, and presence of some suppressor genes etc., which does not allow the pairing between the homeologous chromosomes (Morrison and Rajhathy 1960, Gottschlk 1978). On the other hand in *W. coagulans* the meiosis is highly abnor-

mal with the presence of spindle abnormalities which indicates the absence of multivalents and also indicates that it might be hybrid or more probably due the presence of specific genes which interfere in the pairing and functioning of spindle (Baum *et al.*1992, Risso-Pascotto *et al.* 2003; Kumar and Singhal 2008; Singhal and Kaur 2009). The basic function of the spindle is to attach at kinetochore and separate the chromosome or chromatids at anaphases (Wadsworth *et al*. 2011), these attach to the centromeres (Qu and Vorsa 1999) and rearrange the chromosomes on the equatorial plate and bring them together at metaphase-I (Qu and Vorsa 1999). But, if due to some factors (genetic or enviornmental) the spindle activity fails then chromosomes are unable to line up in the equator and then separate at Anaphases of the meiosis, which leads to abnormal meiotic course. Earlier, a number of plants have been reported with abnormalities like irregular spindle activity, cytomixis and chromatin stickiness leading to abnormal microsporogenesis (Baum *et al*. 1992, Caetano-Pereira and Pagliarinini 2001, Kumar and Singhal 2008, Rai and Kumar 2010, Singhal and Kaur 2009). Spindle irregularities are generally divided into 4 categories-multipolar, monopolar, radial and apolar. Multipolar spindles are those in which 3 or more poles are formed, in monopolar only one spindle formation takes place, in radial spindles ends are located at the periphery and near the equator (Shamina *et al.* 2000a) and apolar spindles have randomly oriented set of fibers (Shamina *et al.* 2000b, Seriukova *et al*. 2003).

Abnormalities like cytomixis, chromosome stickiness, unoriented bivalents, laggards, bridges which ultimately lead to abnormal microsporogenisis with the production of dyads, triads, polyads, tetrads with micronuclei, and sterile and fertile pollen grains.

ACKNOWLEDGMENTS

This study was funded by Department of Biotechnology (DBT), New Delhi, DBT-IPLS Project with reference number BT/PR 4548/NF/22/146/2012. The authors are also thankful to Head, Department of Botany, Punjabi University, Patiala, for all the necessary laboratory facilities.

REFERENCES

Ahmad, Q. N., Britten, E. J. and Byth, D. E. 1984. Effect of interacting genetic factors and temperature on meiosis and fertility in soybean×*Glycine soja* hybrids. Can. J. Genet. Cytol. **26**: 50-56.

Al-Turki, T. A., Filfilan, S. A. and Mehmood, S. F. 2000. A cytological study of flowering plants from Saudi Arabia. Willdenowia **30**: 339-358.

Anesini, C. and Perez, C. 1993. Screening of plants used in Argentine folk medicine for antimicrobial activity. J. Ethnopharmacol. **39**: 119-128.

Bajpai, A. and Singh, A. K. 2006. Meiotic behavior of *Carica papaya* L. spontaneous chromosome instability and elimination in important cvs in North Indian conditions. Cytologia **71**: 131-136.

Baquar, S. R. 1967. Cytomorphological studies in the family Solanaceae from West Pakistan. Genetica **38**: 388-397.

Baum, M. E., Lagudah, E. S. and Appels, R. 1992. Wide crosses in cereals. Annu. Rev. Plant Physiol. Plant Mol. Biol. **43**:117-143.

Bedini, G., Garbari, F. and Peruzzi, L. 2012. Does chromosome number count? Mapping karyological knowledge on Italian flora in a phylogenetic framework. J. Syst. Evol. **298**: 739–750.

Belling, J. 1921. On counting chromosomes in pollen mother cells. American Naturalist. **55**: 573-574.

Bhaduri, P. N. 1933. Chromosome numbers of some Solanaceous plants of Bengal. J. Ind. Bot. Sci. **12**: 56-64.

Bhandari, M. M. 1978. *Flora of Indian desert*. Pp. **471**. Scientific Publishers. Jodhpur.

Bir, S. S. and Sidhu, M. 1979. Cytological observations in weed flora of orchards of Patiala district, Punjab. Recent Res. Plant Sci. **7**: 261-271.

Bir, S. S. and Sidhu, M. 1980. Cyto-palynological studies on weed flora of cultivable lands of Patiala district (Punjab). J. Palynol. **16**: 85-105.

Bir, S. S., Kumari, S., Shoree, S. P. and Saggoo, M. I. S. 1978. Cytological studies in certain Bicarpellatae from North and Central India. J. Cytol. Genet. **13**: 99-106.

Caetano-Pereira, C. M. and Pagliarini, M. S. 2001. A new meiotic abnormality in *Zea mays* multiple spindles associated with abnormal cytokinesis in both divisions. Genome **44**: 865-871.

Cifuentes, M., Grandont, L., Moore, G., Chèvre, A. M. and Jenczewski, E. 2010. Genetic regulation of meiosis in polyploidy species: new insights into an old question. New Phytol. **186**: 29-36.

Datta, A. K., Mukherjee, M. and Iqbal, M. 2005. Persistent cytomixis in *Ocimum basilicum* L. (Lamiaceae) and *Withania somnifera* (L.) Dun. (Solanaceae). Cytologia **70**: 309-313.

de Muyt, A. D., Mercier, R., Mezard, C. and Grelon, M. 2009. Meiotic recombination and crossovers in plants. Genome dynamics **5**: 14-25.

Dymock, W., Waden, C. J. H. and Hopper, D. 1972. Pharmacographia Indica: Institute of health and TB Research, Karachi, pp. 306.

Golubovskaya, I. N. and Distanova, E. E. 1986. Mapping mei gene ms43 by B-A translocation stocks. Genetica **22**: 1173-1180.

Gottschalk, W. 1978. Open problems in polyploidy research. Nucleus 21: 99-112.

Hamant, O., Ma, H. and Cande, W. Z. 2006. Genetics of meiotic prophase I in plants. Anu. Rev. Plant Biol. **57**: 267-302.

Hunziker, A. T. 2001. Genera Solanacearum: the genera of the Solanaceae illustrated, arranged according to a new system; Gantner Verlag: Ruggell, Liechtenstein.

Iqbal, M. and Datta, A. K. 2007. Cytogenetic studies in *Withania somnifera* (L.) Dun. (Solanaceae). Cytologia **72**: 43-47.

Jiao, Y., Wickett, N. J., Ayyampalayam, S., Chanderbali, A. S., Lena. L., Ralph, P. E., Tomsho, L. P., Hu, Y., Liang, H., Soltis, P. S., Soltis, D. E., Clifton, S. W., Schlarbaum, S. E., Schuster, S. C., Ma, H., Leebens-Mack, J. and de Pamphilis, C. W. 2011. Ancestral polyploidy in seed plants and angiosperms. Nature **473**: 97-102.

Khatoon, S. and Ali, S. I. 1982. Chromosome numbers of some plants of Pakistan. Pak. J. Bot. **14**: 117-129.

Koul, A. K., Wakhlu, A. K. and Karihaloo, J. L. 1976. Chromosome numbers of some flowering plants of Jammu (Western Himalayas) II. Chr. Inform. Ser. **20**: 32-33.

Krishnamurthi, A. 1969. The Wealth of India, Vol VIII, Publication Information Directorate, SIR, New Delhi. pp. 582.

Kumar, P. and Singhal, V. K. 2008. Cytology of *Caltha palustris* L. (Ranunculaceae) from cold regions of Western Himalayas. Cytologia **73**:137-143.

Madhavadian, P. 1968. Chromosome numbers in South Indian Solanaceae. Caryologia **21**: 343-347.

Marks, G. E. 1954. An acetocarmine glycerol jelly for use in pollen fertility counts. Stain Tech. **29**: 277.

Masterson, J. 1994. Stomatal size in fossil plants: evidence for polyploidy in majority of angiosperms. Science **264**: 421-423.

Mishra, J., Dash, A. K., Mishra, S. N. and Gupta, A. K. 2013. *Withania Coagulans* in treatment of diabetics and some other diseases: A review. Res. J. Pharm. Bio. Chem. Sci. **4**: 1251-1258.

Ahmad, M. B 2014. Characterization of Genetic Variability in *Withania somnifera* L Dunal using Biochemical and Molecular Markers. http://hdl.handle.net/10603/23450.

Morrison, J. W. and Rajhathy, T. 1960. Frequency of quadrivalents in autotetraploid plants. Nature **187**: 528-530.

Naz, S., Masud, T. and Nawaz, M. A. 2009. Characterization of milk coagulating properties from the extract of *Withania coagulans*. Int. J. Diary Tec. **62**: 315-320.

Olmstead, R. G., Bohs, L., Migid, H. A., Santiago-Valentin, E., Garcia1, V. F. and Collier, S. M. 2008. A molecular phylogeny of the Solanaceae. Taxon **57**: 1159-1181.

Otto, S. P. and Whitton, J. 2000. Polyploid incidence and evolution. Ann. Rev. Genet. **34**: 401-437.

Purohit, S. S. and Vyas, S. P. 2004. Medicinal Plant cultivation: A Scientific Approach. Publisher Agrobios: Jodhpur. pp 547.

Qu, L. and Vorsa, N. 1999. Desynapsis and spindle abnormalities leading to 2*n* pollen formation in *Vaccinium darrowi*. Genome **42**: 35-40.

Rai, P. K. and Kumar, G. 2010. The genotoxic potential of two heavy metals in inbred lines of maize (*Zea mays* L.). Turk. J. Bot. **34**: 39-46.

Ramsey, J. and Schemske, D. W. 1998. Pathways, mechanisms, and rates of polyploid formation in flowering plants. Ann. Rev. Ecol. Syst. **29**: 467-501.

Rezaei, M., Arzani, A. and Syed-Tabatabaei, B. E. 2010. Meiotic behavior of tetraploid wheats (*Triticum turgidum* L.) and their synthetic hexaploid wheat derivates influenced by meiotic restitution and heat stress. J. Genet. **89**: 401-407.

Risso-Pascotto, C., Pagliarini, M. S. and Valle, C. D. 2003. A mutation in the spindle checkpoint arresting meiosis II in *Brachiaria ruziziensis*. Genome 724-728.

Samaddar, T., Nath, S., Halder, M., Sil, B., Roychowdhury, D., Sen, S. and Jha, S. 2012. Karyotype analysis of three important traditional Indian medicinal plants, *Bacopa monnieri*, *Tylophora indica* and *Withania somnifera*. Nucleus **55**: 17-20.

Seriukova, E. G., Dorogova, N. V., Zharkov, N. V. and Shamina, N. V. 2003. Aberrations in prometaphase leading to the formation of restitution nuclei in cereal wide hybrids. Tsitologiya **45**: 244-248.

Shamina, N. V., Dorogova, N. V. and Perelman, P. L. 2000a. Radial spindle and the phenotype of maize meiotic mutant, dv. Cell Bio. Int. **24**: 729-736.

Shamina, N. V., Dorogova, N. V. and Perelman, P. L. 2000b. Disruption of male meiosis in *Pisum sativum* L. induced by mutation ms3. Tsitologiya **42**: 404-411.

Sharma, S. and Tiagi, B. 1979. *Flora of North East Rajasthan*. Kalyani Publishers. New Delhi.

Shetty, B. V. and Singh, V. 1993. *Flora of Rajasthan*, Vol. I, II, III. Botanical Survey of India, Calcutta.

Singhal, V. K. and Kaur, D. 2009. Spontaneous occurrence of meiotic spindle abnormalities in 'Long Headed Poppy' (*Papaver dubium* L.) from Indian cold regions. Cytologia **74**: 385-389.

Soltis, D. E., Albert, V. A., Leebens-Mack, J., Bell, C. D., Paterson, A., Zheng, C., Sankoff, D., dePamphilis, C. W., Wall, P. K. and Soltis, P. S. 2009. Polyploidy and angiosperm diversification. Am. J. Bot. **96**: 336-348.

Staiger, C. J. and Cande, W. Z. 1990. Microtubule distribution in dv, a maize meiotic mutant defective in the prophase to metaphase transition. Dev. Biol. **138**: 213-242.

Stebbins, G. L. 1938. Cytological characteristics associated with the different growth habits in the dicotyledons. Am. J. Bot. **25**: 189-198.

Stebbins, G. L. 1985. Polyploidy, hybridization, and the invasion of new habitats. Ann. Missouri Bot. Gard. **72**: 824-832.

Sun, K., Hunt, K. and Hauser, B. A. 2004. Ovule abortion in *Arabidopsis* triggered by stress. Plant Physiol. **135**: 2358-2367.

Viccini, L. F. and Carvalho, C. R. 2002. Meiotic chromosomal variation resulting from irradiation of pollen in maize. J. Appl. Genet. **43**: 463-469.

Wadsworth, P., Lee, W. L., Murata, T. and Baskin, T. I. 2011. Variations on theme: spindle assembly in diverse cells. Protoplasma **248**: 439-446.

Caryologia
International Journal of Cytology, Cytosystematics and Cytogenetics

Firenze University Press
www.fupress.com/caryologia

OPEN ACCESS

Citation: W. Thongnetr, A. Tanomtong, S. Prasopsin, N. Maneechot, K. Pinthong, I. Patawang (2019) Cytogenetic study of the Bent-toed Gecko (Reptilia, Gekkonidae) in Thailand; I: Chromosomal classical features and NORs characterization of *Cyrtodactylus kunyai* and *C. interdigitalis*. *Caryologia* 72(1): 23-28. doi: 10.13128/cayologia-248

Received: 19th May 2018

Accepted: 19th October 2018

Published: 10th May 2019

Data Availability Statement: All relevant data are within the paper and its Supporting Information files.

Competing Interests: The Author(s) declare(s) no conflict of interest.

Cytogenetic study of the Bent-toed Gecko (Reptilia, Gekkonidae) in Thailand; I: Chromosomal classical features and NORs characterization of *Cyrtodactylus kunyai* and *C. interdigitalis*

Weera Thongnetr[1,2], Alongklod Tanomtong[1,3], Suphat Prasopsin[4], Nuntiya Maneechot[5], Krit Pinthong[5], Isara Patawang[6,7,*]

[1] *Department of Biology, Faculty of Science, Khon Kaen University, Muang, Khon Kaen, Thailand*
[2] *Walai Rukhavej Botanical Research Institute, Mahasarakham University, Kantharawichai, Maha Sarakham, Thailand*
[3] *Toxic Substances in Livestock and Aquatic Animals Research Group, Khon Kaen University, Muang, Khon Kaen, Thailand*
[4] *Research Academic Supports Division, Mahidol University, Kanchanaburi Campus, Saiyok, Kanchanaburi, Thailand*
[5] *Department of Fundamental Science, Faculty of Science and Technology, Surindra Rajabhat University, Muang, Surin, Thailand*
[6] *Department of Biology, Faculty of Science, Chiang Mai University, Muang, Chiang Mai, Thailand*
[7] *Center of Excellence in Bioresources for Agriculture, Industry and Medicine, Chiang Mai University, Muang, Chiang Mai, Thailand*
* Corresponding author: isara.p@cmu.ac.th

Abstract. This study analysed the karyotype of *Cyrtodactylus kunyai* and *C. interdigitalis* from Loei Province in Northeastern Thailand. The metaphase and meiotic chromosome preparations were obtained by squash technique from bone marrow and testes, respectively. The chromosomes were stained by Giemsa staining and Ag-NOR-banding techniques. The results showed diploid chromosome number ($2n$) of 40 for *C. kunyai* and 42 for *C. interdigitalis*. The chromosome types of metacentric, submetacentric, acrocentric and telocentric chromosomes were 8-4-0-28 and 4-2-4-32, respectively. The Ag-NORs banding technique provides the pair of nucleolar organizer regions (NORs) of both two species at telomeric region of the long arm of the pair 12, metacentric type in *C. kunyai* and telocentric type in *C. interdigitalis*. There are no sex differences in karyotypes between males and females of both two species. We found that during metaphase I on meiosis of *C. kunyai* and *C. interdigitalis*, the homologous chromosomes showed synapsis of 20 and 21 bivalents, respectively. Moreover, the meiotic phase on prophase II exhibited 20 and 21 haploid chromosome number (n) as respective diploid species. Their karyotype formulas is as follows: *C. kunyai* ($2n = 40$): $L^m_2 + L^{sm}_4 + L^t_4 + M^t_6 + S^m_6 + S^t_{18}$, and *C. interdigitalis* ($2n = 42$): $L^a_4 + L^t_{14} + M^t_2 + S^m_4 + S^{sm}_2 + S^t_{16}$.

Keywords. *Cyrtodactylus*, *Cyrtodactylus kunyai*, *Cyrtodactylus interdigitalis*, Karyotype stasis.

INTRODUCTION

The bent-toed gecko, genus *Cyrtodactylus* Gray 1827, belong to the class Reptilia, order Squamata, suborder Lacertilia, and family Gekkonidae. The *Cyrtodactylus* is the most diverse gekkonid genus with ~250 species (Uetz et al. 2018). The species distribution of *Cyrtodactylus* found in mainland of Asia, from boundary between middle east and India to southeast Asia, Archipelago of southeast Asia and Pacific to Australia (Shea et al. 2011; Hartmann et al. 2016). In Thailand, there are about 24 species of *Cyrtodactylus* that were reported: including *C. angularis*, *C. auribalteatus*, *C. brevipalmatus*, *C. chanhomeae*, *C. consobrinus*, *C. dumnuii*, *C. erythrops*, *C. feae*, *C. interdigitalis*, *C. intermedius*, *C. jarujini*, *C. lekaguli*, *C. macrotuberculatus*, *C. oldhami*, *C. papilionoides*, *C. peguensis*, *C. phuketensis*, *C. pulchellus*, *C. quadrivirgatus*, *C. sumonthai*, *C. surin*, *C. thirakhupti*, *C. tigroides*, and *C. variegatus* (Chuaynkern and Chuaynkern 2012). Among the Gekkonidae population in Thailand, the *Cyrtodactylus* is the most diverse group than other gekkonid genera and there is continually new species discovered.

Karyological analyses in bent-toed gecko thus far has differentiated species based on mitotic metaphase chromosomal morphology while sporadic reports have based the species differentiation based on meiotic metaphase chromosomal morphology. Thus the basic diploid number of the bent-toed gecko is in the range of 42-48 (Ota et al. 1992). Example of chromosome study of other gekkonid that have been reported such as; *Gekko*: diploid number ranging from 38-42 and mostly 38 (Ota 1989; Shibaike et al. 2009; Trifonov et al. 2011; Patawang et al. 2014; Patawang and Tanomtong 2015a), *Hemidactylus*: diploid distance from 40-56 and mostly 40 or 46 (De Smet 1981; Patawang and Tanomtong 2015b), *Gehyra*: mostly 44 (King 1984), *Ptychozoon*: $2n = 34$ and 42 (Ota and Hikida 1988), *Paroedura*: diploid number ranging from 31-38 and mostly 36 (Aprea et al. 2013; Koubová et al. 2014), *Phelsuma*: $2n = 36$ (Aprea et al. 1996), and *Dixonius*: $2n = 42$ (Ota et al. 2001). Most gekkonid chromosome complements consist of acrocentric or telocentric chromosomes which gradually decrease in size, and karyotype evolution within the group is accompanied by Robertsonian fissions, fusions and pericentric inversions (Gorman 1973). The report of King (1987) presented eight putative ancestral karyomorphs ($2n = 32$, 34, 36, 38, 40, 42, 44, and 46 all acrocentric or telocentric chromosomes) and assigned the genus *Cyrtodactylus* to a group sharing an ancestral karyomorph consisting of $2n = 42$ uni-armed chromosomes.

In Thailand, there are no studies of *Cyrtodactylus*'s chromosome or karyotypic analyses. The present study of the cytogenetic of two *Cyrtodactylus* provides the first report of both two species, overall on the conventional Giemsa, Ag-NOR banding, and meiotic cell division. Data provided here will increase our knowledge of cytogenetic information which can be used as a basis to comprehensively examine the taxonomy and evolutionary relationship of *Cyrtodactylus* species and other gekkonid.

MATERIALS AND METHOD

Five male and four female specimens of *C. kunyai* (Figure 1a) and five male and six female of *C. interdigitalis* (Figure 1b) were collected from Puan Phu Sub-district, Nong Hin District, Loei Province, Northeastern Thailand. Chromosome preparation was conducted by the squash technique, from bone marrow for mitotic cell and testis for male meiotic cell, and followed with colchicine-hypotonic-fixation-air-drying technique (Patawang et al. 2014). The chromosomes were stained with 10% Giemsa for 30 min and NORs were identified through Ag-NOR staining (Howell and Black 1980; Rooney 2001). The length of short arm (Ls) and long arm (Ll) chromosomes were measured and calculated for the length of total arm chromosomes (LT, LT = Ls+Ll). Relative length (RL, $RL = LT/\sum LT$) and centromeric index (CI, CI = Ll/LT) were estimated. CI was also computed to classify the types of chromosomes (Turpin and Lejeune 1965; Chaiyasut 1989). All parameters were used in karyotyping and idiograming.

RESULTS AND DISCUSSION

Mitotic chromosome features from Giemsa staining

Karyomorphology of the *C. kunyai* and *C. interdigitalis* revealed that the diploid chromosome number ($2n$)

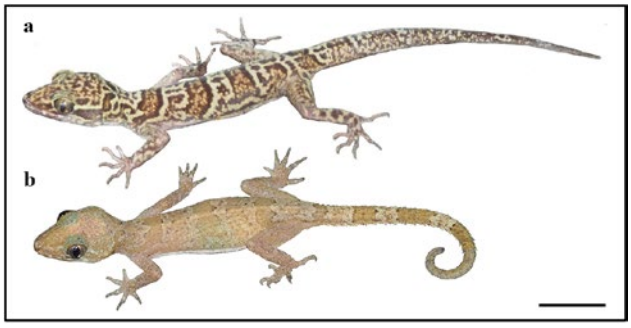

Fig. 1. General characteristic of male *Cyrtodactylus kunyai* (a) and female *C. interdigitalis* (b) (scale bar = 2 cm).

is 40 and 42, respectively. The karyotype of *C. kunyai* composed of 8 metacentric, 4 submetacentric, and 28 telocentric (Table 1 and Figures 2a-b), while the karyotype of *C. interdigitalis* comprised 4 metacentric, 2 submetacentric, 4 acrocentric, and 32 telocentric (Table 2 and Figures 2c-d). Both two species exhibit no sex differences in karyotypes between males and females (Figures 2a-d). Chromosome sizes of *C. kunyai* have pairs 1st to 5th to be large, pairs 6th to 8th to be medium, and pairs 9th to 20th to be small (Figure 3a). For the size of *C. interdigitalis* included large size in pairs 1st to 9th, medium size in the 10th, and small size in pairs 11th to 21st (Figure 3b). The diploid number of *C. kunyai* ($2n$ = 40) and *C. interdigitalis* ($2n$ = 42), both showed difference and accordance with others *Cyrtodactylus* that have been reported (Table 3). However, overall of these karyotypes of *C. kunyai* and *C. interdigitalis* resemble to other *Cyrtodactylus* and other gekkonid, which comprised many gradient mono-armed (telocentric) and few bi-armed chromosomes (meta- or submetacentric). Proximity of chromosome number and karyotype feature within genus *Cyrtodactylus* represents a close evolutionary line in the group.

Nucleolar organizer region and meiotic cell characteristics

The objective of the Ag-NOR banding technique is to detect nucleolar organizer regions (NORs) which represent the location of genes that have a function in ribosome synthesis (18S and 28S ribosomal RNA). The first cytogenetic study of *C. kunyai* and *C. interdigitalis* performed by Ag-NOR banding technique was obtained from this research. We found the clearly observable NORs on the region adjacent to telomere of long arm of the metacentric chromosome pair 12th (Figures 4a-b) for *C. kunyai* and on the region adjacent to telomere of long arm of the telocentric chromosome pair 12th (Figures 5a-b) for *C. interdigitalis*. Compared with other geckos, most showed two NORs appearing near telomeric region of small bi-armed or small mono-armed chromosome. An example of the previous reports of the geckos' NOR

Table 1. Mean length of short arm chromosome (Ls), long arm chromosome (Ll), total chromosomes (LT), centromeric index (CI), relative length (RL) and standard deviation (SD) of CI and RL from 20 metaphases of male and female *Cyrtodactylus kunyai*, $2n$ = 40.

Ch.p	Ls	Ll	LT	CI±SD	RL±SD	Ch.s	Ch.t
1	4.306	6.392	10.698	0.597±0.005	0.106±0.005	L	m
2	2.753	5.639	8.392	0.672±0.036	0.083±0.000	L	sm
3	2.911	5.120	8.031	0.637±0.042	0.080±0.003	L	sm
4	0.000	7.179	7.179	1.000±0.000	0.071±0.003	L	t
5	0.000	6.838	6.838	1.000±0.000	0.068±0.003	L	t
6	0.000	6.452	6.452	1.000±0.000	0.064±0.002	M	t
7	0.000	5.837	5.837	1.000±0.000	0.058±0.003	M	t
8	0.000	5.443	5.443	1.000±0.000	0.054±0.003	M	t
9	0.000	5.210	5.210	1.000±0.000	0.052±0.002	S	t
10	0.000	4.799	4.799	1.000±0.000	0.048±0.003	S	t
11	0.000	4.208	4.208	1.000±0.000	0.042±0.004	S	t
12*	1.946	2.147	4.093	0.525±0.017	0.041±0.003	S	m
13	0.000	3.319	3.319	1.000±0.000	0.033±0.002	S	t
14	0.000	3.300	3.300	1.000±0.000	0.033±0.003	S	t
15	0.000	3.189	3.189	1.000±0.000	0.032±0.003	S	t
16	1.570	1.580	3.150	0.547±0.030	0.035±0.003	S	m
17	0.000	2.793	2.793	1.000±0.000	0.028±0.003	S	t
18	0.000	2.654	2.654	1.000±0.000	0.026±0.002	S	t
19	0.000	2.443	2.443	1.000±0.000	0.024±0.003	S	t
20	1.136	1.156	2.292	0.552±0.020	0.025±0.002	S	m

Abbreviations: *Ch.p*, chromosome pair; *Ch.s*, chromosome size; *Ch.t*, chromosome type; *, nucleolar organizer region; *L*, large size; *M*, medium size; *S*, small size; *m*, metacentric; *sm*, submetacentric; *t*, telocentric.

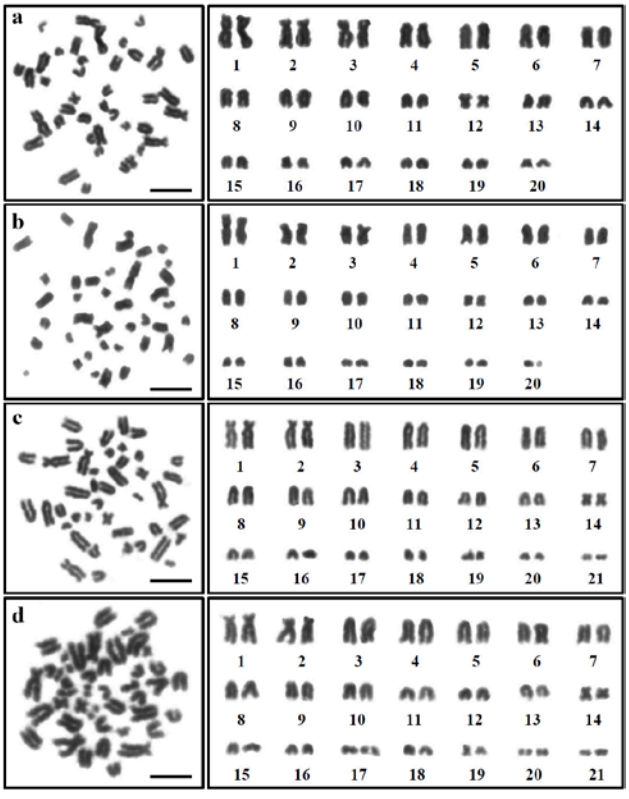

Fig. 2. Conventionally stained somatic metaphase complement and karyotypes of male (a) and female (b) of *Cyrtodactylus kunyai*, $2n$ = 40, and male (c) and female (d) of *C. interdigitalis*, $2n$ = 42, (scale bars = 10 μm).

Table 2. Mean length of short arm chromosome (Ls), long arm chromosome (Ll), total chromosomes (LT), centromeric index (CI), relative length (RL) and standard deviation (SD) of CI and RL from 20 metaphases of male and female *Cyrtodactylus interdigitalis*, $2n = 42$.

Ch.p	Ls	Ll	LT	CI±SD	RL±SD	Ch.s	Ch.t
1	2.715	6.857	9.572	0.716±0.012	0.090±0.005	L	a
2	2.193	6.374	8.567	0.744±0.018	0.081±0.003	L	a
3	0.000	8.136	8.136	1.000±0.000	0.077±0.004	L	t
4	0.000	7.822	7.822	1.000±0.000	0.074±0.003	L	t
5	0.000	7.505	7.505	1.000±0.000	0.071±0.005	L	t
6	0.000	6.513	6.513	1.000±0.000	0.062±0.002	L	t
7	0.000	6.066	6.066	1.000±0.000	0.057±0.003	L	t
8	0.000	5.874	5.874	1.000±0.000	0.056±0.003	L	t
9	0.000	5.677	5.677	1.000±0.000	0.054±0.002	L	t
10	0.000	5.337	5.337	1.000±0.000	0.050±0.003	M	t
11	0.000	4.539	4.539	1.000±0.000	0.043±0.004	S	t
12*	0.000	4.031	4.031	1.000±0.000	0.038±0.003	S	t
13	0.000	3.808	3.808	1.000±0.000	0.036±0.003	S	t
14	1.824	1.830	3.654	0.501±0.027	0.035±0.004	S	m
15	1.102	2.235	3.337	0.670±0.041	0.032±0.004	S	sm
16	0.000	3.113	3.113	1.000±0.000	0.029±0.003	S	t
17	0.000	2.856	2.856	1.000±0.000	0.027±0.003	S	t
18	0.000	2.820	2.820	1.000±0.000	0.027±0.001	S	t
19	1.399	1.410	2.809	0.502±0.038	0.027±0.003	S	m
20	0.000	2.017	2.017	1.000±0.000	0.019±0.003	S	t
21	0.000	1.712	1.712	1.000±0.000	0.016±0.002	S	t

Abbreviations: *Ch.p*, chromosome pair; *Ch.s*, chromosome size; *Ch.t*, chromosome type; *, nucleolar organizer region; *L*, large size; *M*, medium size; *S*, small size; *m*, metacentric; *sm*, submetacentric; *a*, acrocentric; *t*, telocentric.

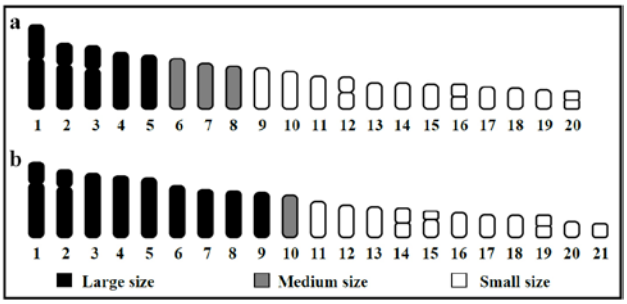

Fig. 3. Standardized idiogram of *Cyrtodactylus kunyai* (a) and *C. interdigitalis* (b) by conventional staining.

localization included in the genus *Gehyra* (King 1983), *Gekko* (Chen et al. 1986; Shibaike et al. 2009; Patawang et al. 2014), *Hemidactylus* (Patawang and Tanomtong 2015b), and *Lepidodactylus* (Trifonov et al. 2015). These previous studies showed the NOR appearing near terminal region of one homologous small chromosome.

The present study on male meiotic cell division in *C. kunyai* and *C. interdigitalis* found the late interphase to early prophase that the cell of each species showed two signals of nucleolus by positive silver staining (Figures 4c, 5c). The characteristics of two nucleolus structure at early phase of cell division supported the appearing of two NORs on one homologous at metaphase chromosome in both two *Cyrtodactylus* species. We found diplotene phase in meiotic cell of both two species (Figures 4d, 5d), which showed synapsis between two of homologous and compacted chromosome. The metaphase I (meiosis I, reductional division) was found in two species, which can be defined as the 20 bivalents for *C. kunyai* (Figure 4e) and 21 bivalents for *C. interdigitalis* (Figure 5e). No metaphase I cells with partially paired bivalents, which are speculated to be male heteromorphic sex chromosomes in both two *Cyrtodactylus* species. Moreover, $n = 20$ in *C. kunyai* (Figure 4f) and $n = 21$ in *C. interdigitalis* (Figure 5f) were found at metaphase II (meiosis II, equational division) of spermatid cells. Form these results, behavior and number of chromosome in metaphase I and metaphase II confirmed of each other's accuracy and also verified the accuracy of diploid chromosome in somatic cells.

Overview of chromosomal feature of the two Cyrtodactylus

Gekkonid chromosome that has been reported in the past, most species show the gradient karyotype, which comprising of many mono-armed chromosomes

Table 3. Review of cytogenetic study of the genus *Cyrtodactylus*.

Species	*2n*	NF	Karyotype	NOR	Locality	Reference
C. consobrinus	48	50	2bi-armed+46t	-	Sarawak, Malaysia	Ota et al. (1992)
C. interdigitalis	42	52	4m+2sm+4a+32t		Loei, Thailand	Present study
C. kunyai	40	52	8m+4sm+28t		Loei, Thailand	Present study
C. pubisulcus	42	44	2bi-armed+40t	-	Sarawak, Malaysia	Ota et al. (1992)

Abbreviations: *2n*, diploid chromosome; *NF*, fundamental number; *NOR*, nucleolar organizer region; *bi-armed*, bi-armed chromosome; *m*, metacentric; *sm*, submetacentric; *a*, acrocentric; *t*, telocentric.

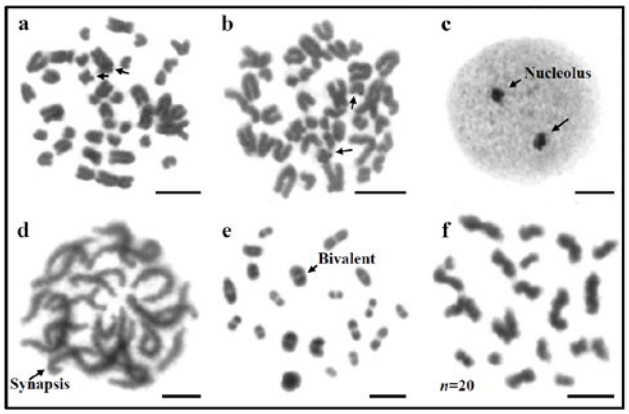

Fig. 4. Silver stained somatic metaphase complement of male (a) and female (b) of *Cyrtodactylus kunyai*, arrows indicate nucleolar organizer region (NOR), and meiotic cell division of the male *C. kunyai* on interphase by silver NOR staining (c), diplotene (d), metaphase I (e), and metaphase II (f) (scale bars = 10 μm).

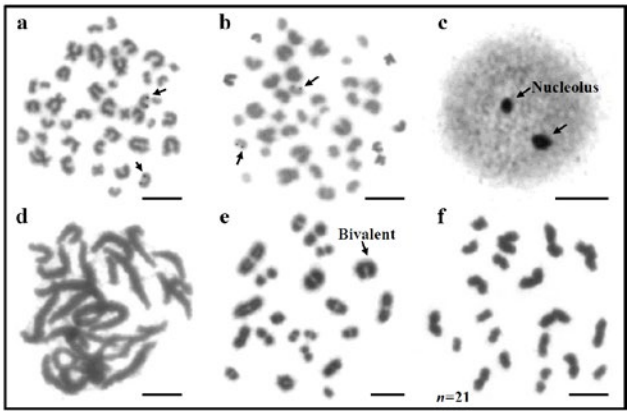

Fig. 5. Silver stained somatic metaphase complement of male (a) and female (b) of *Cyrtodactylus interdigitalis*, arrows indicate nucleolar organizer region (NOR), and meiotic cell division of the male *C. interdigitalis* on interphase by silver NOR staining (c), pachytene (d), metaphase I (e), and metaphase II (f) (scale bars = 10 μm).

and few bi-armed chromosomes. Present results of *C. kunyai* and *C. interdigitalis* agree with chromosomal evolution line hypothesis within the gekkonid group. The karyotype of *C. kunyai* and *C. interdigitalis* showed the gradient of most telocentric while comprised of a few bi-armed chromosome, 12 chromosomes in *C. kunyai* and 10 chromosomes in *C. interdigitalis*. These features conform to the hypothesis of rearrangement from ancestral karyotype by Robertsonian fissions, fusions or pericentric inversions (Gorman 1973; King 1987).

ACKNOWLEDGEMENTS

This research was financially supported by sharing from the Research Fund for Supporting Lecture to Admit High Potential Student to Study and Research on His Expert Program Year 2016, the Toxic Substances in Livestock and Aquatic Animals Research Group, Khon Kaen University, and the Royal Thai Government Scholarship National Science and Technology Development Agency (NSTDA). The project was approved by the Institute of Animals for Scientific Purpose Development of National Research Council of Thailand (Resolution U1-02740-2559).

REFERENCES

Aprea G, Odierna G, Capriglione T, Caputo V, Morescalchi A, Olmo E. 1996. Heterochromatin and NOR distribution in the chromosomes of six gekkonid species of the genus *Phelsuma* (Squamata: Gekkonidae). J Afr Zool. 110(5):341–349.

Aprea G, Andreone F, Fulgione D, Petraccioli A, Odierna G. 2013. Chromosomal rearrangements occurred repeatedly and independently during species diversification in Malagasy Geckos, genus *Paroedura*. Afr Zool. 48(1):96–108.

Chaiyasut K. 1989. Cytogenetic and cytotaxonomy of genus *Zephyranthes*. Bangkok: Department of Botany, Faculty of Science, Chulalongkorn University. [in Thai]

Chen J, Peng X, Yu D. 1986. Studies on the karyotype of three species of the genus *Gekko*. Acta Herpetol Sinica. 5:24–29.

Chuaynkern Y, Chuaynkern C. 2012. Checklist of reptiles in Thailand. J Wildl Thailand. 19(1):75–162.

De Smet WHO. 1981. Description of the orcein stained kariotypes of 27 lizard species (Lacertilia: Reptilia) belonging to the familias Iguanidae, Agamidae, Chamaeleontidae and Gekkonidae (Ascalabota). Acta Zool Pathol Ant. 76:35–72.

Gorman GC. 1973. Cytotaxonomy and vertebrate evolution. New York: Academic Press. The chromosomes of the Reptilia, a cytotaxonomic interpretation; p. 349–424.

Hartmann L, Mecke S, Kieckbusch M, Mader F, Kaiser H. 2016. A new species of bent-toed gecko, genus *Cyrtodactylus* Gray, 1827 (Reptilia: Squamata: Gekkonidae), from Jawa Timur Province, Java, Indonesia, with taxonomic remarks on *C. fumosus* (Müller, 1895). Zootaxa. 4067(5):552–568.

Howell WM, Black DA. 1980. Controlled silver-staining of nucleolus organizer regions with a protective

colloidal developer: a 1-step method. Experientia. 36:1014–1015.

King M. 1983. Karyotypic evolution in *Gehyra* (Gekkonidae: Reptilia) III, the *Gehyra australis* complex. Aust J Zool. 31:723–741.

King M. 1984. Karyotypic evolution in *Gehyra* (Gekkonidae: Reptilia) IV, chromosome change and speciation. Genetica. 64(2):101–114.

King M. 1987. Monophyleticism and polyphyleticism in the Gekkonidae: a chromosomal perspective. Aust J Zool. 35(6):641–654.

Koubová M, Pokorná MJ, Rovatsos M, Farkačová K, Altmanová M, Kratochvíl L. 2014. Sex determination in Madagascar geckos of the genus *Paroedura* (Squamata: Gekkonidae): are differentiated sex chromosomes indeed so evolutionary stable?. Chromosome Res. 22:441–452.

Ota H, Hikida T. 1988. Karyotypes of Two Species of the Genus *Ptychozoon* (Gekkonidae: Lacertilia) from Southeast Asia. JPN J Herpetol. 12(4):139–141.

Ota H. 1989. Karyotypes of five species of *Gekko* (Gekkonidae: Lacertilia) from East and Southeast Asia. Herpetologica. 45(4):438–443.

Ota H, Hikida T, Matsui M, Mori A. 1992. Karyotypes of two species of the genus *Cyrtodactylus* (Squamata: Gekkonidae) from Sarawak, Malaysia. Caryologia. 45(1):43–49.

Ota H, Hikida T, Nabhitabhata J, Panha S. 2001. Cryptic taxonomic diversity in two broadly distributed lizards of Thailand (*Mabuya macularia* and *Dixonius siamensis*) as revealed by chromosomal investigations (Reptilia: Lacertilia). Nat Hist J Chula Univ. 1(1):1–7.

Patawang I, Tanomtong A. 2015a. The variation of tokay gecko, *Gekko gecko* (Linnaeus, 1758) between two populations in southern China and Indochinese Peninsula. SWU Sci J. 31(2): 75–186. [in Thai]

Patawang I, Tanomtong A. 2015b. Karyological analysis of Asian house gecko (*Hemidactylus frenatus*) and frilly house gecko (*H. platyurus*) from northeastern Thailand. In: The 19th National Genetics Conference 2015 –Genetics and Genomics, from Molecular Studies to Applications; 15-17 July 2015; AVANI Khon Kaen Hotel & Convention Centre, Khon Kaen. Bangkok: Genetics Society of Thailand.

Patawang I, Tanomtong A, Jumrusthanasan S, Kakampuy W, Neeratanaphan L, Pinthong K. 2014. Chromosomal characteristics of NORs and karyological analysis of tokay gecko, *Gekko gecko* (Gekkonidae, Squamata) from mitotic and meiotic cell division. Cytologia. 79(3):315–324.

Rooney DE. 2001. Human cytogenetics constitution analysis. London: Oxford University Press.

Shea G, Couper P, Wilmer JW, Amey A. 2011. Revision of the genus *Cyrtodactylus* Gray, 1827 (Squamata: Gekkonidae) in Australia. Zootaxa. 3146:1–63.

Shibaike Y, Takahashi Y, Arikura I, Iiizumi R, Kitakawa S, Sakai M, Imaoka C, Shiro H, Tanaka H, Akakubo N, Nakano M, Watanabe M, Ohne K, Kubota S, Kohno S, Ota H. 2009. Chromosome evolution in the lizard genus *Gekko* (Gekkonidae, Squamata, Reptilia) in the East Asian islands. Cytogenet Genome Res. 127:182–190.

Trifonov VA, Giovannotti M, O'Brien PCM, Wallduck M, Lovell F, Rens W, Parise-Maltempi PP, Caputo V, Ferguson-Smith MA. 2011. Chromosomal evolution in Gekkonidae I. chromosome painting between *Gekko* and *Hemidactylus* species reveals phylogenetic relationships within the group. Chromosome Res. 19:843–855.

Trifonov VA, Paoletti A, Barucchi VC, Kalinina T, O'Brien P CM, Ferguson-Smith MA, Giovannotti M. 2015. Comparative chromosome painting and NOR distribution suggest a complex hybrid origin of triploid *Lepidodactylus lugubris* (Gekkonidae). PLOS ONE. 10(7):e0132380.

Turpin R, Lejeune J. 1965. Les chromosomes humains (caryotype normal et variations pathologiques). Paris: Gauthier-Villars. [in France]

Uetz P, Freed P, Hošek J. 2018. *Cyrtodactylus*. [accessed 2018 March 15]. http://reptile-database.reptarium.cz/search?search=Cyrtodactylus&submit=Search

Caryologia
International Journal of Cytology, Cytosystematics and Cytogenetics

Firenze University Press
www.fupress.com/caryologia

Citation: B. Yilmaz Öztürk (2019) Intracellular and extracellular green synthesis of silver nanoparticles using *Desmodesmus* sp.: their Antibacterial and antifungal effects. *Caryologia* 72(1): 29-43. doi: 10.13128/cayologia-249

Received: 21th april 2018

Accepted: 20th november 2018

Published: 10th May 2019

Data Availability Statement: All relevant data are within the paper and its Supporting Information files.

Competing Interests: The Author(s) declare(s) no conflict of interest.

Intracellular and extracellular green synthesis of silver nanoparticles using *Desmodesmus* sp.: their Antibacterial and antifungal effects

Betül Yilmaz Öztürk

Eskişehir Osmangazi University Central Research Laboratory Application And Research Center (ARUM), 26480 Eskişehir, Turkey
E mail: byozturk@ogu.edu.tr. ORCID: 0000-0002-1817-8240

Abstract. In this study aim was to perform green synthesis of synthesis silver nanoparticles (LAC-AgNPs, RAE-AgNPs and BAE-AgNPs) by using *Desmodesmus* sp., intracellular and extracellular synthesis methods and to compare the obtained products with physicochemical characterization techniques. The structural, morphological and optical properties of the synthesized nanoparticles were characterized using UV-Vis spectroscopy, TEM, SEM-EDS, FTIR, DLS and zeta potential. These results clearly show that silver nanoparticles (AgNPs) could be synthesized in different sizes and stabilities with various biological materials obtained from *Desmodesmus* sp. LAC-AgNPs had size of 10-30 nm, RAE-AgNPs had size of 4-8 nm and BAE-AgNPs had size of 3-6 nm. Also, the antibacterial activity of silver nanoparticles synthesized as intracellular and extracellular showed a strong antibacterial effect against pathogens such as *Salmonella* sp. and *Listeria monocytogenes*. Additionally, they have effective antifungal activity against *Candida parapsilosis*. The broth microdilution method was used for examining antibacterial antifungal effect of synthesis AgNPs. The minimum inhibitory concentration against *Salmonella* sp., *Listeria monocytogenesis* and *Candida parapsilosis* were recorded as 3,125 µl, 1,5625 µl and 0,78125 µl synthesis AgNPs, respectively. As a result, it has thought that different sizes of synthesis AgNPs may have a great potential for biomedical applications.

Keywords. Green synthesis, nanoparticle, algae, antimicrobial, *Desmodesmus* sp.

INTRODUCTION

In nanotechnology studies, the most attract attention topics is the synthesis of nanoparticles (NPs) with strong potency in different sizes and shapes or by using various variables. For example, metal NPs. The area of use for metal NPs are very broad. Even silver NPs alone are used in countless areas with optics, electronics, catalysis, home furnishings and extensive medical applications, and the annual production is estimated to be hundreds of tons worldwide (Ge et al. 2014).

Synthesis of nanomaterials containing noble metal requires alternative strategies because of their high cost. Green synthesis or green chemical synthesis leads the list of these strategies and here the target is a biological synthesis of nanomaterial and to obtain products with positive effects in terms of the environment (Sondi et al. 2000). Green synthesis has preferred because of the high costs of materials used in conventional chemical methods and due to the toxic substances released into the environment. Because the toxic effect of nanoparticles is proven in many studies on aquatic organisms in particular. For example, studies on algae (Dağlıoğlu and Öztürk 2016; Dağlıoğlu and Öztürk 2018; Öztürk and Dağlıoğlu 2018) have shown that aquatic invertebrates (*Artemia salina*) (Dağlıoğlu et al. 2016a), terrestrial invertebrates, honey bee (*Apis mellifera*) (Özkan et al. 2016), aquatic plants (*Lemna minor* and *Myriophyllum spicatum*) (Dağlıoğlu and Türkiş 2017a, b). Nevertheless, it more attracts the attention of researchers for the production of metal nanoparticles because of its low cost, environmental friendliness, and simple approach. In the green synthesis does not use reducing agents like sodium borohydride ($NaBH_4$) used in chemical synthesis (Kozma et al. 2015). These reducing agents are both expensive and may produce oxidized boron species bound to NPs after synthesis. As a result the commercially produced NPs are not appropriate for biological applications. NPs produced by green synthesis are of great importance in terms of environmentally friendly production processes and low costs. Many organisms or a variety of extracts produced by them may be used in the green synthesis process bacteria (Joerger et al. 2000), plant (Khatami et al. 2018a), fungi (Boroumand et al. 2015) and algae (Singh et al. 2013).

Algae will have a great platform for products to be used for various purposes over the next few years has a long-term sustainable potential, especially in the production of food and liquid fuels (Koothari et al. 2017). For this reason algae are commonly chosen for green synthesis because their structures are a rich source of biologically active compounds like chlorophyll, carotenoids, astaxanthin, phenol, flavonoid, protein, vitamin and minerals (Faulker 2000). Additionally, these phytochemical materials are each effective metal reducing agents and their structures contain agents ensuring that hydroxyl, carboxyl, and amino functional groups coat metal NPs (Annamalia and Nallamuthu 2015). It has been supported by various literatures that NPs synthesis can be carried out by using various algae. For example, Kannan et al. (2013) performed AgNP synthesis with extraction from *Chaetomorpha linum* species. The researchers succeeded in synthesizing spherical NPs with nearly 30 nm size without using synthetic reactives. Barwal et al. (2011) used a *Chlamydomonas reinhardtii* model and focused on understanding the role of a variety of cellular proteins in the synthesis and coating of silver NPs. Prasad et al. (2013) studied the extract of the brown algae *Cystophora moniliformis* species and reported that the sizes of NPs may change linked to temperature. Studies mainly use marine macroalgae with insufficient numbers of studies about microalgae.

It has been known for many years that silver (Ag) is an antimicrobial agent and it draws much attention due to its application in fields such as colloidal Ag, catalysis and water purification. It is reported that using AgNP may purify drinking water (Pradeep 2009). Furthermore, the effect of Ag NPs size variability on antibacterial properties has been a matter of interest. As a result, researchers who have successfully achieved green synthesis have simultaneously assessed the antibacterial and antifungal effects on a variety of microorganisms (like bacteria and yeast) (Govindaraju et al. 2009; Rajeshkumar et al. 2014; Salari et al. 2016; Suriya et al. 2012).

Our aim is to use the microalgae *Desmodesmus* sp., which can easily be produced in a laboratory environment, to compare synthesis using both intracellular and extracellular routes. For this, the differences between NPs forming under the same conditions were determined using characterization techniques like UV-Vis, TEM, SEM-EDS, FTIR, DLS and zeta potential. At the same time, antibacterial effects of synthesized NPs on bacterial strains of important food pathogens such as *Salmonella* sp. and *Listeria monocytogenesis* were investigated. Additionally, the antifungal effect on the human pathogen of *Candida parapsilosis* species was investigated.

MATERIAL AND METHOD

Algae Culture

The test organism used in our study, *Desmodesmus* sp. (KR261937), was taken from the algae culture collection of Selçuk University Hydrobiology Laboratory. Algae taken from stock cultures were transferred to the fluid BG-11 medium ($NaNO_3$, 15; K_2HPO_4, 0.4; $MgSO_4{\cdot}7H_2O$, 0.75; $CaCl_2{\cdot}2H_2O$, 0.36; citric acid, 0.06; iron(III) ammonium citrate, 0.06; Na_2-EDTA, 0.01; Na_2CO_3, 0.2 g/L, 1 mL; trace elements solution, (H_3BO_3, 61; $MnSO_4{\cdot}H_2O$, 169; $ZnSO_4$ ·$7H_2O$, 287; $CuSO_4{\cdot}5H_2O$, 2.5; $(NH_4)_6Mo_7O_{24}{\cdot}4H_2O$, 12.5 mg/L) in accordance with the procedure stated in Rippka (1988). The microalgae were transferred to 250 ml erlenmeyer flask and left to proliferate under sterile conditions. The cultures were

left under 3000 lux fluorescent light appropriate for photosynthesis for 12 hours light and 12 hours darkness, at 28±2 °C degrees, and 120 rpm for 15-20 days. When algae passed the log phase stage, cells were centrifuged at 1000 rpm and the biomass was obtained. All chemicals used in this study were analytical quality.

Intracellular AgNP synthesis using live algae cells

Silver nitrate ($AgNO_3$, ≥99.0%; Sigma-Aldrich) was prepared in 100 mM stock solution. Microalgae passing the logarithmic phase were counted with the automatic cell counting device (LUNA-II™ Automated Cell Counter, South). Using LUNA ™ Cell counting slides, counting and viability of cells were determined with trypan blue. Afterwards, live algae cells (LAC) were harvested by centrifugation at 4000 rpm for 20 minutes at 4 °C. The culture filtrate was removed and the pelleted biomass was washed with sterile deionized water to remove foreign absorbed material. The washing procedure was repeated five times and the washed biomass was brought to suspension again in distilled water. The suspension of algal biomass had 5mM $AgNO_3$ added the from stock solution. In the control setup, $AgNO_3$ was not added to the algal biomass. Cultures were incubated at 28 °C under similar conditions to those stated above for 72 hours. Intracellular Ag NPs (LAC-AgNPs) synthesis from LAC was completed. After the reaction, the biomass was separated by the centrifuge and stored at -20 °C until characterization.

Extracellular synthesis of AgNP

Two different algal extracts were obtained using Desmodesmus sp. for the extracellular synthesis of AgNP. These extracts were raw algal extract (RAE) and boiled algal extract (BAE).

Preparation of raw and boiled algae extracts

For the preparation of RAE extract, 3.0 g (wet weight) algal biomass was suspended in 20 ml of deionized water for 5 days. At the end of the 5th day, it was centrifuged at 7000 rpm for 20 minutes. The supernatant (raw algal extract) was separated from cells and prepared for extraction. To begin the reaction, the final concentration of 5 mM $AgNO_3$ was added. After this procedure, continuous mixing began. Later the mixing procedure, a colloidal structure was obtained and after this process repeated centrifugation was completed at 3500 rpm for 5 minutes. These centrifuge cycles were completed to purify AgNP. Extracellular Ag NPs (RAE-AgNPs) synthesis from RAE was completed. After the reaction, the biomass was separated by the centrifuge and stored at -20 °C until characterization.

To prepare the BAE extract, 3.0 g (wet weight) algal biomass was suspended in 20 ml deionized water and heated to 100 °C for 20 minutes in an erlenmeyer flask. After the boiling procedure, it was cooled and filtered with Grade GF/A glass microfiber filters (Whatman™, pore size: 1,6µm). The obtained filtrate had the final concentration of 5 mM $AgNO_3$ added at room temperature to begin the reaction. After the procedure continuous mixing was completed. Later the mixing procedure, a colloidal structure was obtained and after this process repeated centrifugation was completed at 3500 rpm for 5 minutes. These centrifuge cycles were completed to purify AgNP. Extracellular Ag NPs synthesis (BAE-AgNPs) from boiled algal extract was completed. After the reaction had completed, the biomass was separated by the centrifuge and stored at -20 °C until characterization.

Characterization of AgNPs

Biological reduction of silver ions with the green synthesis route was observed by taking 3 ml aliquot samples at different time intervals. Absorption measurements were made with a UV-Vis (AE-S90-2D UV-VIS Spectrophotometer, China.) spectrophotometer between 190 and 1100 nm.

Transmission electron microscope (TEM) images of the intracellular and extracellular synthesized AgNPs were obtained using TEM (JEOL JEM 1220 brand, Japan) working at 100 kV acceleration voltage. Samples used to obtain TEM micrographs were prepared by dropping on a carbon-coated copper grid and dried under a vacuum before investigation. With the aim of investigating the cells at the ultrastructural level, routine TEM monitoring procedure was performed and samples were submerged in epoxy resin. Thin sections were taken at 60 nm thickness with the aid of an ultramicrotome (Leica ultracut UCT, Leica, Germany) (Ilknur et al. 2012; Li et al. 2012; Zhang et al. 2016). Elemental analysis of samples was completed with SEM (a JEOL JSM-5600 LV brand, Japan) device fitted with EDS (E2V Scientific Instruments, United Kingdom).

Algae cells were freeze-dried and algae biomass was obtained. Dried biomass was prepared using the KBr pellet technique and ATR technique. The surface chemistry of reduced Ag samples and the biologically active portions of the live microalgal cells were analyzed to check for comparisons. The fourier transform mid-infra-

red FTIR spectra (Perkin Elmer Spectrum 100 FTIR-ATR unit, Germany) were collected with conduction mode from 400–4,000 cm^{-1} with 0,4 cm^{-1} spatial resolution.

Dynamic light scattering (DLS) and zeta potential are necessary parameters to define the size distribution, particle size, homogeneity and stability of LAC-AgNPs, RAE-AgNPs and BAE-AgNPs. Particle size and polydispersity index (PDI) were determined using the dynamic light scattering technique. DLS studies of LAC-AgNPs, RAE-AgNPs and BAE-AgNPs diluted in deionized water were measured by a Malvern-Zetasizer (Nano-Z590, United Kingdom) device. The zeta potential is a measurement of the attraction or repulsion values between particles. Particles with certain load attractions with opposite polarity within the suspension, as a result, a strong bond surface is formed on the surface of the loaded particle and then a surface extending outward from the loaded particle forms. The behavior of particles within polar fluids is determined not by electric load but by zeta values. Zeta potential studies were measured with a Malvern (SN: MAL1064144, United Kingdom) brand Zeta Sizer ZS device.

Antimicrobial Susceptibility Testing of synthesis NPs

In this study with the aim of determining the antibacterial and antifungal susceptibility of LAC-AgNPs, RAE-AgNPs and BAE-AgNPs, *Salmonella* sp. (gram-) and *Listeria monocytogenesis* (gram+) bacteria and *Candida parapsilosis* yeast was used. To determine the minimal inhibition concentration, the broth microdilution method was taken as a basis. Bacteria cells were left in nutrient broth medium at 37 °C for 1 night, while yeast cells were incubated for 1 night in a shaking incubator at 30 °C in yeast extract-peptone-dextrose (YPD; %1 yeast extract, %2 peptone %2 dextrose) medium and cultures were taken. The density of bacteria and fungal cells were set according to the McFarland 0.5 standard. Tests of minimal inhibitory concentration (MIC) were made in accordance with the CLSI (Clinical Laboratory Standards Institute) criteria M27-A8 for bacteria and M27-A2 for yeast (Zgoda and Porter 2001). The extraction containing lowest NPs that inhibited bacterial and fungal development was determined as the volume MIC value. During this process 40 minutes sonication was applied to obtain the LAC-AgNPs. The 96-well plates (Lp Italiana Spa) was added 100 µl RPMI 1640 and 100 µl the LAC-AgNPs, RAE-AgNPs and BAE-AgNPs. Later they were diluted with microdilution and left for 24 hours incubation. The plate with resazurin added had results assessed in parallel with the colour change.

RESULTS

The test organism *Desmodesmus* sp. (KR261937) is in the Chlorophyceae class and is a water alga generally forming colonies with an oval or shuttle-shaped body. Additionally, it is a photosynthetic microalga with 6-10 horn-like protrusions on the body. In the colonial structure, generally twin cells are found. Additionally, sequences of 4 colonial cells may be seen in low numbers. The count of the automatic cell counting device is given in Table 1. In the current study when algal biomass (LAC) was exposed to Ag ions (Ag^+), the colour of the algal biomass changed from natural bright green to brown and compared with the control biomass, the Ag^+ ion was biologically transformed (Ag metal accumulation) to Ag^0. During exposure the colour change began in the first 24 hours; however, the largest colour difference compared to the first day occurred after 72 hours. LAC-AgNPs was researched with UV-Vis for 72 hours (Figure 1A).

Simultaneously RAE and BAE were treated with 5 mM $AgNO_3$ and extracellular Ag NPs (RAE-AgNPs and BAE-AgNPs) the formation was researched with UV-Vis spectroscopy. The RAE-AgNPs were colourless and had a high peak at 280-300 nm (Figure 1 B). The RAE exposed to Ag displayed a peak at 420 nm especially after the 48 hours day on UV-Vis spectral analysis and it was considered AgNP formation had begun. It is known that the concentration of the reducing agent in the reaction mixture plays an important role in the formation of nucleation points and then controls the size of AgNP; this may have caused less stable AgNP in the RAE (Hiramutsu and Osterloh 2004; Jena et al. 2014).

As a result, another experiment was made to increase the concentration of this type of material in the reaction mixture. The biomass was boiled in water to obtain more reducing and stabilizing agents. Initially, the boiled extract had a light yellow colour, which transformed to brown when exposed to the Ag nitrate solution procedure. The formation of this colour is due to stimulation of surface plasmon resonance (SPR) effect and the reduction in $AgNO_3$ and may indicate the formation of AgNP. With the increase in the reaction duration, the colour of the reaction mixture turned a darker

Table 1. *Desmodesmus* sp. cell counting and cell viability analysis report.

Total cell	Live cell	Dead cell	Viability
$4{,}48x10^8$	$4{,}08x10^8$	$4{,}00x10^7$	80,6 %

*Stain: Trypan blue.

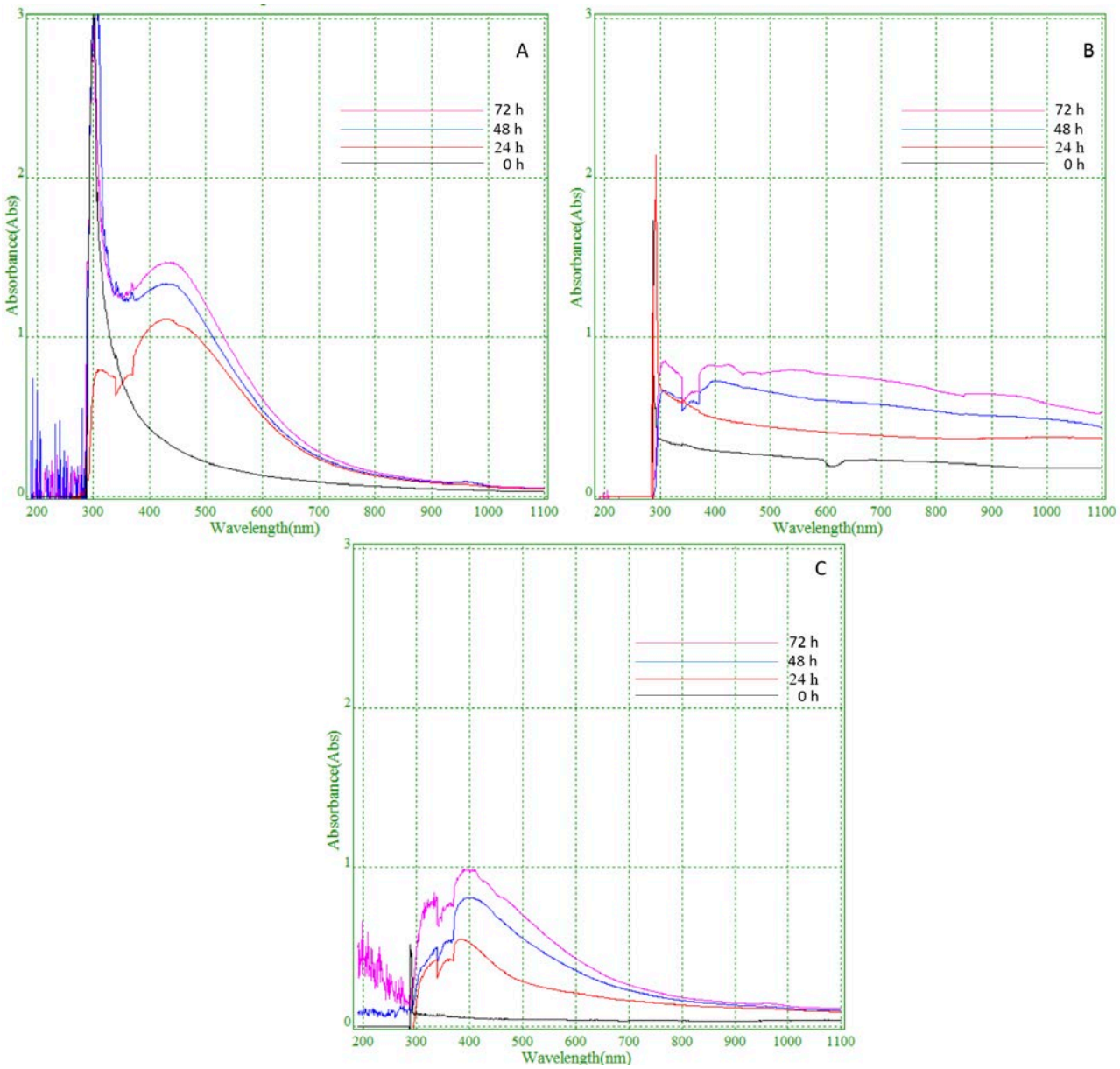

Fig. 1. Examination of intracellular and extracellular synthesis of silver nanoparticles by UV-Vis. A. LAC-AgNPs; B. RAE-AgNPs; C. BAE-AgNPs.

shade for up to 72 hours. The formation of BAE-AgNPs were proven with the UV-Vis spectrum showing the characteristic surface plasmon resonance (SPR) band for AgNPs. Figure 1 C shows the UV-Vis spectra series recorded for the reaction mixture at a variety of time intervals. The BAE showed a peak at 280-320 nm which may be linked to the presence of peptides. The BAE exposed to Ag displayed a peak at 420 nm especially after the 24 hours day on UV-Vis spectral analysis and it was considered BAE-AgNPs formation had begun.

Our UV-Vis results show a steady increase in reduction of Ag ions in LAC up to 420 nm, then it stabilized and appeared to pass to a downward trend. This section is defined as the "surface plasmon resonance band" and is due to the stimulation of free electrons in the NPs. The symmetric shape of the band is an indicator of the regular distribution of the spherical NPs (Travan et al. 2009).

After intracellular synthesis, the exposed biomass had TEM analysis was made to research the morphology

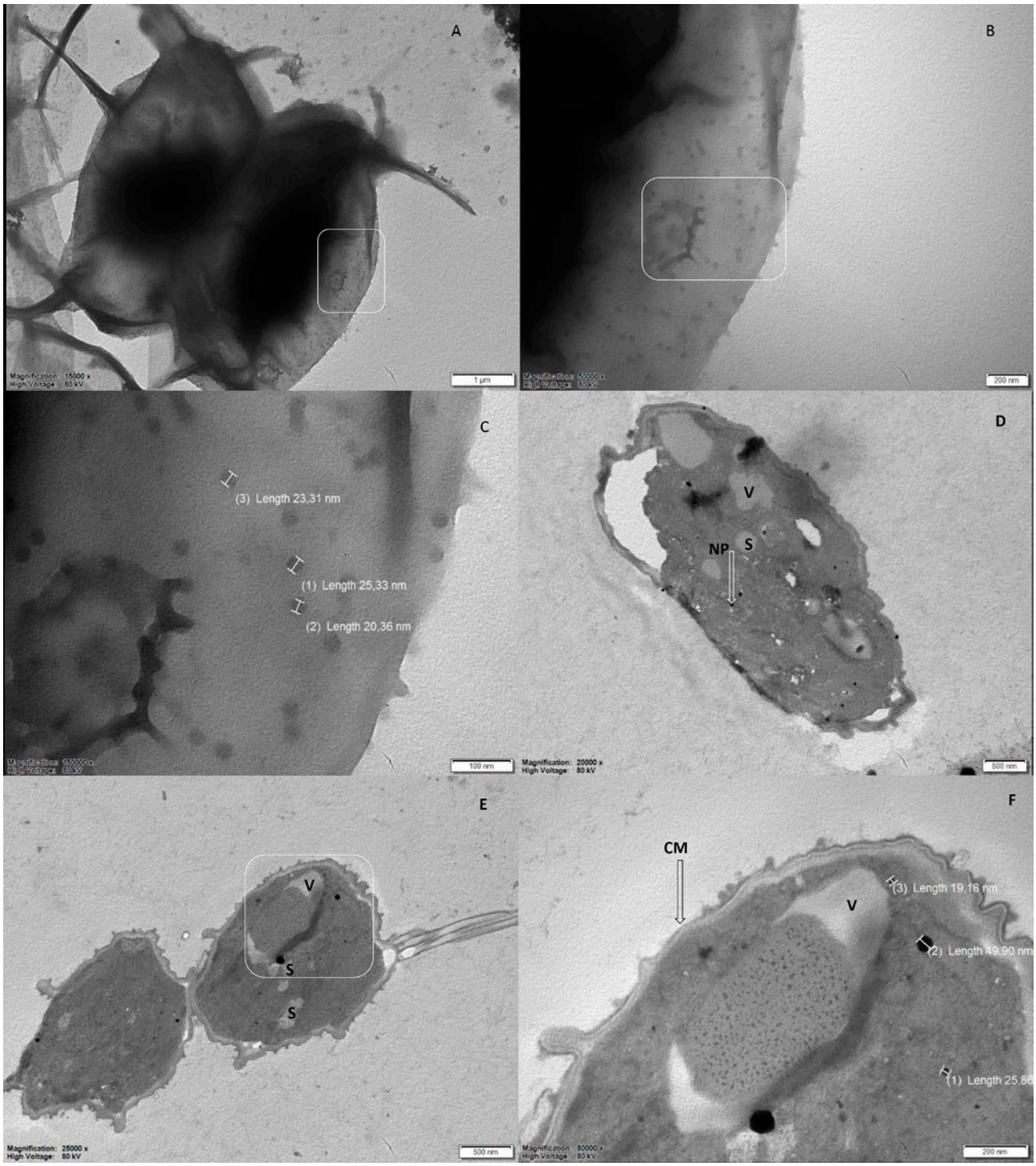

Fig. 2. Morphological characterization of the silver nanoparticles. A, B, C Intracellular synthesis, TEM Image of *Desmodesmus* sp. cell mediated synthesized silver nanoparticles. D, E, F Cellular localization of in Intracellular silver nanoparticles, TEM micrograph of thin section (~ 60 nm). NP:nanoparticle, S starch, V vakuol, CM Cytoplasmic membrane.

and dimensions of the NPs. TEM images revealed the cells were nearly 4.5-5 µm (length) × 2-3 µm (width) size with an oval shape and with 6-9 colonial protrusions (Figure 2A).

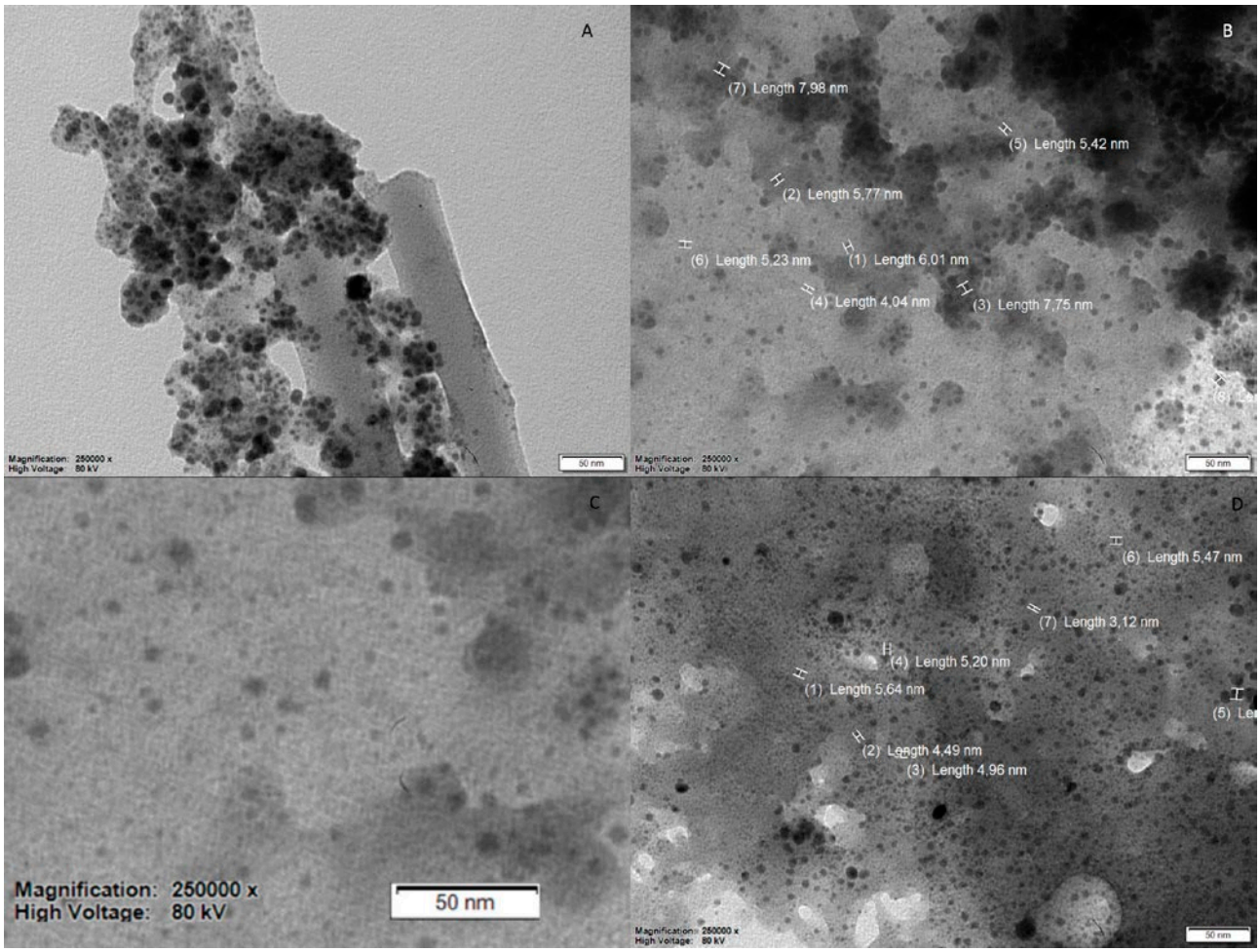

Fig. 3. TEM Image of extracellular synthesized silver nanoparticles A, B. *Desmodesmus* sp. cell RAE mediated synthesized silver nanoparticles (RAE-AgNPs); C, D. *Desmodesmus* sp. cell BAE mediated synthesized silver nanoparticles (BAE-AgNPs).

When the algae cells exposed to $AgNO_3$ were investigated with TEM on a grid with the dropping method, distributed metal NPs were observed, as shown in Figure 2 A, B and C. As seen at different magnifications of the metal nanoparticle shapes, the periphery of the cells is observed more clearly and homogeneously, while the interior sections were not fully identified due to a more compact and electron-dense zone observed (Figure 2 A, B). When micrographs of LAC-AgNPs at high magnifications are investigated, the spherical structures of the AgNPs are clearly observed. The intracellular LAC-AgNPs are in the range of 10-30 nm in size and appear to display a homogeneous distribution. In TEM analysis, a section of 60 nm in thickness was taken from the cells in order to be able to see the LAC-AgNPs. Additionally, sections were taken of these cells to identify where the NPs were localized (Figure 2 D, E, F). According to the results of these sections, NPs were localized especially in areas close to the cell membrane, while also in other regions of the cell, e.g., in areas close to starch storage areas (Figure 2 F).

The nanoparticle dimensions obtained after RAE-AgNPs were mean 4-8 nm (Figure 3 A, B). NPs synthesized in this manner were less stable according to both TEM and zeta potential results. When morphology and size of NPs are examined after extracellular synthesis, the NPs produced by BAE-AgNPs were mean 3-6 nm. These NPs had a homogeneous distribution without aggregation or flocculation (Figure 3 C, D). The reason for this is that some stabilizing agents in the algal extract were released by boiling and entered the reaction (Mohseniazar et al. 2011; Nithya and Ragunathan, 2009). At the same time, control of dimension and structure may be associated with interactions between biocomponents like polysaccharides, proteins, polyphenols and phenolic compounds with metal atoms (Shao et

Table 2. EDS reported from biosynthesized AgNPs.

AgNPs	Intensity (c/s)	Error 2-sig	Conc.	Units
Control	0.060	0.129	0.023	wt.%
LAC-AgNPs	130.34	7.217	34.385	wt.%
RAE- AgNPs	130.01	7.209	20.975	wt.%
BAE- AgNPs	293.68	10.837	54.920	wt.%

*kV 20.0, Takeoff Angle 35.0°.
Elapsed Livetime 10.0.
Conc: Concentration.

al. 2004). As a result, BAE-AgNPs showed the NPs had equal distribution.

Analysis through Energy dispersive SEM-EDS spectrometers confirmed the presence of an elemental Ag signal of the Ag NPs. Recognition lines for the major emission energies for Ag are displayed and these match with peaks in the spectrum, thus giving confidence that Ag has been correctly identified. In this study, the synthesized AgNPs were subjected to elemental analysis with SEM-EDS, the Ag element was observed in all three situations (LAC-AgNPs, BAE-AgNPs, RAE-AgNPs) at the rate (Table 2) (Figure 4 A, B, C). The highest Ag was identified in the BAE-AgNPs groups (Figure 4 B). When these results are considered, they provide information about the purity of the formed NPs.

Extracts obtained with different methods (BAE and RAE) and live cell algae (LAC) the AgNPs obtained from these extracts (LAC-AgNPs, RAE-AgNPs and BAE-AgNPs) had FTIR analysis completed on these samples to define the functional groups of chemical components. The analysis results observed many peaks (transmittance a.u) at 3284, 2919, 2851, 2161, 2027, 2034, 1638, 1535, 1380, 1242, 1149, 1023, 812, 717, and 551.

When vibrations of biomass exposed to Ag are investigated, the dense broadband at 3400 cm^{-1} is vibrations from alcoholic, phenolic and carboxylic groups (Figure 1 F). Primarily in addition to hydroxyl groups equivalent to O-H strain, vibrations equivalent to primary and secondary amines and amides are shown with N-H strain were observed. The band at nearly 2920 cm^{-1} reflects the C-H strain of alkanes. The lack of absorption in this region shows hydrogen linked to aliphatic carbon is not present (Rónavári et al. 2017). The band at 2851 cm^{-1} from the aldehyde group reflects C-H strain. The band at 2161 cm^{-1} is -S-CΞN thiocyanate, while the bands at 2027 and 2034 cm^{-1} are -N=C=S isothiocyanate. This situation shows that cyanate, elemental carbon and thiocyanate may be found within total organic carbon. The peak at nearly 1,638 cm^{-1} is equivalent to C = C vibration of aromatic structures, with the peak at 1242 cm^{-1} equivalent to C-O strain of phenolic groups. The peak at 1380 cm^{-1} is NO_2 asymmetric strain of

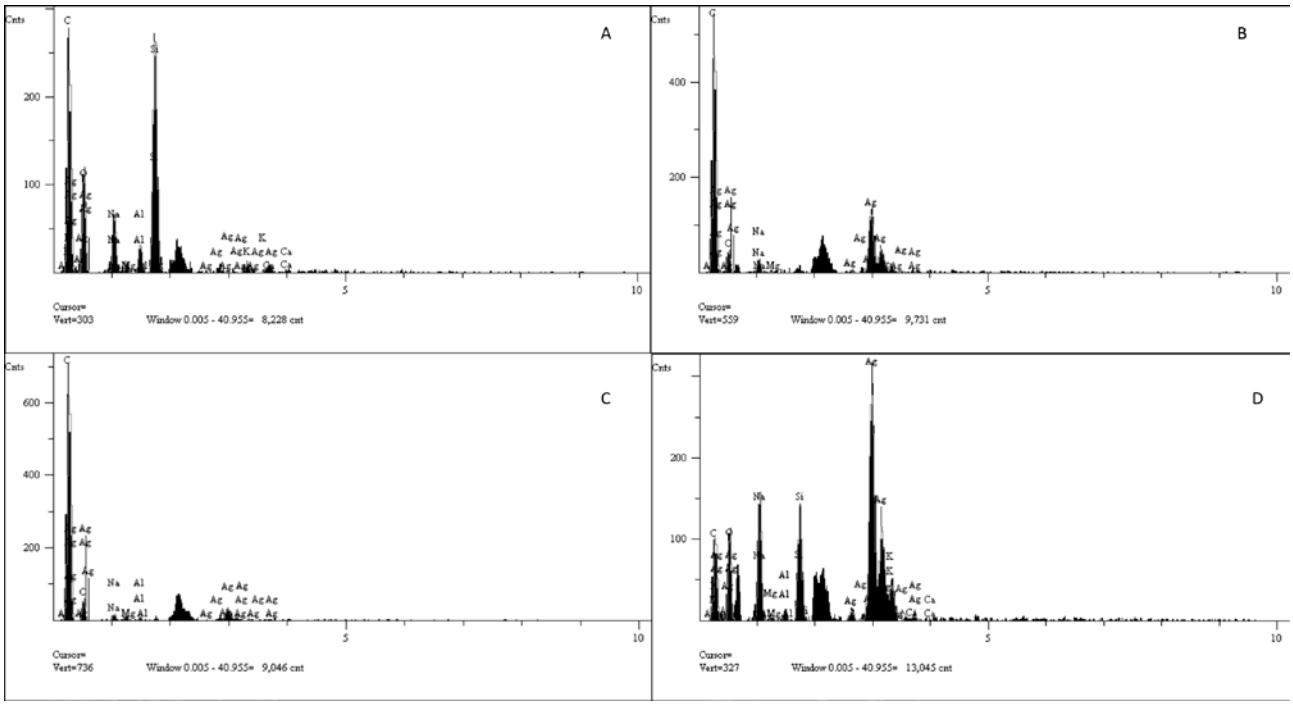

Fig. 4. SEM-EDS spectrum recorded from biosynthesized AgNPs A. Control group; B. LAC-AgNPs; C. RAE-AgNPs; D. BAE-AgNPs.

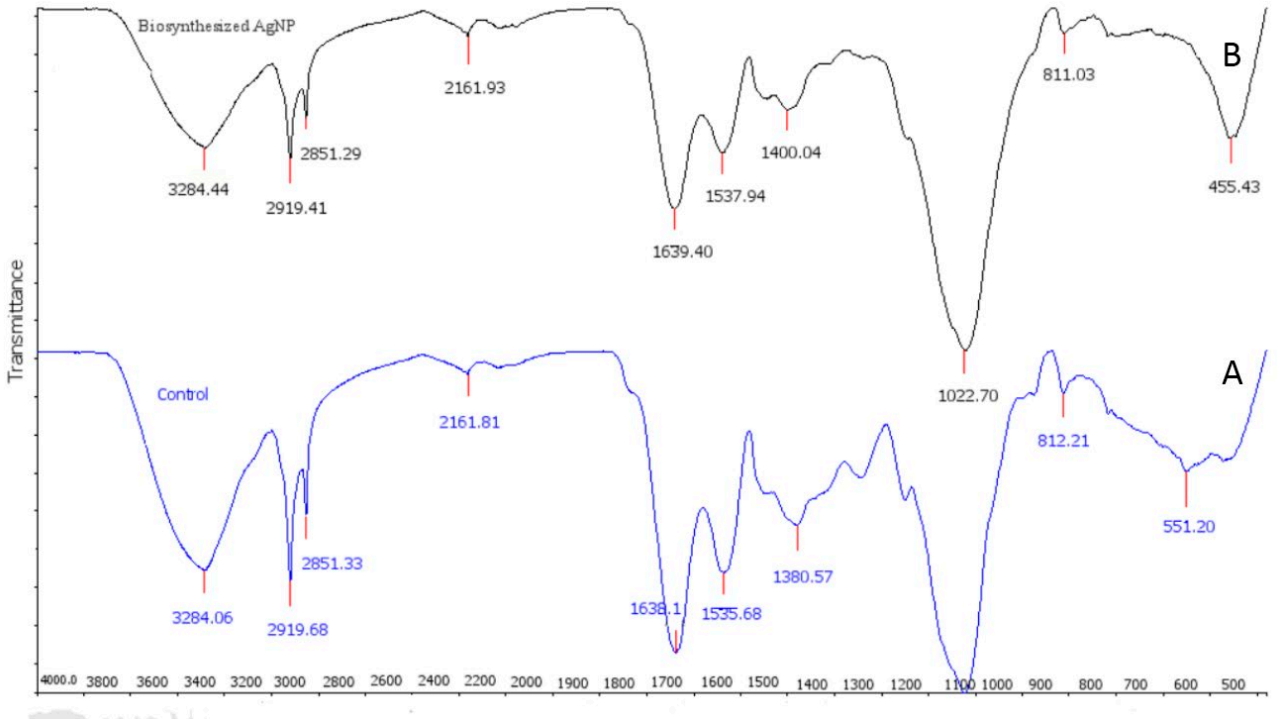

Fig. 5. FT-IR spectrum for A. *Desmodesmus* sp. control group; B. *Desmodesmus* sp. formed LAC-AgNPs.

alkyl groups, and the peak at 1535 cm^{-1} is equivalent to C = C strain of biphenol group. Around 1145 cm^{-1} the C-N strain vibration of aromatic primary and secondary amines is observed. Aromacity may be mentioned between 900-690 cm^{-1} (Jena et al. 2014).

The extracellular BAE-AgNPs obtained with the boiling method may have bonded to amine groups, while the RAE-AgNPs may have bonded to alkyne groups. Our FTIR results comply well with the literature data, with the surface of AgNPs obtained from intracellular *Desmodesmus* sp. coated with organic components found in the extract, as shown in Figure 3 B. As a result, successful green synthesis is revealed with the soluble organic components or proteins able to bind to Ag ions and reduce Ag ions to form NPs (Jegadeeswaran et al. 2012) (see 800-2919 cm^{-1} region).

Particle size and zeta potential are very important parameters for green synthesized Ag NPs. The particle size of Ag NPs, especially, has a large effect on the antimicrobial properties. Another important value for particle size is PDI. PDI reveals homogeneity (Sharma et al. 2018). Both intracellular and extracellular AgNPs were well distributed in colloidal solution and the mean size distribution of these particles were as follows; the mean particle distribution for LAC-AgNPs were 10-30 nm, with this value 4-8 nm and 3-6 nm from RAE-AgNPs and BAE-AgNPs (Figure 6 A, C, E). According to PDI values for the results, homogeneous particle size distribution within the solution was observed to be highest for LAC-AgNPs. Though different sizes were found during synthesis, higher numbers of small-scale NPs were observed in terms of numbers (Table 3).

Zeta potential values are obtained from the high repulsion and attraction forces between each nanoparticle and these values define particle stability. Intracellular and extracellular AgNPs have high negative zeta potential values. The high negative value affects the push between the particles, thereby increasing the stability of the formulation (Rao et al. 2013). In our study, the zeta potential of AgNPs were measured as -20.2 mV for LAC-AgNPs (Figure 6 B), -19.9 mV for BAE-AgNPs (Figure 6 D) and -14.2 mV for RAE-AgNPs (Figure 6 F). All values for particle sizes, PDI and zeta potentials are shown in

Table 3. The particle size of silver nanoparticles, polydispersity index and Zeta potential.

	Particle size (nm) DLS	PDI	Zeta potential (mV)
LAC-AgNPs	20-40	0.445	-20.2
BAE-AgNPs	10-15	0.452	-19.9
RAE-AgNPs	10-20	0.613	-14.2

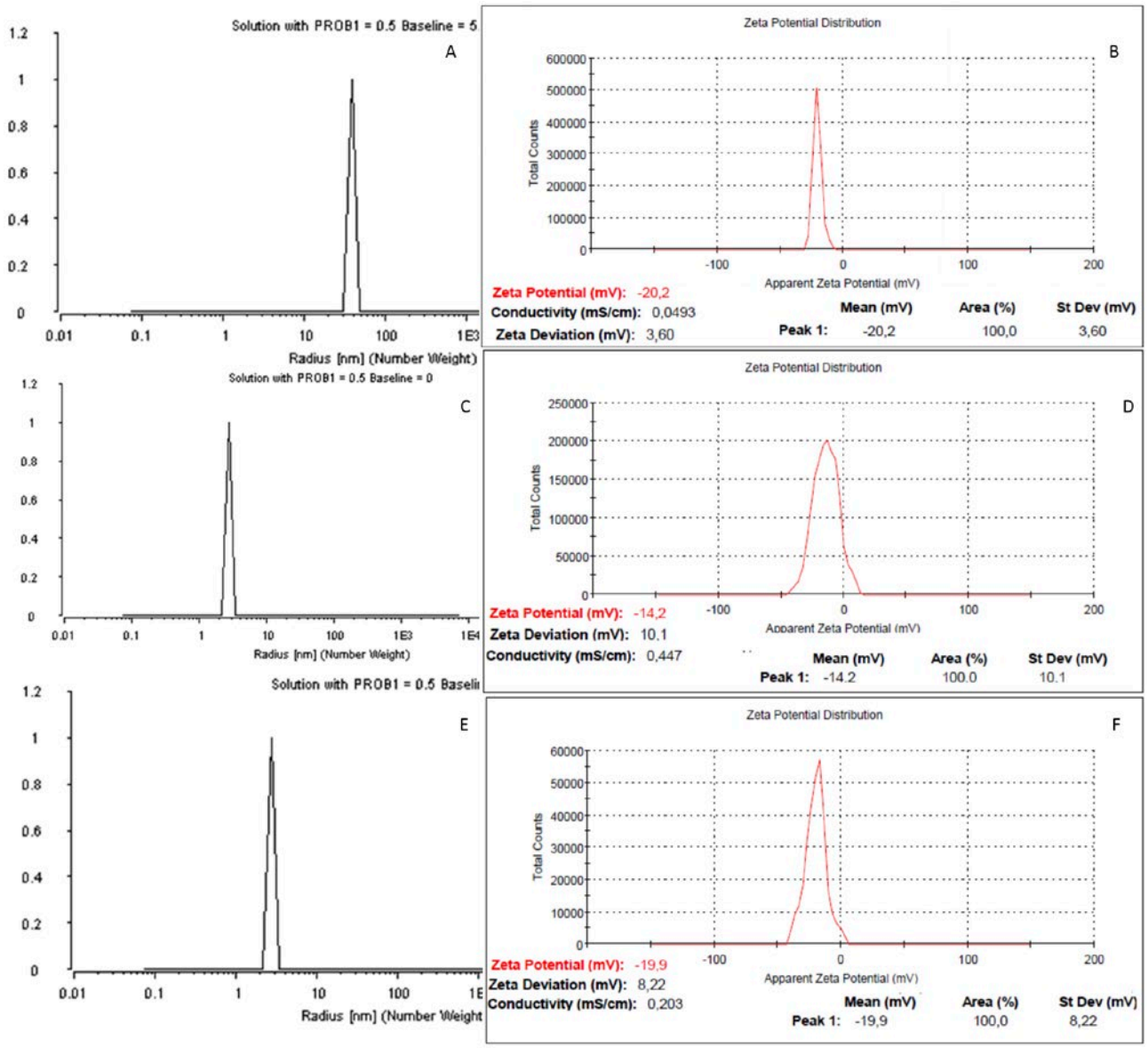

Fig. 6. Size distribution by dynamic light scattering and zeta potential measurement of biyosenthesis silver nanoparticles A, B. LAC-AgNPs; C, D. RAE-AgNPs; E, F. BAE-AgNPs.

Table 3. The observed result contains some differences compared with the TEM studies but is well-correlated. The differences may be due to the tendency of Ag NPs to agglomerate within an aqueous solution; thus the values obtained from DLS will be higher than TEM values (Domingos et al. 2009).

Antimicrobial and antifungal effect of synthesis AgNPs

LAC-AgNPs, RAE-AgNPs and BAE-AgNPs have been tested on *Salmonella* sp. (gram +) and *Listeria monocytogenesis* (gram -), the most frequently encountered bacteria in food poisoning (Cantero et al. 2018; Ma et al. 2018). The MIC values of the synthesized NPs were calculated on these bacteria. It was initiated by adding 100 µl of synthesized NPs so that the MIC values could be found. The LAC-AgNPs, RAE-AgNPs and BAE-AgNPs inhibited 3,125 µl of *Salmonella* sp. Thus, this value was determined as the MIC value. There was a larger effect on *Listeria monocytogenesis* compared to *Salmonella* sp. with 1,5625 µl MIC value determined. *Candida parapsilosis* is a pathogenic yeast strain with

high biofilm formation capacity (Soldini et al. 2017). *Candida parapsilosis* appeared to be more affected compared to bacteria and the MIC value was determined as 0,78125 µl (The synthesized AgNPs were initially used in 100 µl). The LAC-AgNPs, BAE-AgNPs and RAE-AgNPs obtained from *Desmodesmus* sp. with different methods showed significant degree of effect with different MIC values for bacteria and yeast.

DISCUSSION

AgNP is used in a variety of applications like catalysis, biosensing, imaging and antibacterial activity. As result researchers in recent times have performed many studies to synthesize AgNP more economically and easily. Green synthesis is an alternative method developed to produce metal NPs using natural compounds or plant components. The most important advantages of these methods are the lack of toxic material involved in the chemical synthesis and the lack of high costs. In addition to green synthesis and sustainable synthetic methods can decrease environmental pollution to some extent (Khatami et al. 2018c) . Another significant advantage is that NPs may be synthesized in an easy and reliable manner using only live organisms (algae, bacteria, fungus and plant), without requiring reducing or stabilizing agents (Tippayawat et al. 2016; Khatami et al. 2018b). Microorganisms such as bacteria and algae have proven to be well suited for nanoparticle synthesis, where particle size and morphology must be stabilized by different methods in green synthesis (Metuku et al. 2014). Algae or plants or their extracts, many prokaryotic organisms and biocompatible macromolecules are very important for nanoparticle synthesis (Poulose et al. 2014). Algae are unique due to the lipids, minerals and some vitamin wealth contained in these organisms (Namvar et al. 2012; Zuercher et al. 2006). Additionally, polysaccharides, proteins, and polyphenols are known as functional food as a variety of bioactive material with some medical uses like in cancer, oxidative stress, inflammation, allergies, thrombosis and lipidemia (Mahdavi et al. 2013). As a result, hydroxyl, carboxyl and amino functional groups are found among this phytochemical material that is capable of acting in a single step as both effective metals reducing agents and as capping agents. Generally many natural essences in cell contents or released after extraction are biologically active compounds and may be responsible for the reduction of Ag ions and stabilization of the obtained NPs.

The carbonyl groups in proteins have strong binding ability against metal NPs and as a result, proteins may form a coating layer on the surface of AgNPs (Dhand et al, 2016; Vivek et al. 2012). This may prevent agglomeration and increase the stability of NPs synthesized in aqueous media. In our study, UV-Vis data from algal cells exposed to Ag nitrate support the view that of Ag^{+} ions were taken into cells within 24 hours and L-AgNPs formed (Peaked at 420 nm within 24 h.). As metal ions (Ag^{+}) are on the algal surface, they were identified to be held by electrostatic interaction between the functional groups with the negative load on the cell surface, and following this, the metal ions were reduced (Barwal et al. 2011). In this way, high intracellular accumulation and formation of metal particles may be linked to several probable mechanisms in the process. These mechanisms vary according to type and metal accumulation occurs with two processes. The first is adsorption or biosorption at the cell surface independent of metabolism, while the second is metabolism-dependent absorption by organelles or cytoplasmic ligands (Chakraborty et al. 2006).

Metal NPs synthesized with green methods may produce colloids with different sizes, shapes, and distributions. If changing the method used provides better results, the green approach may be chosen. As a result of our study, the focus was on the biosynthesis of both intracellular and extracellular AgNP using different extraction techniques with *Desmodesmus* sp. microalgae and AgNP production was successfully achieved. In this study during intracellular synthesis, algal cells have pores of 3-5 nm width ensuring passage of low molecular weight material like water, inorganic ions, gases and other small nutritional material required for growth and metabolism (Wang and Chen 2009). Large molecules or macromolecules cannot pass these pores. Similarly, in our study, the intracellular LAC-AgNPs appeared to be larger than the size of the pores in the algal cell walls (10-30 nm) (Figure 2 A, B, C). The BAE-AgNPs and RAE-AgNPs also had spherical shape without agglomeration. Sections through the cells transversely and longitudinally observed nanoparticle formation distributed through intracellular cytoplasm, with larger size NPs in some regions, e.g., in regions close to vacuoles. In previous research, it was reported that maximum metal accumulation occurred within the cytoplasm, periplasm, nucleus and pyrenoids of organisms like *Chlamydomonas* (Ag), *Chlorella* (Au, Pd, Ru, Rh), *Klebsormidium flaccidum* (Au) and *Shewanella* (Au, Pt) (Barwal et al. 2011; Dahoumane et al. 2012; Luangpipat et al. 2011).

FTIR can be used to identify the type of functional groups and biomolecules that are responsible for capping and efficient stabilization of NPs and qualitative and quantitative identification of the molecular structure

of organic compounds in the NPs structure (Khatami et al. 2018d). In thi study, the results of FTIR spectroscopic investigations showed the presence of organic particles especially in the 800-2919 cm^{-1} region. Linked to this result, the protein building block of amino acids was confirmed as having strong binding ability to metals and formed a layer surrounding metal NPs. They acted as a coating material preventing agglomeration and thus are considered to have ensured high stability of metal NPs. These results confirm the presence of proteins or peptides with possible function as stabilizing agents for AgNPs (Singhal et al. 2011).

The extracellular RAE-AgNPs synthesized was found to be less stable and have a tendency to agglomerate compared to extracellular synthesized BAE-AgNPs and intracellular synthesized L-AgNPs. Additionally, the RAE-AgNPs synthesis process was slower compared to the others. When BAE was used, both high rates of BAE-AgNPs biosynthesis occurred and the stability of these NPs were higher. However, according to the UV results, L-AgNPs were more rapid biosynthesised than extracellular BAE-AgNPs and RAE-AgNPs. This situation may be related to macromolecules like protein or peptide released by boiling directly reducing Ag^{+} ions. A study by Jena et al. (2014) produced similar results. The researchers explained that in this situation the protein or peptide concentration has a vital role in AgNP formation and stabilization. A similar study by Barwal et al. (2011) prepared *Chlamydomonas* cell extract treated with Ag nitrate with both whole cell esence and protein-removed extraction. When the results are compared, the protein-removed cell extraction was identified to synthesize larger sizes of AgNP. The researchers explained that the protein concentration is directly correlated with particle formation rate and inversely correlated with particle size (Barwal et al. 2011; Jena et al. 2014).

Due to a variety of reasons in the antimicrobial mechanism, Ag ions or salts only have limited use as an antimicrobial agent. However, the use of AgNPs may overcome these limitations. In biological systems (animal cell culture, plants, bacteria) the effect of AgNPs in different concentrations has been investigated (Sobieh et al. 2016, Khatami et al. 2018). For the use of Ag against microorganisms in a variety of areas, it is important to prepare Ag with appropriately priced methods and to know the antimicrobial effect mechanism to increase this effect (Kim et al. 2007). Green synthesized NPs may expand these areas of use significantly. In this study, AgNPs may be a potential antibacterial and antifungal agent and could be prepared cost-effectively. Because, *Desmodesmus* sp., a green algae, could be a low-cost production house for intracellular and extracellular AgNPs synthesis because of the minimum growth regimens required for growth, such as water, sunlight and commercial fertilizers, and high biomass efficiency.

CONCLUSION

In this study different sizes of AgNP were successfully synthesized from *Desmodesmus* sp. microalgae using both intracellular and extracellular green synthesis routes. In particular, intracellular UV results of LAC-AgNPs peaked at 420 nm within the first 24 hours. The purity of Ag NPs was confirmed with SEM-EDS. Nanoparticle size and stability were determined according to DLS and Zeta potential results. AgNPs with optimized size were determined to have lethal potential against bacteria and yeast. Thus this study is considered to support sustainable development of green synthesis using the green microalgae of *Desmodesmus* sp.

ACKNOWLEDGEMENTS

The author are thankful to Associate professor İlknur Dağ, Dr. Bükay Yenice Gürsu, Dr. Yeşim Dağlıoğlu and Phd Tayfun Şengel from Eskişehir Osmangazi University for their valuable discussions, advices, and shares on their expertise related to the subject.

REFERENCES

Annamalai J and Nallamuthu T. 2015. Characterization of biosynthesized gold nanoparticles from aqueous extract of *Chlorella vulgaris* and their anti-pathogenic properties. Applied Nanoscience, 5(5), 603-607. DOI 10.1007/s13204-014-0353-y

Barwal I, Ranjan P, Kateriya S, Yadav SC. 2011. Cellular oxido-reductive proteins of *Chlamydomonas reinhardtii* control the biosynthesis of silver nanoparticles. Journal of nanobiotechnology, 9(1), 56. DOI 10.1186/1477-3155-9-56

Boroumand Moghaddam A, Namvar F, Moniri M, Md Tahir P, Azizi S, Mohamad R. 2015. Nanoparticles biosynthesized by fungi and yeast: a review of their preparation, properties, and medical applications. Molecules, 20(9), 16540-16565. DOI 10.3390/molecules200916540

Cantero G, Correa-Fiz F, Ronco T, Strube M, Cerdà-Cuéllar M, Pedersen K. 2018. Characterization of Campylobacter jejuni and Campylobacter coli Broiler

Isolates by Whole-Genome Sequencing. Foodborne pathogens and disease, 15(3), 145-152. DOI 10.1089/fpd.2017.2325

Chakraborty N, Pal R, Ramaswami A, Nayak D, Lahiri S. 2006. Diatom: a potential bio-accumulator of gold. Journal of radioanalytical and nuclear chemistry, 270(3), 645-649. DOI 10.1007/s10967-006-0475-0

Dağlıoğlu Y, Çelebi SM, Önalan Ş. 2016. Determination of acute toxic effects of poly (Vinylferrocenium) supported palladium nanoparticle (Pd/PVF+) on *Artemia salina*. Pakistan Journal of Zoology, 48(1), 187–193.

Dağlıoğlu Y, Kabakcı D, Akdeniz G, Çelebi MS. 2016. Determining the acute toxic effects of poly(vinylferrocenium) supported platinum nanoparticle (PT/PVF+ NPs) on *Apis mellifera*.

Dağlıoğlu Y, Öztürk BY. 2016. The assessment of biological accumulation on exposure in boron particles of *Desmodesmus multivariabilis*. Biological Diversity and Conservation. 9(3), 204-209.

Dağlıoğlu Y, Öztürk BY. 2018. Effect of concentration and exposure time of ZnO-TiO_2 nanocomposite on photosynthetic pigment contents, ROS production ability, and bioaccumulation of freshwater algae (*Desmodesmus multivariabilis*). Caryologia, 71(1), 13-23, DOI 10.1080/00087114.2017.1400262

Dağlıoğlu Y, Türkiş S. 2017. Effect of nano and microparticle boron on hydrogen peroxide (H_2O_2) and lipid peroxidation (MDA) enzyme activity superoxide dismutase (SOD) of *Myriophyllum spicatum*. 6(2), 62-70.

Dağlıoğlu Y, Türkiş S. 2017. Effect of TiO_2 nanoparticles application on photosynthetic pigment contents of duckweed (*Lemna minor* L.). Acta Biologica Turcica, 30(4), 108-115.

Dahoumane SA, Djediat C, Yéprémian C, Couté A, Fiévet F, Coradin T, Brayner R. 2012. Recycling and adaptation of Klebsormidium flaccidum microalgae for the sustained production of gold nanoparticles. Biotechnology and bioengineering, 109(1), 284-288. DOI doi.org/10.1002/bit.23276

Dhand V, Soumya L, Bharadwaj S, Chakra S, Bhatt D, Sreedhar B. 2016. Green synthesis of silver nanoparticles using Coffea arabica seed extract and its antibacterial activity. Materials Science and Engineering: C, 58, 36-43. DOI 10.1016/j.msec.2015.08.018

Domingos RF, Baalousha MA, Ju-Nam Y, Reid MM, Tufenkji N, Lead JR, Wilkinson, KJ. 2009. Characterizing manufactured nanoparticles in the environment: multimethod determination of particle sizes. Environmental science & technology, 43(19), 7277-7284. DOI 10.1021/es900249m

Faulkner DJ. 2000. Marine natural products. Natural Product Reports, 17(1), 7-55.

Ge L, Li Q, Wang M, Ouyang J, Li X, Xing MM. 2014. Nanosilver particles in medical applications: synthesis, performance, and toxicity. International journal of nanomedicine, 9, 2399. DOI 10.2147/IJN.S55015

Govindaraju K, Kiruthiga V, Kumar VG, Singaravelu G. 2009. Extracellular synthesis of silver nanoparticles by a marine alga, *Sargassum wightii* Grevilli and their antibacterial effects. Journal of Nanoscience and Nanotechnology, 9(9), 5497-5501. DOI 10.1166/jnn.2009.1199

Hiramatsu H, Osterloh FE. 2004. A simple large-scale synthesis of nearly monodisperse gold and silver nanoparticles with adjustable sizes and with exchangeable surfactants. Chemistry of Materials, 16(13), 2509-2511. DOI 10.1021/cm049532v

Ilknur D, Yasemin O, Nuri K. 2012. Effect of disinfectants on biofilm development by five species of Candida. African Journal of Microbiology Research, 6(10), 2380-2386. DOI 10.5897/AJMR11.1427

Jegadeeswaran P, Shivaraj R, Venckatesh R. 2012. Green synthesis of silver nanoparticles from extract of *Padina tetrastromatica* leaf. Digest Journal of Nanomaterials and Biostructures, 7(3), 991-998.

Jena J, Pradhan N, Nayak RR, Dash BP, Sukla LB, Panda PK, Mishra BK. 2014. Microalga *Scenedesmus* sp.: a potential low-cost green machine for silver nanoparticle synthesis. Journal of Microbiology and Biotechnology, 24(4), 522-533. DOI 10.4014/jmb.1306.06014

Joerger R, Klaus T, Granqvist CG. 2000. Biologically Produced Silver–Carbon Composite Materials for Optically Functional Thin-Film Coatings. Advanced Materials, 12(6), 407-409. DOI 10.1002/(SICI)1521-4095(200003)12:6<407::AID-ADMA407>3.0.CO;2-O

Kannan RRR, Arumugam R, Ramya D, Manivannan K, Anantharaman P. 2013. Green synthesis of silver nanoparticles using marine macroalga *Chaetomorpha linum*. Applied Nanoscience, 3(3), 229-233. DOI 10.1007/s13204-012-0125-5

Khatami M, Alijani HQ, Heli H, Sharifi I. 2018a. Rectangular shaped zinc oxide nanoparticles: Green synthesis by Stevia and its biomedical efficiency. Ceramics International. DOI 10.1016/j.ceramint.2018.05.224

Khatami M, Sharifi I, Nobre MA, Zafarnia N, Aflatoonian MR. 2018b. Waste-grass-mediated green synthesis of silver nanoparticles and evaluation of their anticancer, antifungal and antibacterial activity. Green Chemistry Letters and Reviews, 11(2), 125-134. DOI 10.1080/17518253.2018.1444797

Khatami M, Alijani HQ, Nejad MS, Varma RS. 2018c. Core@ shell nanoparticles: greener synthesis using

natural plant products. Applied Sciences, 8(3), 411. DOI 10.3390/app8030411

Khatami M, Alijani H, Sharifi I. 2018d. Biosynthesis of bimetallic and core shell nanoparticles: their biomedical applications: A review. IET Nanobio, 1-19. DOI 10.1049/iet-nbt.2017.0308

Khatami M, Varma RS, Zafarnia N, Yaghoobi H, Sarani M, Kumar VG. 2018. Applications of green synthesized Ag, ZnO and Ag/ZnO nanoparticles for making clinical antimicrobial wound-healing bandages. Sustainable Chemistry and Pharmacy, 10, 9-15. DOI 10.1016/j.scp.2018.08.001

Kim JS, Kuk E, Yu KN, Kim JH, Park SJ, Lee HJ, Jeong, DHo, Hwang CY. 2007. Antimicrobial effects of silver nanoparticles. Nanomedicine: Nanotechnology, Biology and Medicine, 3(1), 95-101. DOI 10.1016/j.nano.2006.12.001

Kothari R, Pandey A, Ahmad S, Kumar A, Pathak VV, Tyagi V. 2017. Microalgal cultivation for value-added products: a critical enviro-economical assessment. 3 Biotech, 7(4), 243. DOI10.1007/s13205-017-0812-8

Kozma G, Rónavári A, Kónya Z, Kukovecz A. 2015. Environmentally benign synthesis methods of zerovalent iron nanoparticles. ACS Sustainable Chemistry & Engineering, 4(1), 291-297. DOI 10.1021/acssuschemeng.5b01185

Li L, Shi C, Yin Z, Jia R, Peng L, Kang S, Li Z. 2014. Antibacterial activity of α-terpineol may induce morphostructural alterations in *Escherichia coli*. Brazilian Journal of Microbiology, 45(4), 1409-1413. DOI 10.1590/S1517-83822014000400035

Luangpipat T, Beattie IR, Chisti Y, Haverkamp RG. 2011. Gold nanoparticles produced in a microalga. Journal of Nanoparticle Research, 13(12), 6439-6445. DOI doi.org/10.1007/s11051-011-0397-9

Ma X, Xu X, Xia Y, Wang Z. 2018. SERS aptasensor for *Salmonella typhimurium* detection based on spiny gold nanoparticles. Food Control, 84, 232-237. DOI 10.1016/j.foodcont.2017.07.016

Mahdavi M, Namvar F, Ahmad MB, Mohamad R. 2013. Green biosynthesis and characterization of magnetic iron oxide (Fe3O4) nanoparticles using seaweed (*Sargassum muticum*) aqueous extract. Molecules, 18(5), 5954-5964. DOI 10.3390/molecules18055954

Metuku RP, Pabba S, Burra S, Gudikandula K, Charya MS. 2014. Biosynthesis of silver nanoparticles from *Schizophyllum radiatum* HE 863742.1: their characterization and antimicrobial activity. 3 Biotech, 4(3), 227-234. DOI 10.1007/s13205-013-0138-0

Mohseniazar M, Barin M, Zarredar H, Alizadeh S, Shanehbandi D. 2011. Potential of microalgae and Lactobacilli in biosynthesis of silver nanoparticles. BioImpacts: BI, 1(3), 149. DOI 10.5681/bi.2011.020

Namvar F, Mohamed S, Fard SG, Behravan J, Mustapha NM, Alitheen NBM, Othman F. 2012. Polyphenol-rich seaweed (*Eucheuma cottonii*) extract suppresses breast tumour via hormone modulation and apoptosis induction. Food chemistry, 130(2), 376-382. DOI 10.1016/j.foodchem.2011.07.054

Nithya R, Ragunathan R. 2009. Synthesis of silver nanoparticle using Pleurotus sajor caju and its antimicrobial study. Digest Journal of Nanomaterials and Biostructures, 4(4), 623-629.

Özkan Y, İrende İ, Akdeniz G, Kabakçı D, Sökmen M. 2015. Evaluation of the comparative acute toxic effects of TiO_2, Ag-TiO_2 and ZnO-TiO_2 composite nanoparticles on *Apis mellifera* (Honey Bee). J. Int. Environmental Application & Science, 10 (1), 26–36.

Öztürk BY, Dağlıoğlu Y. 2018. ZnO-TiO2 nanocomposite in *Chodatodesmus mucranulatus*. Fresenius Environmental Bulletin, 27(5), 2951-2962.

Poulose S, Panda T, Nair PP, Theodore T. 2014. Biosynthesis of silver nanoparticles. Journal of Nanoscience and Nanotechnology, 14(2), 2038-2049. DOI 10.1166/jnn.2014.9019

Pradeep T. 2009. Noble metal nanoparticles for water purification: a critical review. Thin solid films, 517(24), 6441-6478. DOI 10.1016/j.tsf.2009.03.195

Prasad TN, Kambala VSR, Naidu R. 2013. Phyconanotechnology: synthesis of silver nanoparticles using brown marine algae Cystophora moniliformis and their characterisation. Journal of applied phycology, 25(1), 177-182. DOI 10.1007/s10811-012-9851-z

Rajeshkumar S, Malarkodi C, Paulkumar K, Vanaja M, Gnanajobitha G, Annadurai G. 2014. Algae mediated green fabrication of silver nanoparticles and examination of its antifungal activity against clinical pathogens. International Journal of Metals, 2014. DOI 10.1155/2014/692643

Rao YS, Kotakadi VS, Prasad T, Reddy A, Gopal DS. 2013. Green synthesis and spectral characterization of silver nanoparticles from Lakshmi tulasi (*Ocimum sanctum*) leaf extract. Spectrochimica Acta Part A: Molecular and Biomolecular Spectroscopy, 103, 156-159. DOI 10.1016/j.saa.2012.11.028

Rippka R. 1988. [1] Isolation and purification of cyanobacteria. In Methods in Enzymology, Academic Press, 167, 3-27. DOI 10.1016/0076-6879(88)67004-2

Rónavári A, Kovács D, Igaz N, Vágvölgyi C, Boros IM, Kónya Z, Pfeiffer I, Kiricsi M. 2017. Biological activity of green-synthesized silver nanoparticles depends on the applied natural extracts: a comprehensive study. International journal of nanomedicine, 12, 871. DOI 10.2147/IJN.S122842

Salari Z, Danafar F, Dabaghi S, Ataei SA. 2016. Sustainable synthesis of silver nanoparticles using macroalgae *Spirogyra varians* and analysis of their antibacterial activity. Journal of Saudi Chemical Society, 20(4), 459-464. DOI 10.1016/j.jscs.2014.10.004

Shao Y, Jin Y, Dong S. 2004. Synthesis of gold nanoplates by aspartate reduction of gold chloride. Chemical Communications (9), 1104-1105. DOI 10.1039/B315732F

Sharma P, Pant S, Rai S, Yadav RB, Sharma S, Dave V. 2018. Green synthesis and characterization of silver nanoparticles by *Allium cepa* L. to produce silver nano-coated fabric and their antimicrobial evaluation. Applied Organometallic Chemistry, 32(3). DOI 10.1002/aoc.4146

Sharma VK, Yngard RA, Lin Y. 2009. Silver nanoparticles: green synthesis and their antimicrobial activities. Advances in colloid and interface science, 145(1), 83-96. DOI 10.1016/j.cis.2008.09.002

Singh CR, Kathiresan K, Anandhan S. 2015. A review on marine based nanoparticles and their potential applications. African Journal of Biotechnology, 14(18), 1525-1532. DOI 10.5897/AJB2015.14527

Singhal G, Bhavesh R, Kasariya K, Sharma AR, Singh RP. 2011. Biosynthesis of silver nanoparticles using *Ocimum sanctum* (Tulsi) leaf extract and screening its antimicrobial activity. Journal of Nanoparticle Research, 13(7), 2981-2988. DOI 10.1007/s11051-010-0193-y

Sobieh SS, Kheiralla ZMH, Rushdy AA, Yakob NAN. 2016. In vitro and in vivo genotoxicity and molecular response of silver nanoparticles on different biological model systems. Caryologia, 69(2), 147-161. DOI 10.1080/00087114.2016.1139416

Soldini S, Posteraro B, Vella A, De Carolis E, Borghi E, Falleni M, Losito AR, Maiuro G, Trecarichi EM, Sanguinetti, M, Tumbarello M. (2017). Microbiologic and clinical characteristics of biofilm-forming *Candida parapsilosis* isolates associated with fungaemia and their impact on mortality. Clinical Microbiology and Infection. DOI 10.1016/j.cmi.2017.11.005

Sondi I, Siiman O, Koester S, Matijević E. 2000. Preparation of aminodextran– CdS nanoparticle complexes and biologically active antibody– aminodextran–CdS nanoparticle conjugates. Langmuir, 16(7), 3107-3118. DOI 10.1021/la991109r

Suriya J, Raja SB, Sekar V, Rajasekaran R. 2012. Biosynthesis of silver nanoparticles and its antibacterial activity using seaweed *Urospora* sp. African Journal of Biotechnology, 11(58), 12192-12198. DOI 10.5897/AJB12.452

Tippayawat P, Phromviyo N, Boueroy P, Chompoosor A. 2016. Green synthesis of silver nanoparticles in *Aloe vera* plant extract prepared by a hydrothermal method and their synergistic antibacterial activity. PeerJ, 4, e2589. DOI 10.7717/peerj.2589

Travan A, Pelillo C, Donati I, Marsich E, Benincasa M, Scarpa T, Semeraro S, Turco G, Gennaro R, Paoletti, S. 2009. Non-cytotoxic silver nanoparticle-polysaccharide nanocomposites with antimicrobial activity. Biomacromolecules, 10(6), 1429-1435. DOI 10.1021/bm900039x

Vigneshwaran N, Nachane R, Balasubramanya R, Varadarajan P. 2006. A novel one-pot 'green'synthesis of stable silver nanoparticles using soluble starch. Carbohydrate research, 341(12), 2012-2018. DOI 10.1016/j.carres.2006.04.042

Vivek R, Thangam R, Muthuchelian K, Gunasekaran P, Kaveri K, Kannan S. 2012. Green biosynthesis of silver nanoparticles from *Annona squamosa* leaf extract and its in vitro cytotoxic effect on MCF-7 cells. Process Biochemistry, 47(12), 2405-2410. DOI 10.1016/j.procbio.2012.09.025

Wang J, Chen C. 2009. Biosorbents for heavy metals removal and their future. Biotechnology advances, 27(2), 195-226. DOI 10.1016/j.biotechadv.2008.11.002

Zgoda J, Porter J. 2001. A convenient microdilution method for screening natural products against bacteria and fungi. Pharmaceutical Biology, 39(3), 221-225. DOI 10.1076/phbi.39.3.221.5934

Zhang Y, Liu X, Wang Y, Jiang P, Quek S. 2016. Antibacterial activity and mechanism of cinnamon essential oil against *Escherichia coli* and *Staphylococcus aureus*. Food Control, 59, 282-289. DOI 10.1016/j.foodcont.2015.05.032

Zuercher AW, Fritsche R, Corthésy B, Mercenier A. 2006. Food products and allergy development, prevention and treatment. Current opinion in biotechnology, 17(2), 198-203. DOI 10.1016/j.copbio.2006.01.010

Caryologia
International Journal of Cytology, Cytosystematics and Cytogenetics

Firenze University Press
www.fupress.com/caryologia

OPEN ACCESS

Citation: İ. Genç, M. Firat (2019) Karyological study of the genus *Gundelia* (Compositae) in Turkey. *Caryologia* 72(1): 45-53. doi: 10.13128/cayologia-250

Received: 13th june 2018

Accepted: 4th December 2018

Published: 10th May 2019

Data Availability Statement: All relevant data are within the paper and its Supporting Information files.

Competing Interests: The Author(s) declare(s) no conflict of interest.

Karyological study of the genus *Gundelia* (Compositae) in Turkey

İlker Genç[1,*], Mehmet Firat[2]

[1] *Department of Pharmaceutical Botany, Faculty of Pharmacy, İstanbul University, İstanbul, Turkey*
[2] *Department of Biology Education, Faculty of Education, Van Yüzüncü Yıl University, Van, Turkey*
* Corresponding author: gencilker1@gmail.com

Abstract. Karyotypes in 12 taxa of *Gundelia* are compared, based on Feulgen-stained somatic metaphase chromosomes. The karyotypes of *G. anatolica*, *G. asperrima*, *G. cilicica*, *G. colemerikensis*, *G. dersim*, *G. glabra*, *G. komagenensis*, *G. mesopotamica*, *G. munzuriensis* and *G. vitekii* are described for the first time. Karyological analyses indicate relationships among the species with respect to their asymmetry indices. All *Gundelia* species studied were diploid with $2n = 2x = 18$ chromosomes. All karyotypes are symmetrical, consisting of metacentric and submetacentric chromosomes. The submetacentric chromosomes of all the investigated specimens contain a secondary constriction. Three chromosome types were identified according to the position of the secondary constrictions. The chromosomes ranged in size from 2.00 µm to 7.02 µm. The total haploid chromosome length (THL) varied from 24.97 µm (*G. asperrima*) to 42.56 µm (*G. rosea*). To determine the karyological relationships among taxa, PCoA (Principal Coordinate Analysis) with six uncorrelated parameters was performed.

Keywords. Chromosome number, karyotype asymmetry, secondary constriction, *Cichorieae, Scolyminae.*

INTRODUCTION

Gundelia L. was first recorded in one of the earliest natural history collections made in the Near East by the German physician, botanist and traveller, Leonhard Rauwolf (1535–1596) at 16. century. However, the plant was first evaluated in *Silybum* then *Eryngium* groups. About 125 years later, in the early years of the 18th century, Joseph Pitton de Tournefort saw the plant in the natural habitat. Moreover, he concluded that the plant should be called *Gundelia* (Hind 2013). Finally, the plant was named *Gundelia tourneforti* by Linnaeus, in accordance with the binomial nomenclature (Linnaeus 1753).

The infrafamilial position of *Gundelia* has also changed over time (Hind 2013). The last tribal position of genus *Gundelia* was *Cichorieae* Lam. & DC., subtribe *Scolyminae* Less., along with *Catananche* L., *Hymenonema* Cass., and *Scolymus* L. (Kilian et al. 2009). The genus grows in the semi-desert areas, and it is distributed in the Mediterranean to Central/Eastern Asia (Karis et al. 2001).

Some different species and varieties have been described over the years, although many authors have treated *Gundelia* as monospecific and the wide variation in corolla colour was considered unrelated to gross morphology (Komarov 1961; Kupicha 1975; Feinbrun Dothan 1978; Meikle 1985; Rechinger 1989). However, in the last decades, researches on *Gundelia* increased. Numerous new species have been published as a result of research on live and more abundant materials. The genus is currently represented by 16 species, of which 12 (10 endemic) in Turkey (Vitek et al. 2010, 2014, 2017; Nersesyan 2014; Armağan 2016; Fırat 2016, 2017a, 2017b, 2017c; Vitek and Noroozii 2017; Vitek 2018). These are *Gundelia anatolica* Fırat, *G. asperrima* (Trautv.) Fırat, *G. cilicica* Fırat, *G. colemerikensis* Fırat, *G. dersim* Vitek, Yüce & Ergin, *G. glabra* Mill., *G. komagenensis* Fırat, *G. mesopotamica* Fırat, *G. munzuriensis* Vitek, Yüce & Ergin, *G. rosea* M.Hossain & Al-Taey (non-endemic), *G. tournefortii* L. (non-endemic), and *G. vitekii* Armağan.

The chromosome numbers of *Cichorieae* range between $2n = 14x = 126$ chromosomes in *Sonchus* (Beuzenberg and Hair 1984; Dawson 2000) and $2n = 2x = 6$ in some species of *Crepis* (Ikeda 1988; Gupta and Gill 1989; Dimitrova and Greilhuber 2001). The basic chromosome number in the majority of the subtribes is $x = 9$, or a descending series starting with $x = 9$ to $x = 3$. Subtribe *Scolyminae* has the basic chromosome numbers $x = 9$ and 10 (Kilian et al. 2009). The only chromosome number *Gundelia* is $2n = 18$ (Waisel 1962; Al-Taey and Hossain 1984; Ghaffari and Chariat-Panahi 1985; Nersesyan and Nazarova. 1989; Ghukasyan and Janjughazyan 2015).

Fig. 1. Synflorescences of the studied taxa. (a) *G. anatolica*; (b) *G. asperrima*; (c) *G. cilicica*; (d) *G. colemerikensis*; (e) *G. dersim*; (f) *G. glabra*; (g) *G. komagenensis*; (h) *G. mesopotamica*; (i) *G. munzuriensis*; (j) *G. rosea*; (k) *G. tournefortii*; (l) *G. vitekii*.

This study aimed to determine the chromosome numbers and karyomorphology of al the 12 *Gundelia* species occurring in Turkey (Figure 1).

MATERIALS AND METHODS

Twelve *Gundelia* species were analysed in this study. A list of examined specimens is provided in Table 1. All endemic taxa were collected from their type localities. Voucher specimens were deposited in the Herbarium of University of Van Yüzüncü Yıl (VANF) and in a private herbarium (Herb. M. Fırat). For karyological observations, four to eight individuals were used for each species in this study. Mitotic metaphase cells of root tips were obtained from germinated seeds which were collected in natural habitats from Turkey.

Mitotic chromosomes were prepared from root tips and pre-treated with 0.002 M 8-Hydroxyquinoline at +4 °C for 24 h. Roots were fixed for a minimum of 2 h in absolute ethanol:glacial acetic acid, (3:1,v/v), hydrolysed at 60 °C in 1 N HCl for 12 min. and stained with the Feulgen method. Finally, root tips were squashed in 1% aceto-orcein. Permanent slides were prepared with entellan mounting medium. Microphotographs of good quality metaphase plates were taken using an Olympus BX53 (Tokyo, Japan) microscope equipped with a high-resolution digital camera. Metaphase observations and chromosome measures were made using the image analysis systems KAMERAM (ARGENİT Microsystems, İstanbul, Turkey). The somatic chromosome number and karyotype details were studied in five to eighteen well-spread metaphase plates from different individuals; mean values were used for the analysis.

Chromosome pairs were identified and arranged on the basis of their length and any other evident karyomorphological features. The nomenclature used for describing karyotype composition followed Levan et al. (1964). To determine the karyological relationships among taxa, we performed a PCoA (Principal Coordinate Analysis) with six uncorrelated parameters as suggested by Peruzzi and Altinordu (2014). These parameters are chromosome number (*2n*), basic chromosome number (x), total haploid length (THL), mean centromeric asymmetry (M_{CA}), coefficient of variation of chromosome length (CV_{CL}), and coefficient of variation of centromeric index (CV_{CI}) (Paszko 2006; Peruzzi et al. 2009; Zuo and Yuan 2011, Peruzzi and Eroğlu 2013). The software Past 3.03 (Hammer et al. 2001, Hammer 2018) was used to perform this analysis.

Mitotic metaphase chromosomes are given in Figure 3. Idiograms of these taxa are arranged in order of centromere position and then decreasing the length of homologue chromosome pairs (Figure 4).

In this study, chromosome types were determined according to the position of the secondary constrictions of *Gundelia* chromosomes for the purpose of chromosome comparison. General description of these chromo-

Table 1. Localities and voucher specimens of *Gundelia* taxa examined in the present study.

Taxa	Locality	Collector (M. Fırat) /voucher
G. anatolica Fırat	Kırıkkale: Delice province, Tuzkayası region, dry steppe, 700 m, 10 July 2017	*33866*
G. asperrima (Trautv.) Fırat	Erzurum: Palandöken mountain, mountain slope, steppe, 2444 m, 30 July 2017	33845
G. cilicica Fırat	Mersin: Erdemli province, Tozlu village, open forrest, 1460 m, 11 July 2017	*33868*
G. colemerikensis Fırat	Hakkâri: Hakkâri Province (Colemerîk) Berçelan plateau, open erode region and steppe, 2284 m, 7 July 2017	*33861*
G. dersim Vitek, Yüce & Ergin	Tunceli (Dersim): Ovacık, c. 11.7 km SW Ovacık, 1.9 km NE Ziyaret (fountains of river Munzur), 1300 m, 28 July 2017	*33872*
G. glabra Mill.	Bayburt: Kop mountain arround, near Kop Village, 1897 m, 19 July 2017	33867
G. komagenensis Fırat	Adıyaman: Kahta Province, Nemrut mountain, rocky steppe, 1445 m, 30 July 2017	*33783*
G. mesopotamica Fırat	Mardin: 2-3 km from Mardin to Nusaybin (Nisêbîn), eroded slopes, aride steppe, 807 m, 11 July 2017	33865
G. munzurensis Vitek, Yüce & Ergin	Tunceli (Dersim): Ovacık, c. 2 km SW Ovacık, near road Ovacık plain, 1275 m, 28 July 2017	*33871*
G. rosea M.Hossain & Al-Taey	Hakkari: Şemdinli Province, Sad Mountain, Derîyê Kera region, meadows and stony slopes, 1662 m, 7 July 2017	*33862*
G. tournefortii L.	Hatay: Reyhanli district, near Syria (Aleppe) border, 121 m, 9 July 2017	33864
G. vitekii Armağan	Tunceli (Dersim): c. 8-9 km N of Tunceli, mountain slope NW of Tüllük Bucağı, rocky steppe, 1760 m, 28 July 2017	*33870*

some types is given below, followed by the karyotype description.

Type A: Longest metacentric chromosomes with two constrictions, secondary constrictions in the distal position of the long arm.

Type B: Submetacentric chromosomes with two constrictions, secondary constrictions nearly in the median position of the long arm.

Type C: Submetacentric chromosomes with two constrictions and secondary constrictions located very close to the centromere on the short arm.

RESULTS

All species showed basic chromosome number x = 9 and diploids with *2n* = 18 (Figures 3 and 4). Chromosome measurements and karyotype formula of the twelve analysed species are indicated in Table 2. Total haploid length, asymmetry indices, chromosome types and flower number within the partial synflorescences in the middle part are summarised in Table 3.

Secondary constrictions were observed at the long or short arms of all submetacentric chromosomes, and in the distal regions of the long arms of some of the longest

Table 3. Karyo-morphometric parameters, symmetry indices, Chromosome types and cephaloid flowers number for investigated taxa (**THL**: total haploid length; $\mathbf{M_{CA}}$: mean centromeric asymmetry; $\mathbf{CV_{CL}}$: coefficient of variation of chromosome length; $\mathbf{CV_{CI}}$: coefficient of variation of centromeric index).

	THL	M_{CA}	CV_{CL}	CV_{CI}	Chromosome Types	Cephaloid. Flowers numbers
G. anatolica	34.48	14.13	16.87	9.73	_/B/_	6
G. asperrima	24.97	13.08	21.58	9.83	A/B/C	3(–4)
G. cilicica	34.26	12.06	20.01	7.44	_/_/C	6(–7)
G. colemerikensis	29.84	13.03	22.42	10.75	_/B/C	(3–)5(–6)
G. dersim	34.52	13.27	21.57	9.56	A/_/C	6–7
G. glabra	35.60	13.27	20.84	9.94	_/B/C	3–5(–6)
G. komagenensis	37.90	13.95	20.56	11.94	_/B/C	3(–4)
G. mesopotamica	32.64	14.38	19.70	12.44	A/B/C	6–7
G. munzurensis	27.87	13.27	20.24	10.21	A/B/C	3–5
G. rosea	42.56	14.40	21.42	8.12	A/_/C	(6–) 7–8
G. tournefortii	27.16	11.41	20.20	8.83	A/_/C	(5–)6(–7)
G. vitekii	30.57	13.76	21.64	11.82	A/B/C	3(–5)

Table 2. Karyotype formula according to Levan et al. (1964) and measurements of the investigated taxa. (SC: the shortest chromosome length; LC: the longest chromosome length; p: mean long arm length; q: mean short arm length; SD: standard deviation; m: metacentric; sm: submetacentric).

	SC–LC	q (μm) Mean (±SD)	p (μm) Mean (±SD)	p+q Mean (±SD)	Karyotype formula
G. anatolica	2.90 – 5.15	1.64(±0.30)	2.19(±0.44)	3.83(±0.65)	16 m + 2 sm
G. asperrima	2.00 – 4.01	1.19(±0.23)	1.58(±0.42)	2.77(±0.60)	14 m + 4 sm
G. cilicica	2.77 – 5.35	1.67(±0.35)	2.14(±0.46)	3.81(±0.76)	16 m + 2 sm
G. colemerikensis	2.40 – 4.90	1.43(±0.33)	1.89(±0.50)	3.32(±0.74)	14 m + 4 sm
G. dersim	2.78 – 5.78	1.66(±0.40)	2.18(±0.50)	3.84(±0.83)	16 m + 2 sm
G. glabra	2.86 – 5.61	1.70(±0.35)	2.25(±0.56)	3.96(±0.82)	14 m + 4 sm
G. komagenensis	3.10 – 6.08	1.79(±0.37)	2.42(±0.61)	4.21(±0.87)	14 m + 4 sm
G. mesopotamica	2.73 – 5.27	1.55(±0.36)	2.08(±0.47)	3.63(±0.71)	14 m + 4 sm
G. munzurensis	2.28 – 4.43	1.33(±0.26)	1.77(±0.43)	3.10(±0.63)	14 m + 4 sm
G. rosea	3.30 – 7.02	2.03(±0.49)	2.70(±0.58)	4.73(±1.01)	16 m + 2 sm
G. tournefortii	2.31 – 4.45	1.33(±0.30)	1.68(±0.37)	3.02(±0.61)	16 m + 2 sm
G. vitekii	2.49 – 5.04	1.45(±0.31)	1.95(±0.51)	3.40(±0.74)	14 m + 4 sm

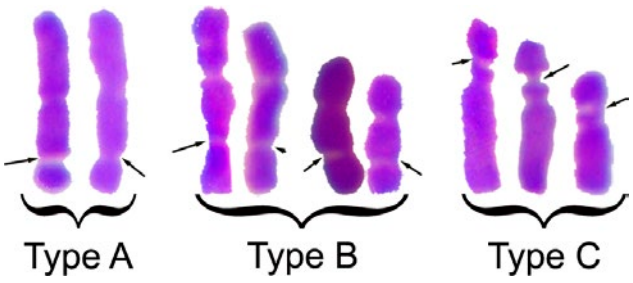

Fig. 2. Chromosome types according to the position of the secondary constrictions (indicated by arrows).

metacentric chromosomes (Figure 2). Moreover, three chromosome types were determined according to the position of the secondary constrictions (Figure 2).

The chromosomes ranged in size from 2.00 µm to 7.02 µm. *G. asperrima* showed the smallest mean chromosome length (2.77 µm), while *G. rosea* the biggest (4.73 µm).

Similarly, the smallest mean short arm length (q) was observed in *G. asperrima* (1.19 µm) and the largest mean long arm length (p) was observed in *G. rosea* (2.70 µm). The idiograms of the analysed species are shown in Figure 3.

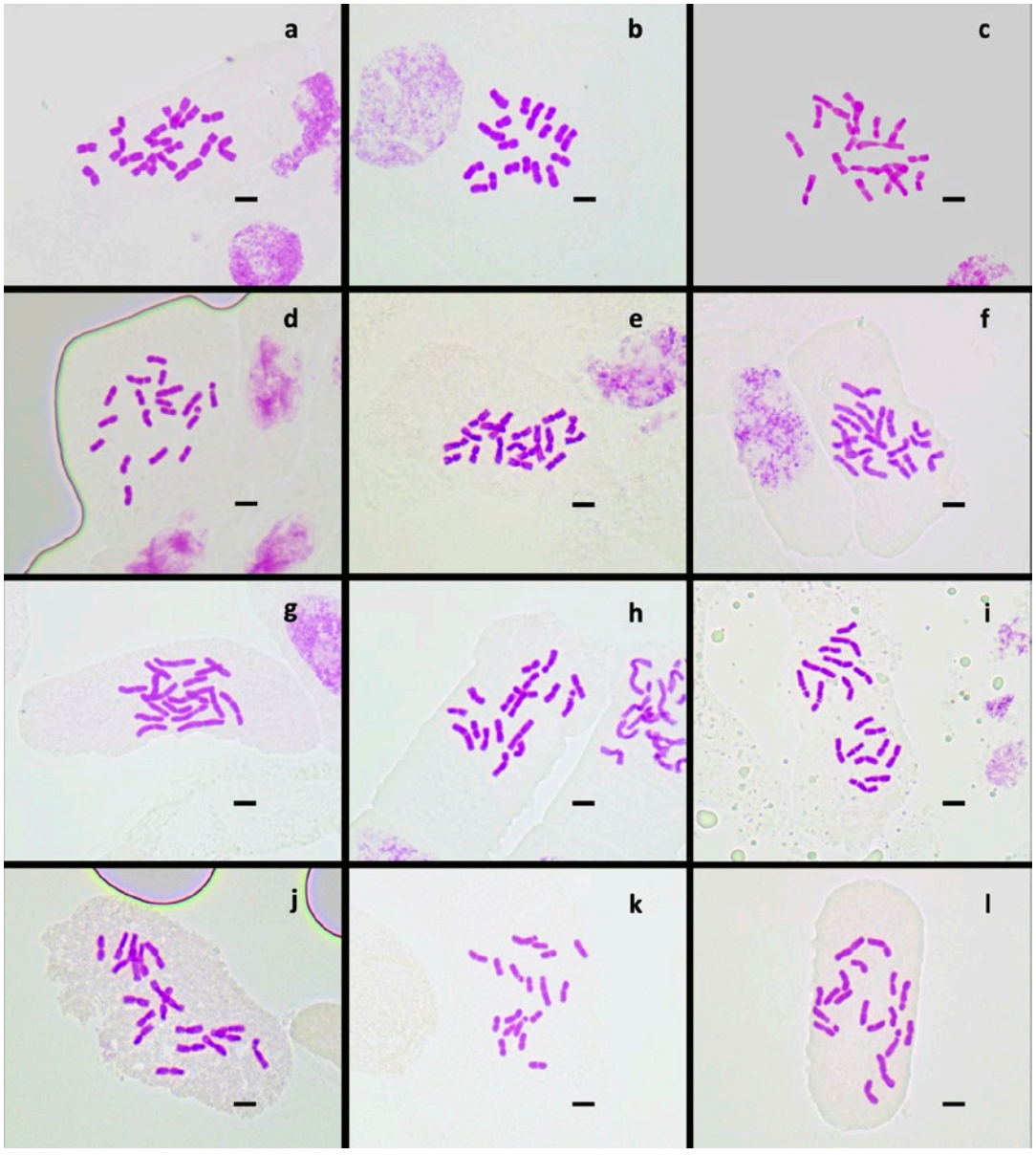

Fig. 3. Somatic chromosomes (*2n* = 18) in the studied taxa. (a) *G. anatolica*; (b) *G. asperrima*; (c) *G. cilicica*; (d) *G. colemerikensis*; (e) *G. dersim*; (f) *G. glabra*; (g) *G. komagenensis*; (h) *G. mesopotamica*; (i) *G. munzuriensis*; (j) *G. rosea*; (k) *G. tournefortii*; (l) *G. vitekii*. Scale bars 3 *µm*.

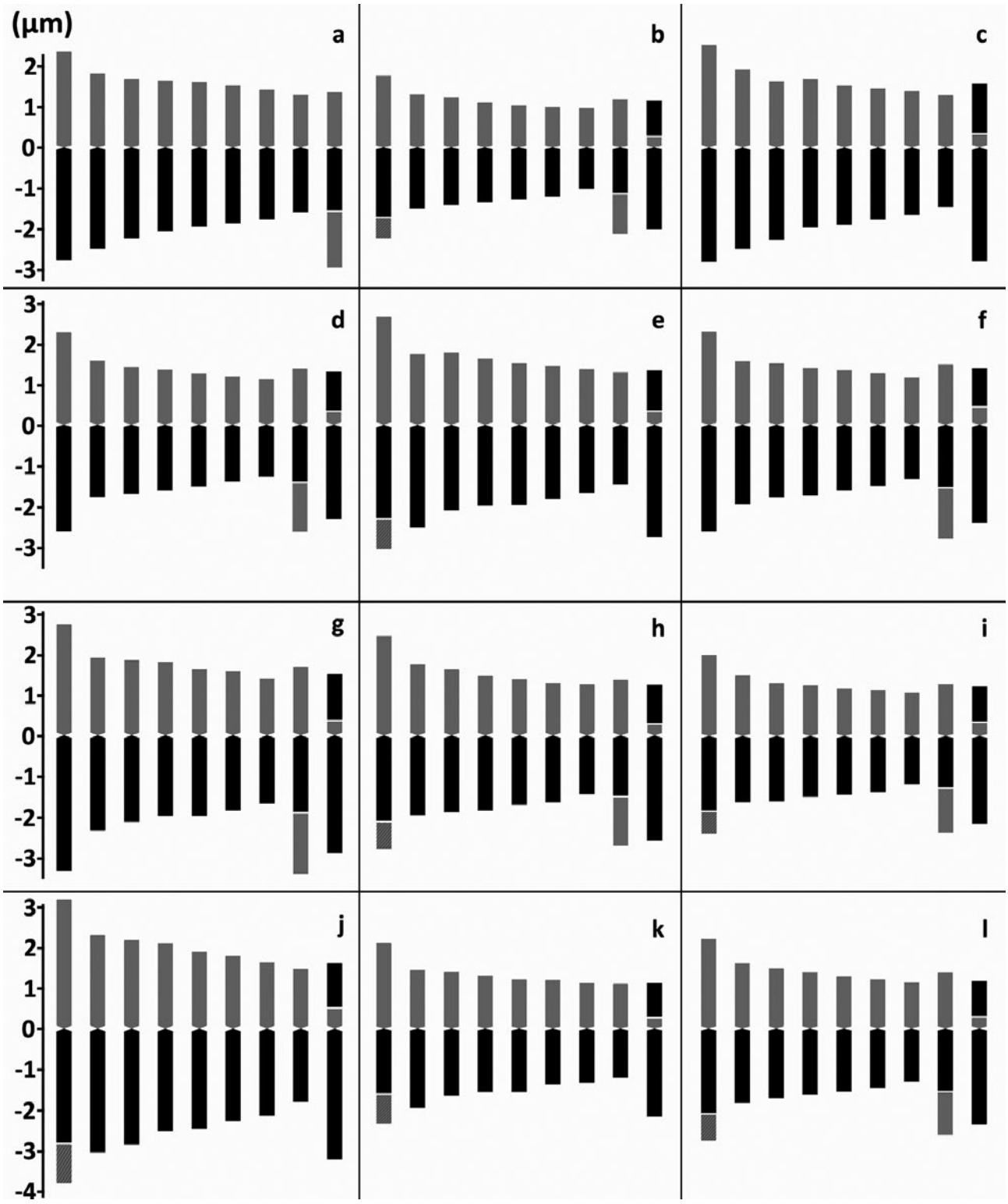

Fig. 4. Haploid idiograms in the studied taxa. (a) *G. anatolica*; (b) *G. asperrima*; (c) *G. cilicica*; (d) *G. colemerikensis*; (e) *G. dersim*; (f) *G. glabra*; (g) *G. komagenensis*; (h) *G. mesopotamica*; (i) *G. munzuriensis*; (j) *G. rosea*; (k) *G. tournefortii*; (l) *G. vitekii*.

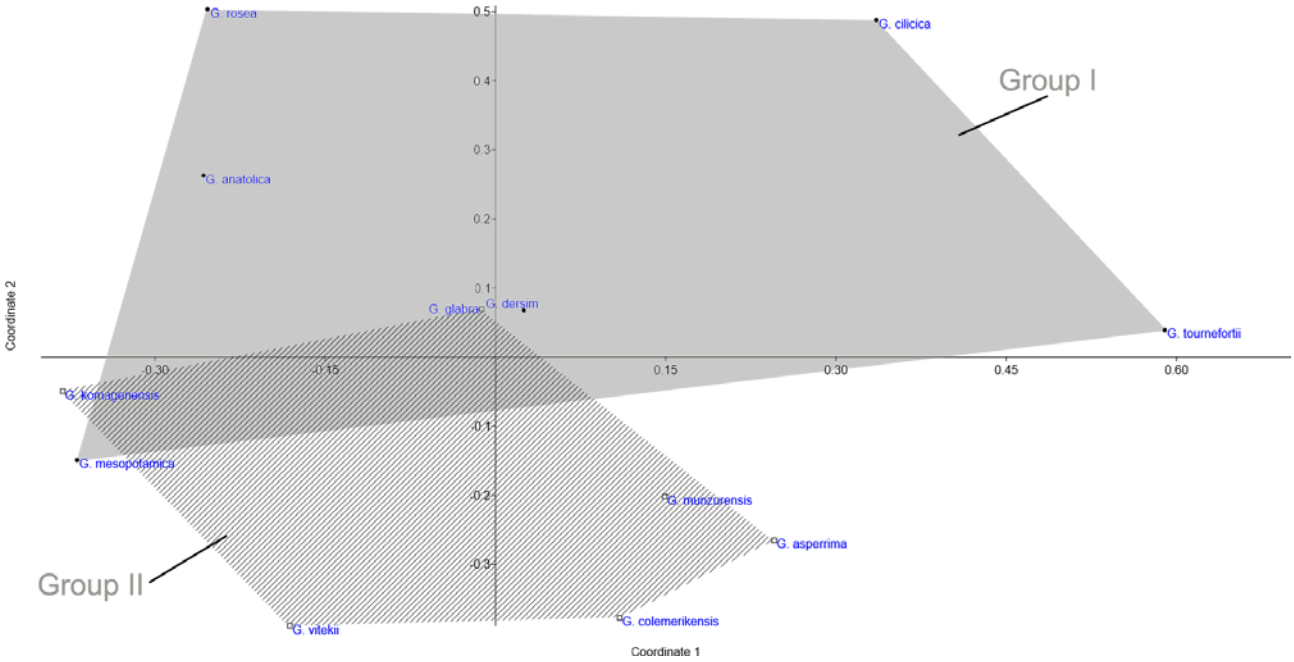

Fig. 5. PCoA analysis based on six quantitative karyological parameters of investigated taxa.

The chromosomes with secondary constriction ranged from 2 to 6 in number. The total haploid chromosome length (THL) varied from 24.97 µm (*G. asperrima*) to 42.56 µm (*G. rosea*).

Karyotypes of the analysed species exhibit a predominance of metacentric chromosomes. However, one or two submetacentric chromosomes were detected in each taxon. Due to the prevalence of metacentric pairs and to the absence of strong differences between smaller and larger chromosomes, asymmetry indices were in general low. However, some species show a tendency to have karyotypes distinct on asymmetry grounds:

Gundelia rosea, with relatively high intrachromosomal (MCA) and *G. tournefortii* with low intrachromosomal asymmetry, also, *G. vitekii* with high interchromosomal (CVCL) and *G. anatolica* low interchromosomal asymmetry.

DISCUSSION

Karyotype data for all taxa are reported for the first time in the present study with the exception *G. tournefortii* and *G. rosea*. The present investigation on *Gundelia* supports earlier data about $2n = 2x = 18$ (Waisel 1962; Al-Taey and Hossain 1984; Ghaffari and Chariat-Panahi 1985; Nersesyan and Nazarova 1989; Ghukasyan and Janjughazyan 2015). The article by Nersesyan and Nazarova (1989) is the most detailed work published on the karyology of *Gundelia tournefortii*. Three chromosome types were also seen in that study. However, according to our results, type B chromosome was not observed in *Gundelia tournefortii* chromosomes. However, earlier works accepted only one species in the genus, and this could be the cause of this difference.

According to Trautvetter (1876), flower number within the partial synflorescences differs between different populations of *Gundelia*. Moreover, the partial synflorescences in the middle part of the synflorescence are formed by 3 to 8 flowers according to the articles published in recent years. These flowers have been defined as "cephaloid flowers" in the following sections of the article. The taxa examined in this article were evaluated according to cephaloid flowers, and two groups have been recognised. Group I consists of mainly 3(-5) cephaloid flowers; Group II consists of mainly 6 or more cephaloid flowers (Table 3). In addition to this, according to chromosome types (A-C), taxa are divided into two main groups too. In agreement with our results, these groups are quite overlapping. Namely, type B chromosomes were present in all the taxa of Group I and no type B chromosomes was observed in the taxa of Group II with the exception of *G. mesopotamica* and *G. anatolica*. These species differ from others by having 6-8 cephaloid flowered and type B chromosomes. Also, *G. anatolica* is the only species in which there are no type C chromosomes. According to Tarıkahya Hacıoğlu and Fırat (2017), *G.*

anatolica is a derived species. This difference in chromosomal morphology supports this argument.

According to PCoA analysis, the species belonging to the same group tend to cluster together substantially (Figure 5). The presence of type A and type B chromosomes does not show variation at intraspecific level, these chromosome types were observed in all metaphase stages. However, type A chromosomes showed some infraspecific variation.

In conclusion, this study illustrated that two different groups can be distinguished, according to chromosome morphology. Therefore, the chromosome types can be used, in addition to other characters, for species identification and classification in the genus *Gundelia*.

REFERENCES

Al-Taey RA, Hossain M. 1984. Studies in *Gundelia*: 1 A new species from Iraq. Notes Roy. Bot. Gard. Edinburgh. 42: 39–44.

Armağan M. 2016. *Gundelia vitekii* (Compositae), a new species from Turkey. Ann. Naturhist. Mus. Wien, B 118: 129–134.

Beuzenberg EJ, Hair JB. 1984. Contributions to a chromosome atlas of the New Zealand flora - 27: Compositae. New Zealand J. Bot. 22: 353–356

Dawson MI. 2000. Index of chromosome numbers of indigenous New Zealand spermatophytes. New Zealand J. Bot. 38: 47–150.

Dimitrova D, Greilhuber J. 2001. C-Banding patterns and quantitative karyotype characteristics of Bulgarian species of *Crepis* (Asteraceae). Pl. Biol. (Stuttgart). 3: 88–97.

Feinbrun Dothan N. 1978. *Gundelia* L. in: Flora Palaestina: Part 3. Ericaceae to Compositae. Jerusalem: Israel Academy of Sciences and Humanities; p. 360-361

Fırat M. 2016. Four new species of *Gundelia* L. (Asteraceae) from Anatolia: *G. komagenensis*, *G. colemerikensis*, *G. cilicica* and *G. anatolica*. – Van: Sitav.

Fırat M. 2017a. *Gundelia rosea* (Asteraceae), a new record for the Flora of Turkey with contributions to its systematics. Acta Biologica Turcica. 30 (2): 31-35.

Fırat M. 2017b. *Gundelia mesopotamica* (Asteraceae), a new lactiferous species from Mardin (Turkey). Acta Biologica Turcica. 30 (3): 64-69.

Fırat M. 2017c: The resurrection and a new status of *Gundelia tournefortii* L. var. *asperrima* Trautv. (*Asteraceae*). OT Sistematik Botanik Dergisi. 24(2): 57-67

Ghaffari SM, Chariat-Panahi MS. 1985. Chromosome counts of some angiosperms from Iran. Iran. J. Bot. 3: 67–73.

Ghukasyan A, Janjughazyan K. 2015. Chromosome numbers of some rare flowering plants of Armenian flora. *Естественные Науки* 1: 24.

Gupta RC, Gill BS. 1989. Cytopalynology of north and central Indian Compositae. J. Cytol. Genet. 24: 96–105.

Hammer Ø. 2018. PAST 3.19. http://folk.uio.no/ohammer/past [accessed March 2018]

Hammer Ø, Harper DAT, Ryan PD. 2001. PAST: Paleontological statistics software package for education and data analysis. Palaeontologia Electronica 4(1): 9pp.

Hind N. 2013. 763. *Gundelıa tournefortii*: Compositae. Curtis's Botanical Magazine. 30(2): 114–138.

Ikeda H. 1988. Karyomorphological studies on the genus *Crepis* with special reference to C-banding pattern. J. Sci. Hiroshima Univ., Ser. B, Div. 2, Bot. 22: 65–117.

Karis PO, Eldenäs P, Källersjö M. 2001. New evidence for systematic position of *Gundelia* L. with notes on delimitation of Arctoteae (Asteraceae). Taxon. 50: 105-114.

Kilian N, Gemeinholzer B, Lack HW. 2009. Chapter 24. *Cochorieae*. In: Funk VA, Susanna A, Stuessy TF, Bayer RJ. editors. Systematics, Evolution, and Biogeography of Compositae. Vienna: International Association for Plant Taxonomy; pp. 343–383.

Komarov VL 1961. *Gundelia* L. in Flora of the USSR [in Russian], Vol. XXVI. Moscow and Leningrad: Izd. Akad. Nauk SSSR.

Kupicha FK. 1975. *Gundelia*. In: Davis PH, Matthews VA, Kupicha FK, Parris BS editors. Flora of Turkey and the East Aegean Islands, Vol. 5. Edinburgh: Edinburgh University Press. pp. 325–326.

Levan A, Fredga K, Sandberg AA. 1964. Nomenclature for centromeric position on chromosomes. Hereditas. 52(2):201–220.

Linnaeus C. 1753. *Species Plantarum*. Tomus II. Salvii, Holmiae.

Meikle RD. 1985. *Gundelia* L. in Flora of Cyprus Vol. 2. Bentham-Noxon Trust.

Nersesyan A. 2014: *Gundelia armeniaca* Nersesyan (Compositae) – a new species from Armenia. Ann. Naturhist. Mus. Wien, B. 116: 191–196.

Nersesyan AA, Nazarova EA. 1989. Karyosystematic study of *Gundelia tournefortii* (Asteraceae). Bot. Žhurn. (Moscow & Leningrad). 74: 837–839.

Paszko B. 2006. A critical review and a new proposal of karyotype asymmetry indices. Plant Syst Evol. 258(1-2):39–48.

Peruzzi L, Altınordu F. 2014. A proposal for a multivariate quantitative approach to infer karyological relationships among taxa. Comp. cytogen. 8(4): 337-349.

Peruzzi L, Eroğlu HE. 2013. Karyotype asymmetry: again, how to measure and what to measure? Comp. Cytogen. 7(1):1–9.

Peruzzi L, Leitch IJ, Caparelli KF. 2009. Chromosome diversity and evolution in Liliaceae. Ann. Bot. 103: 459–475.

Rechinger KH. 1989. *Gundelia* L. In: Rechinger KH. editor. Flora Iranica. (Flora des Iranischen Hochlandes und der Umrahmenden Gebirge Persien, Afghanistan, teile von West-Pakistan, Nord-Iraq,Azerbaidjan, Turkmenistan) Compositae VII , Vol. 164. Graz: Akademische Druck- u. Verlangsanstalt; pp. 107–109 & tab. 75, 76.

Tarıkahya Hacıoğlu B, Fırat M. 2017. ITS Phylogeny and Molecular Dating of some *Gundelia* (Asteraceae) of Anatolia. Anadolu. 27(2): 74-77.

Trautvetter ER. 1876. Plantarum messes anno 1874 in Armenia a Dre. G. Radde et in Daghestania ab A. Becker factas commentatus est ER a Trautvetter. Trudy Imperatorskago S.-Petersburskago Botanicheskago Sada. 4(1): 97-192.

Vitek E, Noroozi J. 2017. *Gundelia tehranica* (Compositae), a new species from Iran. Ann. Naturhist. Mus. Wien, B. 119: 243–248.

Vitek E, Fayvush G, Tamanyan K, Gemeinholzer B. 2010. New taxa of *Gundelia* (Compositae) in Armenia. Ann. Naturhist. Mus. Wien, B. 111: 85–99.

Vitek E, Yüce E, Çakilcioğlu U. 2017. *Gundelia glabra* Miller (Compositae) – an ignored taxon. Ann. Naturhist. Mus. Wien, B. 119: 235–242.

Vitek E, Yüce E, Ergin C. 2014. *Gundelia dersim* and *Gundelia munzuriensis* (Compositae), two new species from Turkey. Phytotaxa. 161: 130–138.

Vitek E. 2018. *Gundelia microcephala* (Compositae)– a taxon deserving rank of species. Ann. Naturhist. Mus. Wien, B. 120: 233-240.

Waisel Y. 1962. Ecotypic differentiation in the flora of Israel. II. Chromosome counts in some ecotype pairs. Bull. Res. Counc. Israel. 2: 174-176.

Zuo J, Yuan G. 2011. The difference between the heterogeneity of the centromeric index and intrachromosomal asymmetry. Plant Syst. Evoln. 297: 141–145.

Caryologia
International Journal of Cytology, Cytosystematics and Cytogenetics

Firenze University Press
www.fupress.com/caryologia

OPEN ACCESS

Citation: N. Nazar, J.J. Clarkson, D. Goyder, E. Kaky, T. Mahmood, M.W. Chase (2019) Phylogenetic relationships in Apocynaceae based on nuclear PHYA and plastid *trnL-F* sequences, with a focus on tribal relationships. *Caryologia* 72(1): 55-81. doi: 10.13128/cayologia-251

Received: 24th July 2018

Accepted: 18th October 2018

Published: 10th May 2019

Data Availability Statement: All relevant data are within the paper and its Supporting Information files.

Competing Interests: The Author(s) declare(s) no conflict of interest.

Phylogenetic relationships in Apocynaceae based on nuclear PHYA and plastid *trnL-F* sequences, with a focus on tribal relationships

Nazia Nazar[1,2,3,*], James J. Clarkson[3], David Goyder[3], Emad Kaky[4,5], Tariq Mahmood[2], Mark W. Chase[3]

[1] *Department of Plant Sciences, University of Nottingham, LR12 5RD, United Kingdom*
[2] *Department of Plant Science, Quaid-i-Azam University Islamabad, Pakistan*
[3] *Royal Botanic Gardens Kew, Richmond, Surrey, TW9 3AE, United Kingdom*
[4] *Kalar Technical Institute, Sulaimani Polytechnic University, Iraq*
[5] *Life Science School, University of Nottingham, NG7 2RD, United Kingdom*
* Corresponding author, E-mail: Nazia.Nazar1@nottingham.ac.uk

Abstract. To date, most molecular phylogenetic studies of Apocynaceae have been based on plastid DNA regions or nuclear ribosomal DNA. In this study, we used part of the PHYA (phytochrome A) exon, a low-copy nuclear gene, and combined it with the *trnL-F* region (intron and spacer) to investigate placement of Periplocoideae, intergeneric relationships of Asclepiadoideae and relationships within Rauvolfioideae. We included 112 taxa representing most major clades of Apocynaceae. The study confirms that both subfamilies Apocynoideae and Rauvolfioideae are paraphyletic and that Periplocoideae are nested within Apocynoideae. The APSA clade (Apocynoideae, Periplocoideae, Secamonoideae and Asclepiadoideae) is strongly supported here, but the crown clade of Apocynaceae (comprised of subfamilies Asclepiadoideae, Secamonoideae, Periplocoideae and Echiteae, Mesechiteae, Odontadenieae and Apocyneae of Apocynoideae) has only moderate support. The present study places Periplocoideae as part of the sister group to the rest of the crown clade. This contrasts with results from the previous only PHYA and plastid marker–based studies in which periplocoids appeared as sister to a clade comprising Baisseeae (Apocynoideae) plus Secamonoideae and Asclepiadoideae. Old World Cynanchinae form a well-supported clade with the New World MOG (Metastelmatinae, Oxypetalinae and Gonolobinae) tribes rather than with the largely Old World. Asclepiadinae and Tylophorinae, as suggested by earlier studies. In our combined analyses, resolution among most groups is improved as compared to previous plastid-only analyses.

Keywords. Apocynaceae, Asclepiadeae, Baisseeae, Periplocoideae, Phylogeny, Phytochrome A.

1. INTRODUCTION

Since Endress and Bruyns (2000), Apocynaceae sensu lato have been investigated with molecular data, mostly plastid, to evaluate relationships among various groups proposed in their classification (Potgieter and Albert 2001; Rapini et al. 2003 and 2006; Livshultz et al. 2007; Simões et al. 2007; Livshultz 2010). Subfamilies Rauvolfioideae and Apocynoideae have been recovered as non-monophyletic (e.g., Sennblad et al. 1998; Potgieter and Albert 2001; Livshultz et al. 2007; Simões et al. 2004). In more recent classifications (Endress et al. 2007a; Simões et al. 2007; Endress et al., 2014)), ten tribes have been proposed in Rauvolfioideae: Tabernaemontaneae, Alstonieae, Alyxieae, Carisseae, Hunterieae, Melodineae, Plumerieae, Vinceae, Willughbeieae, Aspidospermeae and Amsonieae. Monophyly of most tribes in the subfamily has always remained suspect (Potgieter and Albert 2001; Sennblad and Bremer 2002); however, in the recent phylogenetic analysis by Simões et al. (2007), six clades (out of nine tribes sensu Endress and Bruyns 2000) were identified in Rauvolfioideae, which could be referred to Willughbeieae, Tabernaemontaneae, Hunterieae, Alyxieae, Plumerieae, and Carisseae, while Melodineae, Alstonieae and Vinceae were polyphyletic

Similarly, in Apocynoideae, five tribes were recognized by Endress and Bruyns (2000): Wrightieae, Malouetieae, Apocyneae, Echiteae and Mesechiteae. Since this publication, five more tribes, Nerieae (Sennblad and Bremer 2002), Odontadenieae (Endress et al. 2007a), Baisseeae (Endress et al. 2007a) and Rhabdadenieae (Endress et al., 2014) have been recognized in this subfamily. Baisseeae are considered a sister group of the milkweeds (Asclepiadoideae-Secamonoideae) rather than subfamily Periplocoideae on the basis of various phylogenetic studies (Sennblad and Bremer 1996, 2000 and 2002; Potgieter and Albert 2001; Lahaye et al. 2005; Livshultz et al. 2007). Also phylogenetic analyses firmly support placement of Periplocoideae in the APSA (Apocynoideae, Periplocoideae, Secamonoideae, Asclepiadoideae) clade (Judd et al. 1994; Sennblad and Bremer 1996, 2002; Civeyrel et al. 1998; Potgieter and Albert 2001). Periplocoideae were recognized until the last decades of the 20th century as members of Asclepiadaceae (Kunze 1990 and 1993; Venter et al. 1990; Dave and Kuriachen 1991; Liede and Kunze 1993; Nilsson et al. 1993; Swarupanandan et al. 1996). In subfamily Asclepiadoideae five tribes have been recognized: Asclepiadeae, Ceropegieae, Marsdenieae, Fockeeae and Eustegieae (Endress et al. 2007a; Endress et al., 2014)). Endress and Bruyns (2000) delimited the tribes of Asclepiadoideae on the basis of the orientation of pollinia in pollen sacs: upwardly directed in Ceropegieae-Marsdenieae and pendulous in Asclepiadeae. Erect pollinia are considered a primitive character and also found in Secamonoideae and Fockeeae (Kunze 1993). Recognition of Fockeeae as a tribe separate from Marsdenieae in Asclepiadoideae by Kunze et al. (1994) is disputed by Endress and Bruyns (2000) due to insufficient taxon sampling in Marsdenieae. The isolated basal position of Fockeeae has been confirmed by subsequent phylogenetic analyses (Potgieter and Albert, 2001; Rapini et al., 2003; Verhoeven et al., 2003).

Rapini et al. (2003) identified three main clades in Asclepiadeae that could be referred to as subtribes: Astephaninae and two multiple subtribe clades, ACTG (Asclepiadinae, Cynanchinae, Tylophorinae and Glossonematinae) and MOG. Subtribe Glossonematinae was later dissolved by Liede et al. (2002), *Glossonema* and *Odontanthera* were included in Cynanchineae and a third genus of the tribe *Solenostemma* belongs to none of the subtribes presently recognized in the Asclepiadeae (Endress et al. 2007a).

Cynanchinae within the ACT clade are divided into a monophyletic Old World succulent group (containing Malagasy *Cynanchum* species), but New World sections of the subtribe are polyphyletic (Liede and Taüber 2002; Rapini et al. 2006). Furthermore, cladistic analyses of Goyder et al. (2007) and Fishbein et al. (2011) have emphasized that generic delimitation of subtribe Asclepiadineae is problematic. These studies concluded that Asclepiadoideae still needs further investigation to identify monophyletic groups and find morphological characters by which to recognize them. To date, almost all broader molecular phylogenetic studies of Apocynaceae have been based on plastid DNA, either alone or in combination with morphological datasets.

Livshultz (2010) presented a study using the low-copy nuclear gene, PHYA (phytochrome A, exon 1) for a number of Apocynaceae groupings. Her approach proved useful in describing the status of tribe Baisseeae as the sister group of the milkweeds (i.e. Asclepiadoideae and Secamonoideae) rather than Periplocoideae. However, there are still many other areas within the family where resolution/support is low. For this study, we sequenced the same region of PHYA 1 (first exon) as in Livshultz (2010) for a broader dataset sampled across the family and combined these data with the widely sampled plastid *trnL-F* (intron/spacer) region. Our main goals are to: 1) further improve resolution in the primary clades of Asclepiadoideae (one of the groups from the crown clade defined by Livshultz 2010), 2) examine the position of Periplocoideae in Apocynaceae and 3) improve resolution within the subfamily Rauvolfioideae.

2. MATERIALS AND METHODS

2.1. DNA extraction and amplification

Taxa of Apocynaceae used here were either collected from the field in Pakistan or sampled from the DNA Bank at The Royal Botanic Gardens, Kew (https://dnabank.science.kew.org/). A complete list of taxa including voucher details, taxonomic treatment and provenance are provided in Table 1.

Total genomic DNA was extracted from silica-dried field collections following the 2 ×CTAB protocol of Richard (1997) with modifications described by Nazar and Mahmood (2010). DNA from herbarium specimens was isolated by pulverising dry material in tubes containing plastic beads (using a Genogrinder 2010, SPEX CertiPrep Ltd, Harrow, Middlesex, UK) and then following a modified Doyle and Doyle (1987) 2 ×CTAB method. To isolate DNA from these samples, we used precipitation in chilled ethanol (-20 °C) for at least 24 hr and then resuspended in 1.55 g/ml caesium chloride/ethidium bromide. Samples were then purified using a density gradient, followed by removal of the ethidium and caesium chloride with butanol/dialysis and storage in Tris EDTA.

Primers (PHYA 2059F, 2745F, 2971R, 3560R) used to amplify the first exon of PHYA are those of Livshultz (2010). The region was amplified using ReddyMix PCR Mastermix (Thermo Scientific, Epsom, Surrey, UK) in a 25 µl reaction volume. Degraded DNA (and/or possibly impure DNA), in some samples caused problems for amplification using the ReddyMix PCR Mastermix. To amplify the target regions from degraded DNA, especially from herbarium samples, Platinum® taq DNA polymerase (Invitrogen) was used. The reaction mix (25 µl total volume) consisted of 2.5 µl 10 ×PCR buffer, 2 µl MgCl2 (50 mM/ml), 1 µl of BSA (50 mg/ml), 0.6 µl of each primer (0.1 ng/µl), 0.2 µl of 5 U/µl of Platinum taq DNA polymerase, made up to volume with nuclease free water. The following PCR program was used for amplification: initial denaturation at 94 °C for 2 min, followed by 35 cycles of denaturation at 94 °C for 20 sec, annealing at 50 °C for 30 sec and extension at 72 °C for 2 min. A final extension was carried out at 72 °C for 7 min. Higher annealing temperatures reduced yields, and we found that using 50 °C did not cause amplification of more than one region (i.e. the sequencing reactions were free from obvious polymorphisms.

PCR products were cleaned using NucleoSpin® Extract II mini-columns (Macherey-Nagel, Duren, Germany) following the manufacturer's protocols. For cleaning of cycle sequencing products, we used precipitation in ethanol (using EDTA). Samples were sequenced on an ABI 3730 automated sequencer according to the manufacturer's protocols (Applied Biosystems, Inc.). Electropherograms were edited and assembled using Sequencher version 4.5 (Gene Codes, Ann Arbor, Michigan, USA); these sequences were easily aligned by eye in PAUP following the suggestions of Kelchner (2000).

2.2. Data analysis

Incongruence between *trnL-F* and PHYA results was assessed by looking for contradictory clades in both PHYA and *trnL-F* Bayesian and parsimony trees by following the same criteria regarding bootstrap support used by Livshultz (2010). Several studies have shown that the incongruence length test (ILD) proposed by Ferris et al. (1994) is too sensitive and unreliable for detection of incongruence (Darlu and Lecointre, 2002), so we did not use it here and have instead relied on inspection for well supported but different tree topologies as the basis for assessing incongruence (which we did not observe here). For the Bayesian results, we considered posterior probabilities (PP) > 0.95 as well-supported; < PP 0.95 is considered weakly supported and not indicative of incongruence. For the parsimony results, we considered bootstrap percentages (BP) of 80 as the cut-off for assessing incongruence. The separate analyses did not produce any clear evidence for incongruent clades, so we produced combined analyses of *trnL-F* and PHYA.

The combined dataset (*trnL-F* and PHYA) comprises of 112 sequences — 47 sequences from study of Livshultz (2010) are included (Table 2). Phylogenetic analyses were performed using maximum parsimony (MP; PAUP version 4.0b10, Swofford 2002) and Bayesian methods (Mr. Bayes ver.3.1, Huelsenbeck and Ronquist, 2001). Gaps were treated as missing data. For the parsimony analyses, the combined data matrix was analysed using tree bisection-reconnection (TBR) swapping and 1000 replicates of random taxon-addition, holding 10 trees at each step to reduced time searching islands of equally parsimonious trees. DELTRAN character optimization was used to illustrate branch lengths (due to reported errors with ACCTRAN optimization in PAUP version 4.0b).

For Bayesian analysis, a HKY85 model was specified in which all transitions and transversions have potentially different rates. More complex models were also tested, but these yielded the same tree with similar PP. The analysis was performed with 500,000 generations of Markov chain Monte Carlo with equal rates and a sampling frequency of 10. Microsoft excel was used to plot

Table 1. A list of the samples from Pakistan and The Royal Botanic Gardens Kew, London with vouchers information and place of collection are given.

Taxa	Voucher detail	Country	Regions sequenced
Asclepiadoideae – Asclepiadeae: Metastelmatinae			
Blepharodon lineare (Decne.) Decne.	Forzza *et al*. 2027	Argentina	*trnL-F* and *PHYA*
Asclepiadoideae – Asclepiadeae: Oxypetalinae			
Araujia sericifera Brot.	Forster 7656	Australia	*PHYA*
Funastrum clausum (Jacq.) Schltr.	Mello- Silva *et al*. 1919	Argentina	*PHYA*
Oxypetalum capitatum Mart.	Mello- Silva *et al*. 1924	Argentina	*PHYA*
Philibertia discolor (Schltr.) Goyder	Mello- Silva *et al*. 1887	Argentina	*PHYA*
Philibertia lysimachioides (Wedd.) T. Mey.	Mello- Silva *et al*. 1886	Argentina	*PHYA*
Asclepiadoideae – Asclepiadeae: Gonolobinae			
Matelea pseudobarbata (Pitter) Woodson	M. Endress 97-08	Costa Rica	*PHYA*
Asclepiadoideae – Asclepiadeae: Asclepiadinae			
Calotropis procera (Aiton) W. T. Aiton	Naz001*	Pakistan	*trnL-F* and *PHYA*
Kanahia laniflora (Forssk.) R. Br.	Goyder *et al*. 3931	Tanzania	*PHYA*
Pergularia daemia (Forssk.) Chiov.	Naz024*	Pakistan	*PHYA*
Pergularia tomentosa L.	Naz012*	Pakistan	*trnL-F* and *PHYA*
Stenostelma corniculatum (E. Mey.) Bullock	Balkwill 10908	South Africa	*PHYA*
Xysmalobium parviflorum Harv. ex Scott-Elliot	Killick & Vahrmeijer 3658	South Africa	*PHYA*
Asclepiadoideae – Asclepiadeae: Cynanchinae			
Cynanchum viminale (L.) Bassi	Chase 731	**	*PHYA*
Cynanchum jacquemontianum Decne.	Naz010*	Pakistan	*trnL-F* and *PHYA*
Cynanchum obtusifolium L.f.	P. Bruyns Vch	South Africa	*PHYA*
Asclepiadoideae – Asclepiadeae: Tylophorinae			
Tylophora hirsuta (Wall.) Wight	Naz014*	Pakistan	*trnL-F* and *PHYA*
Unplace genus			
Oxystelma esculentum (L. f.) Sm.	Naz020*	Pakistan	*trnL-F* and *PHYA*
Asclepiadoideae – Asclepiadeae: Astephaninae			
Eustegia minuta (L. F.) N. E. Br.	P. Bruyns 4357	South Africa	*PHYA*
Oncinema lineare (L. F.) Bullock	P. Bruyns Vch?	South Africa	*PHYA*
Schubertia grandiflora Mart.	Irwin *et al*. 31285	Brazil	*PHYA*
Asclepiadoideae – Marsdenieae			
Dischidia lanceolata Decne.	Chase 734	Indonesia	*PHYA*
Dregea abyssinica K.Schum.	Goyder *et al*. 3918	Tanzania	*PHYA*
Gymnema sylvestre (Retz.) Schultz.	Chase 3902	India	*trnL-F* and *PHYA*
Hoya finalasonii Wight	Chase 17138	India	*PHYA*
Hoya manipurensis Deb.	Chase 733	Thailand	*PHYA*
Marsdenia carvalhoi Morillo & Carnevali	Chase 3904	Brazil	*trnL-F* and *PHYA*
Rhyssolobium dumosum E. Mey.	P. V. Bruyns 3948	South Africa	*PHYA*
Staphanotis floribunda Brongn.	Chase 732	Senegal	*trnL-F* and *PHYA*
Wattakaka volubilis (Linn.f.) Stapf.	Naz006*	Pakistan	*trnL-F* and *PHYA*
Asclepiadoideae – Ceropegieae			
Caralluma tuberculata N.E. Br.	Naz019*	Pakistan	*trnL-F* and *PHYA*
Ceropegia sandersonii Decne.ex Hook.	Chase 17507	**	*PHYA*
Duvalia polita N. E. Br.	Kew	**	*PHYA*
Boucerosia indica Dalzell	Chase 2861	India	*PHYA*
Leptadenia pyrotechnica	Naz018*	Pakistan	*trnL-F* and *PHYA*
Neoschumannia kamerunensis	Chase 3903	Cameroon	*PHYA*
Quaqua incarnata (L. f.) Bruyns	Chase 9818	South Africa	*PHYA*
Heterostemma acuminatum Decne.	Forster 5090	**	*PHYA*

Taxa	Voucher detail	Country	Regions sequenced
Secamonoideae			
Secamone alpini Schult.	P. Bruyns Vch	South Africa *trnL-F* and *PHYA*	
Periplocoideae			
Cryptolepis buchananii Roemer & Schult.	Naz002*	Pakistan	*trnL-F* and *PHYA*
Cryptolepis decidua (Planch. ex Benth.) N. E. Br.	P. V. Bruyns s.n. (east of Fish R.)	Namibia	*trnL-F* and *PHYA*
Hemidesmus indicus (L.) R.Br. ex Schult.	Chase 725	Tamil Nadu	*PHYA*
Periploca aphylla Decne.	Naz004*	Pakistan	*trnL-F* and *PHYA*
Raphionacme hirsuta (E.Mey.sec.N.E.Brown) R.A.Dyer	CFR 15	South Africa	*PHYA*
Schlechterella abyssinicum (Chiov.) Venter & R. L. Verh.	Chase 720	Ethopia	*trnL-F* and *PHYA*
Apocynoideae - Malouetieae			
Kibatalia gitingensis (Elmer) Woodson	Liede 3268	**	*trnL-F* and *PHYA*
Pachypodium leallii Welw.	Chase 735	South Africa *trnL-F* and *PHYA*	
Apocynoideae - Nerieae			
Adenium obesum (Forssk.) Roem. & Schult.	Chase 727	Somalia	*trnL-F* and *PHYA*
Nerium oleander L.	Naz015*	Pakistan	*trnL-F* and *PHYA*
Apocynoideae - Apocyneae			
Beaumontia grandiflora (Roxb.) Wall.	Naz008*	Pakistan	*trnL-F* and *PHYA*
Trachelospermum jasminoides (Lindl.) Lem.	Naz022*	Pakistan	*trnL-F* and *PHYA*
Apocynoideae - Echiteae			
Fernaldia pandurata (A.DC.) Woodson	M Endress, Zurich	**	*PHYA*
Rauvolfioideae - Wrightieae			
Pleioceras barteri Baill.	Endress, P. 99-10	Ivory Coast	*PHYA*
Rauvolfioideae - Carisseae			
Carissa spinarum L.	Naz017*	Pakistan	*trnL-F* and *PHYA*
Rauvolfioideae - Plumerieae			
Anechites nerium Urb.	Bremer *et al*. 3386 UPS	**	*PHYA*
Skytanthus acutus Meyen	M. Endress, Zurich	**	*PHYA*
Thevetia peruviana (Pers.) K. Schum.	Naz013*	Pakistan	*trnL-F* and *PHYA*
Rauvolfioideae - Vinceae			
Amsonia hurbritchii Woodson	Chase 19252	USA	*trnL-F* and *PHYA*
Petchia ceylanica (Wight) Livera	R. Olmor s. n	Germany	*trnL-F* and *PHYA*
Rauvolfia serpentina (L.) Benth.	Naz003*	Pakistan	*trnL-F* and *PHYA*
Rhazya orientalis A.DC.	M. Endress s.n.	Zurich	*trnL-F* and *PHYA*
Vinca major L.	Naz025*	Pakistan	*trnL-F*
Rauvolfioideae - Tabernaemontaneae			
Tabernaemonta divericata (L.) R. Br. exRoem.Schult	Chase 5571	Bangladesh	*PHYA*
Rauvolfioideae - Hunterieae			
Gonioma kamassi E.Mey.	Chase 5806	South Africa *trnL-F* and *PHYA*	
Rauvolfioideae - Alyxieae			
Alyxia buxifolia R. Br.	Smith, R.J. (RJS202)	Australia	*PHYA*
Rauvolfioideae - Alstonieae			
Alstonia scholaris (L.) R. Br.	Naz007*	Pakistan	*trnL-F* and *PHYA*

*Vouchers specimens are preserved in the Plant Biochemistry and Molecular Biology Laboratory of Quaid-i-sAzam University, Islamabad, Pakistan.

** Information not present in Kew's databases.

generation number against InL to find the 'burn in'. Trees of low PP were deleted, and all remaining trees were imported into PAUP 4.0b10. A Bayesian tree (i.e., a majority-rule consensus tree) was produced showing frequencies of all observed bi-partitions (i.e. the posterior probabilities for each node).

Table 2. A list of taxa with GenBank accession numbers used in *trnL-F* and *PHYA* analyses, sequenced in present study, previously published in Rapini et al. (2003), Sennblad and Bremer (1998) and Livshultz (2010) with updated nomenclature (Endress et al., 2014).

Species Name	*PHYA*	*trnL-F*	Subtribe	Tribe	Subfamily
Adenium obesum (Forssk.) Roem. & Schult.	LT972249	HE805526		Nerieae	Apocynoideae
Aganosma wallichii G. Don.	GU901319	EF456127	Ichnocarpinae	Apocyneae	Apocynoideae
Alstonia scholaris (L.) R. Br.	LR027092	HE805532		Alstonieae	Rauvolfioideae
Alyxia buxifolia R. Br.	LT972244	AF214152		Alyxieae	Rauvolfioideae
Amsonia hurbritchii Woodson	LR027376			Amsonieae	Rauvolfioideae
Anechites nerium Urb.	LT972245	AM295087	Thevetiinae	Plumerieae	Rauvolfioideae
Angadenia berteroi (A.DC.) Miers	GU901358	EF456246		Echiteae	Apocynoideae
Anodendron paniculatum A. DC.	GU901327	EF456194	Papuechitinae	Apocyneae	Apocynoideae
Apocynum androsaemifolium L.	GU901328	AF214308	Apocyinae	Apocyneae	Apocynoideae
Araujia sericifera Brot.	LT972246	AJ704332	Oxypetalinae	Asclepiadeae	Asclepiadoideae
Artia balansae (Baillon) Pichon ex Guillaumin	GU901372	EF456142		Echiteae	Apocynoideae
Baissea multiflora A. DC.	GU901330	EF456199		Baisseeae	Apocynoideae
Beaumontia grandiflora (Roxb.) Wall.	LR027094	HE805527	Beaumontiinae	Apocyneae	Apocynoideae
Blepharodon linere (Decne.) Decne.	LR026999	AY163668	Metastelmatinae	Asclepiadeae	Asclepiadoideae
Boucerosia indica Dalzell	HF969013	AF214202		Ceropegieae	Asclepiadoideae
Calotropis procera (Aiton) W. T. Aiton	LT972247	HE805509	Asclepiadinae	Asclepiadeae	Asclepiadoideae
Caralluma tuberculata N.E. Br.	LT972248	HE805510		Ceropegieae	Asclepiadoideae
Carissa spinarum L.	LR027375	HE805533		Carisseae	Rauvolfioideae
Ceropegia sandersonii Decne.ex Hook.	HF969012	AF214179		Ceropegieae	Asclepiadoideae
Chonemorpha fragrans (Moon) Alston	GU901332	EF456132	Chonemorphinae	Apocyneae	Apocynoideae
Cleghornia malaccensis (Hook. f.) King & Gamble	GU901333	EF456241	Apocyinae	Apocyneae	Apocynoideae
Cryptolepis buchananii Roemer & Schult.	HG004619	HE805522			Periplocoideae
Cryptolepis decidua (Planch. ex Benth.) N. E. Br.	HG004618	HE805523			Periplocoideae
Cycladenia humilis Bentham	GU901367	EF456140		Odontadenieae	Apocynoideae
Cynanchum jacquemontianum Decne.	LR027368	HE805511	Cynanchinae	Asclepiadeae	Asclepiadoideae
Cynanchum obtusifolium L.f.	HF969010	AJ428692	Cynanchinae	Asclepiadeae	Asclepiadoideae
Cynanchum viminale (L.) Bassi	HG004632	AJ290912	Cynanchinae	Asclepiadeae	Asclepiadoideae
Dischidia lanceolata Decne.	LR028004			Marsdenieae	Asclepiadoideae
Dregea abyssinica K.Schum.	HG004620			Marsdenieae	Asclepiadoideae
Duvalia polita N. E. Br.	HF969009	AJ488374		Ceropegieae	Asclepiadoideae
Echites umbellatus Jacq.	GU901387	EF456186		Echiteae	Apocynoideae
Elytropus chilensis Müll. Arg.	GU901398	EF456171		Odontadenieae	Apocynoideae
Epigynum cochinchinense (Pierre) D.J. Middleton	GU901340	EF456147	Ichnocarpinae	Apocyneae	Apocynoideae
Eustegia minuta (L.f.) N.E.Br.	LR027089	AJ410207	Eustegieae	Asclepiadeae	Asclepiadoideae
Fernaldia pandurata (A.DC.) Woodson	GU901329	EF456209		Echiteae	Apocynoideae
Finlaysonia insularum (King & Gamble) Venter	GU901341	EF456105			Periplocoideae
Fockea edulis K. Schum.	LR027374	AF214199		Fockeeae	Asclepiadoideae
Forsteronia guyanensis Müll.Arg.	GU901359	EF456153		Mesechiteae	Apocynoideae
Funastrum clausum (Jacq.) Schltr.	HG004645	AJ428794	Oxypetalinae	Asclepiadeae	Asclepiadoideae
Gonioma kamassi E.Mey.	HG004623	HE805535		Hunterieae	Rauvolfioideae
Gymnanthera oblonga (Burm. f.) P.S. Green	GU901348	EF456106			Periplocoideae
Gymnema sylvestre (Retz.) Schultz.	HG004637	HE805512		Marsdenieae	Asclepiadoideae
Hemidesmus indicus (L.) R.Br. ex Schult.	HG004617	DQ916877			Periplocoideae
Heterostemma acuminatum Decne.		AJ574827		Ceropegieae	Asclepiadoideae
Hoya finalasonii Wight	HG004636			Marsdenieae	Asclepiadoideae
Hoya manipurensis Deb.	LR027373	AF214227		Marsdenieae	Asclepiadoideae
Ichnocarpus frutescens R. Br.	GU901356	EF456136	Ichnocarpinae	Apocyneae	Apocynoideae
Kanahia laniflora (Forssk.) R. Br.	HG004642	AY163695	Asclepiadinae	Asclepiadeae	Asclepiadoideae
Kibatalia gitingensis (Elmer) Woodson	HG004629	HE805528		Malouetieae	Apocynoideae

Species Name	*PHYA*	*trnL-F*	Subtribe	Tribe	Subfamily
Laubertia contorta (Mart.& Galeotti) Woodson	GU901375	EF456180		Echiteae	Apocynoideae
Leptadenia pyrotechnica	HG004614	HE805513		Ceropegieae	Asclepiadoideae
Mandevilla boliviensis Decne.	GU901343	EF456134		Mesechiteae	Apocynoideae
Marsdenia carvalhoi Morillo & Carnevali	LR027091	DQ334521		Marsdenieae	Asclepiadoideae
Marsdenia glabra Costantin	LR027370	EF456114		Marsdenieae	Asclepiadoideae
Matelea pseudobarbata (Pitter) Woodson	HG004621		Gonolobinae	Asclepiadeae	Asclepiadoideae
Microloma tenuifolium (L.) Kuntze	LR027371	AJ410230	Astephaninae	Asclepiadeae	Asclepiadoideae
Motandra guineensis A. DC.	GU901361	EF456210		Baisseeae	Apocynoideae
Neoschumannia kamerunensis Schltr.	HG004613	AJ410054		Ceropegieae	Asclepiadoideae
Nerium oleander L	LR027093	HE805529		Nerieae	Apocynoideae
Odontadenia perrotteti (A. DC.) Woodson	GU901335	EF456211		Odontadenieae	Apocynoideae
Oncinema lineare (L. F.) Bullock	LR027090	AJ428827	Astephaninae	Asclepiadeae	Asclepiadoideae
Oncinotis tenuiloba Stapf	GU901368	EF456141		Baisseeae	Apocynoideae
Orthanthera jasminiflora Schinz		AJ574827		Ceropegieae	
Oxypetalum capitatum Mart.	HG004644	AY163710	Oxypetalinae	Asclepiadeae	Asclepiadoideae
Oxystelma esculentum (L. f.) Sm.	HF969014	AJ290887		Asclepiadeae	Asclepiadoideae
Pachypodium leallii Welw.	HG004628	HE805530		Malouetieae	Apocynoideae
Papuechites aambe Markgr.	GU901370	EF456189	Papuechitinae	Apocyneae	Apocynoideae
Parameria laevigata (Juss.) Mold.	GU901371	EF456197	Urceolinae	Apocyneae	Apocynoideae
Parsonsia eucalyptophylla F. Muell.	GU901380	EF456215		Echiteae	Apocynoideae
Peltastes isthmicus Woodson	GU901324	EF456129		Echiteae	Apocynoideae
Pentalinon luteum (L.) B.F. Hansen & R.P. Wunderlin	HG004631	EF456191		Echiteae	Apocynoideae
Pergularia daemia (Forssk.) Chiov.	HG004641	JN205300	Asclepiadinae	Asclepiadeae	Asclepiadoideae
Pergularia tomentosa L.	HG004640	HE805514	Asclepiadinae	Asclepiadeae	Asclepiadoideae
Periploca aphylla Decne.	HG004616	HE805524			Periplocoideae
Petchia ceylanica (Wight) Livera	HG004624	AM295093	Catharanthinae	Vinceae	Rauvolfioideae
Petopentia natalensis (Schltr.) Bullock	GU901376	EF456107			Periplocoideae
Philibertia discolor (Schltr.) Goyder	LR027369	AY163700	Oxypetalinae	Asclepiadeae	Asclepiadoideae
Philibertia lysimachioides (Wedd.) T. Mey.	HG004643	AJ290900	Oxypetalinae	Asclepiadeae	Asclepiadoideae
Phyllanthera grayi (P.I. Forst.) Venter	GU901377	EF456103			Periplocoideae
Pinochia corymbosa (Jacq.) M.E. Endress & B.F. Hansen	GU901378	EF456167		Odontadenieae	Apocynoideae
Pleioceras barteri Baill.	LR027096	EF456251		Wrightieae	Apocynoideae
Prestonia lagoensis (Müll. Arg.) Woodson	GU901337	EF456237		Echiteae	Apocynoideae
Quaqua incarnata (L. f.) Bruyns	HG004612	AJ488455		Ceropegieae	Asclepiadoideae
Raphionacme hirsuta (E.Mey.sec.N.E.Brown) R.A.Dyer	HG004615	AJ581825			Periplocoideae
Rauvolfia serpentina (L.) Benth.	HG004625	HE805539	Rauvolfiinae	Vinceae	Rauvolfioideae
Rhabdadenia biflora Müll.Arg.	LR028003			Rhabdadenieae	Apocynoideae
Rhazya orientalis A.DC.		AM295095		Vinceae	Rauvolfioideae
Rhodocalyx rotundifolius Müll. Arg.	GU901396	EF456238		Echiteae	Apocynoideae
Rhyssolobium dumosum E. Mey.	HG004635	AM233378		Marsdenieae	Asclepiadoideae
Schlechterella abyssinicum (Chiov.) Venter & R. L. Verh.	HG004611	HE805525			Periplocoideae
Schubertia grandiflora Mart.	HG004622	AJ428827	Astephaninae	Asclepiadeae	Asclepiadoideae
Secamone alpini Schult.	LR027095	HE805519			Secamonoideae
Secamone elliptica R. Br.	GU901389	EF456116			Secamonoideae
Secondatia densiflora A. DC.	GU901339	EF456228		Odontadenieae	Apocynoideae
Sindechites chinensis Oliv. & Tsiang:	GU901393	EF456244	Amphineuriinae	Apocyneae	Apocynoideae
Skytanthus acutus Meyen	HG004627	AF214269	Thevetiinae	Plumerieae	Rauvolfioideae
Staphanotis floribunda Brongn.	HG004634	HE805517		Marsdenieae	Asclepiadoideae
Stenostelma corniculatum (E. Mey.) Bullock	HG004639	AY163722	Asclepiadinae	Asclepiadeae	Asclepiadoideae
Stipecoma peltigera Müll. Arg.	GU901394	EF456193		Echiteae	Apocynoideae
Tabernaemonta divericata (L.) R. Br. exRoem.Schult		AF214399		Tabernaemontaneae	Rauvolfioideae

Species Name	*PHYA*	*trnL-F*	Subtribe	Tribe	Subfamily
Temnadenia odorifera (Vell.) J.F. Morales:	GU901373	EF456179		Echiteae	Apocynoideae
Thevetia peruviana (Pers.) K. Schum.	LR027097		Thevetiinae	Plumerieae	Rauvolfioideae
Thyrsanthella difformis (Walter) Pichon	GU901391	EF456177		Odontadenieae	Apocynoideae
Toxocarpus villosus(Blume) Decne	GU901399	EF456117			Secamonoideae
Trachelospermum jasminoides (Lindl.) Lem.	HG004630	HE805531	Chonemorphinae	Apocyneae	Apocynoideae
Tylophora hirsuta (Wall.) Wight		HE805515	Tylophorinae	Asclepiadeae	Asclepiadoideae
Urceola lucida Benth. & Hook. f.	GU901400	EF456226	Urceolinae	Apocyneae	Apocynoideae
Vallaris solanacea (Roth) *O. Kuntze*	GU901401	EF456162	Beaumontiinae	Apocyneae	Apocynoideae
Vinca major L.	LR028005	HE805541	Vincinae	Vinceae	Rauvolfioideae
Wattakaka volubilis (Linn.f.) Stapf.	HF969011	HE805516		Marsdenieae	Asclepiadoideae
Xysmalobium parviflorum Harv. ex Scott-Elliot	HG004638	AM295674	Asclepiadinae	Asclepiadeae	Asclepiadoideae
Zygostelma benthamii Baill	GU901404	EF456109			Periplocoideae

3. RESULTS

3.1. Incongruence

As mentioned above, well-supported clades incongruent between the Bayesian and parsimony results were not observed. In some cases, *trnL-F* provided higher support for certain clades than did PHYA, but in other cases the reverse was true. Overall resolution produced by *trnL-F* for both Bayesian and parsimony analyses was lower than for PHYA. We will not describe the results of the separate analyses (they are highly similar), but we do include figures here for comparison (Supplementary data (Figures 1a, 1b, 2a, 2b)); we confine our discussion to only the combined results because the individual gene trees are congruent and the combined results are better resolved and have higher support.

3.2. Combined trnL-F *and PHYA analyses*

The dataset comprises 112 taxa and 2325 characters, of which 1400 are contributed by PHYA and 975 from *trnL-F*. In the parsimony analysis, 701 characters (479 from PHYA and 222 from *trnL-F*) proved to be parsimony informative. Analysis produced 13960 equally most-parsimonious trees with 3284 steps and a consistency index of 0.49 and retention index of 0.71. Mr Modeltest indicated that the best fit model was a general time reversible model with an alpha parameter for the shape of the gamma distribution to account for rate heterogeneity among sites (GTR+G+I). A burn in period of 2 10^6 generations per run was removed. The Bayesian tree (Figure 2) generally depicts more resolved groups as compared to the parsimony tree (Figure 1). Rauvolfioideae and Apocynoideae are non-monophyletic, but the subfamilies of the traditional Asclepiadaceae are strongly supported. The APSA clade receives high support (BP 99; PP 1.0), and Wrightieae emerge as sister to the rest of the clade.

In Rauvolfioideae, resolution of groups is low in both analyses. Monophyly of Plumerieae receives low support in both analyses (BP 59; PP 0.93), whereas Vinceae are paraphyletic in the MP analysis and poorly supported in the Bayesian tree (PP 0.83). In both analyses *Tabernaemontana* falls with Vinceae, whereas Hunterieae cluster with the *Amsonia-Rhazya* clade (BP 100; PP 1.0), but this relationship is not well supported. The position of Carisseae is found here as sister to the APSA clade with weak support (BP 59; PP 0.91).

APSA is well supported (BP 100; PP 1.0). *Rhabdadenia*, the only genus of Rhabdadenieae, forms a weakly supported clade with members of Malouetieae in the MP analysis (Figure 1), whereas in the Bayesian tree *Rhabdadenia* appears elsewhere (Figure 2). Periplocoideae receive good support in both analyses (BP 100; PP 1.0), but they are embedded in Apocynoideae. The clade comprising Odontadenieae, Mesechiteae, Echiteae and Apocyneae (all Apocynoideae) is well supported (BP 99; PP 1.0).

Baisseeae (sensu Endress et al. 2007a) are supported (BP 99; PP1.0) with *Dewevrella* as their sister. This clade forms a strongly supported sister to the milkweeds in the Bayesian tree (PP 1.0) and is relatively less well supported in the parsimony tree (BP 78).

The Secamonoideae-Asclepiadoideae clade receives strong support in both analyses (BP 100; PP 1.0), and the position of Fockeeae as sister to the rest is confirmed (BP 100; PP1.0). Members of Ceropegieae form a well-supported clade (BP 99; PP 1.0) in Asclepiadoideae. The monophyly of Marsdenieae receives strong support only in the Bayesian analysis (PP 0.99; BP 78). The close relationship between these tribes receives strong support also only in the Bayesian tree (PP 1.0; BP 53).

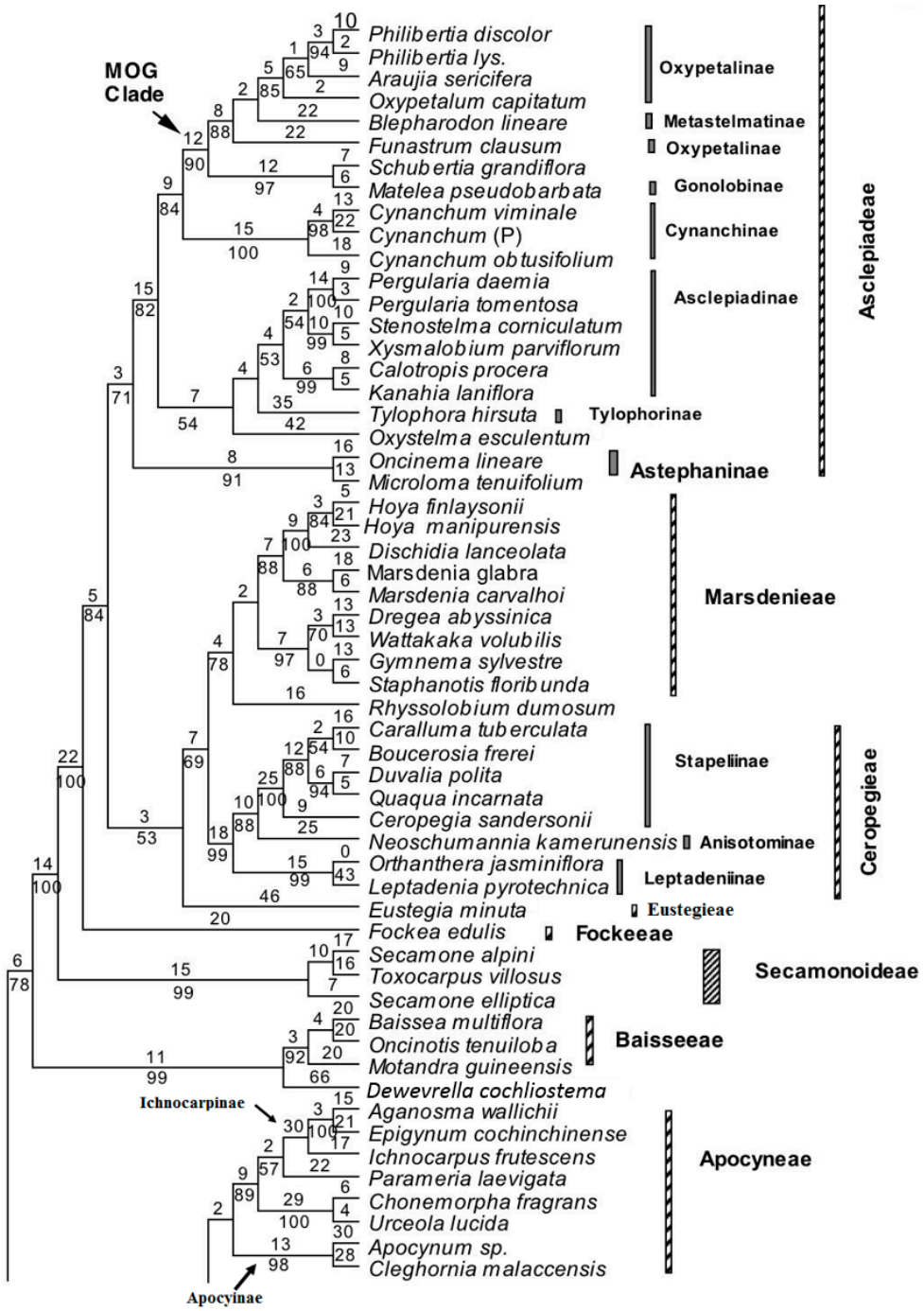

Fig. 1. One of the most parsimonious trees for Apocynaceae based on sequences of the combined dataset (PHYA and *trnL-F*). Bootstrap percentages > 50 and consistent with the strict consensus tree are indicated below branches. *Cynanchum* (P) = *Cynanchum jacquemontianum*.

Eustegia of the new tribe Eustegieae is recovered as sister to the combined Marsdenieae-Ceropegieae clade (BP 53; PP 1.0). The major clades in Asclepiadeae receive strong support in the Bayesian analysis, whereas resolution is relatively poor in the parsimony analysis. Subtribe Astephaninae (PP 1.0) is sister to rest of Asclepiadeae. The informally named ACT clade is not recovered here due to the position of Cynanchineae (Figures 1, 2).

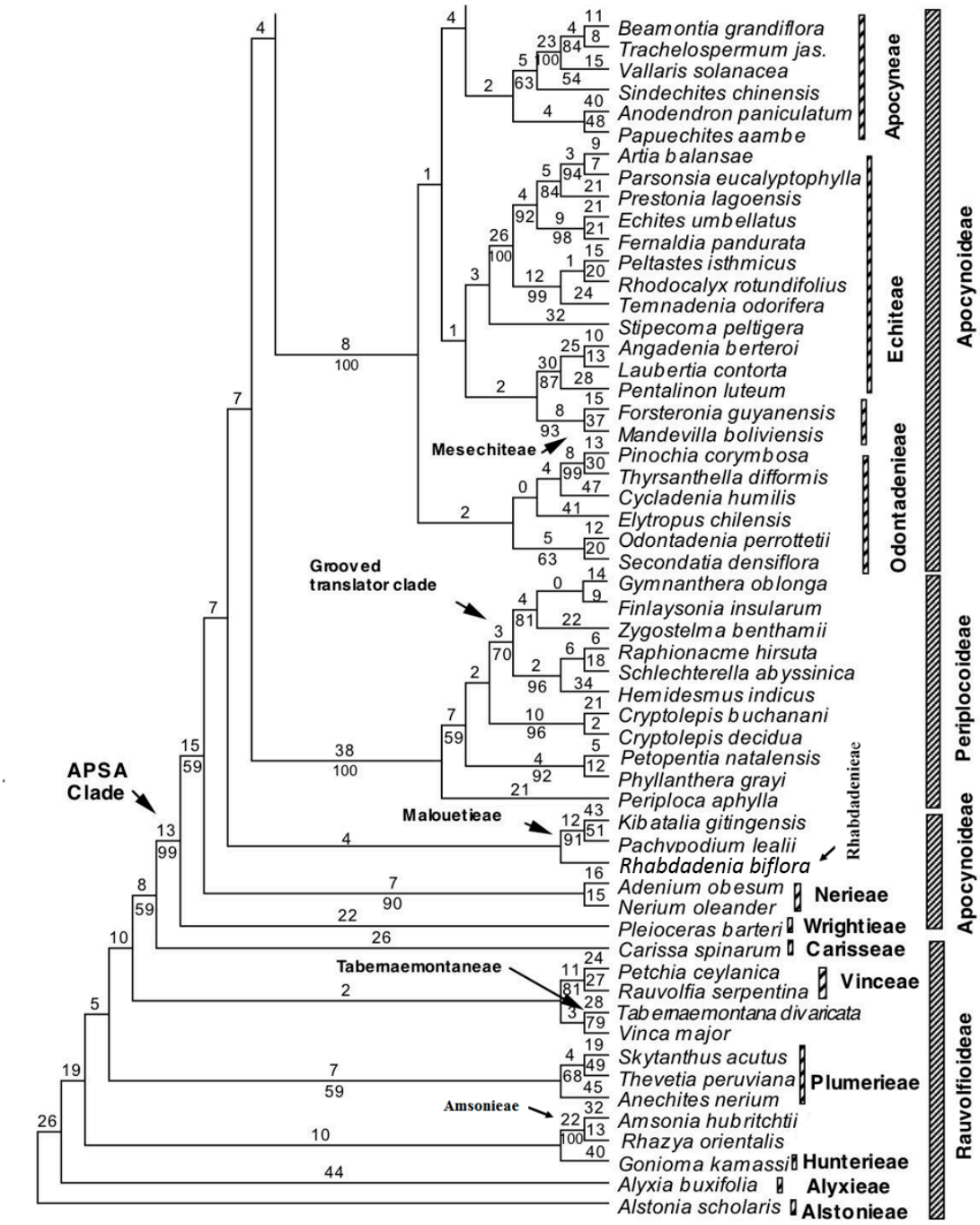

Fig. 1. (Continued).

Asclepiadineae and Tylophorinae form a well-supported clade (the AT clade) with *Oxystelma* as their sister (PP 1.0). Cynanchineae here comprise just the Old World genus *Cynanchum*, which forms a strongly supported clade sister to the MOG clade (BP 84; PP 1.0).

The MOG clade (all New World) receives strong support only in the Bayesian tree (PP 1.0). Within MOG, Gonolobineae are monophyletic (PP 1.0). *Blepharodon* (Metastelmatinae) is weakly supported (PP 0.61) as sister to *Funastrum* (Oxypetalinae), resulting in Oxypetalinae not being monophyletic. Within Oxypetalinae, *Araujia*, *Philibertia* and *Oxypetalum* form a well-supported clade (PP 1.0).

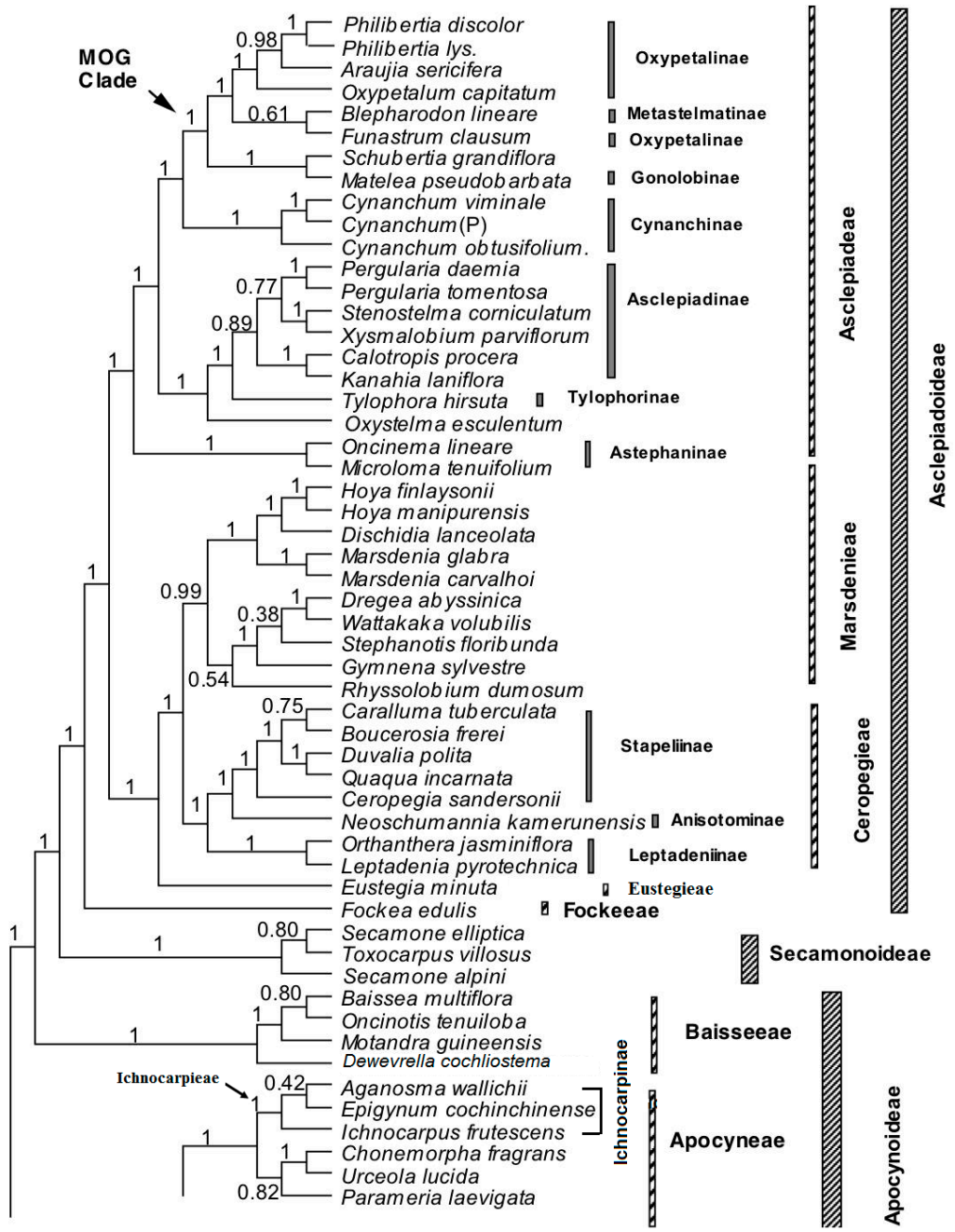

Fig 2. Bayesian analysis of Apocynaceae using combined datasets (PHYA and *trnL-F*). Posterior probabilities are shown along branches. *Cynanchum* (P) = *Cynanchum jacquemontianum*.

4. DISCUSSION

In the separate Bayesian and MP analyses, well-supported incongruent nodes are not observed, which was also reported by Livshultz (2010). Relationships are better supported in the combined results (Figures 1, 2) compared to the separate *trnL-F* and PHYA trees. Here, we confine our discussion of results to the combined analyses.

These results are broadly congruent with previously published phylogenetic studies of Apocynaceae (Livshultz et al. 2007; Simões et al. 2007; Endress et al. 2007a), and like these both subfamilies of Apocynaceae sensu stricto are not resolved as monophyletic. On the

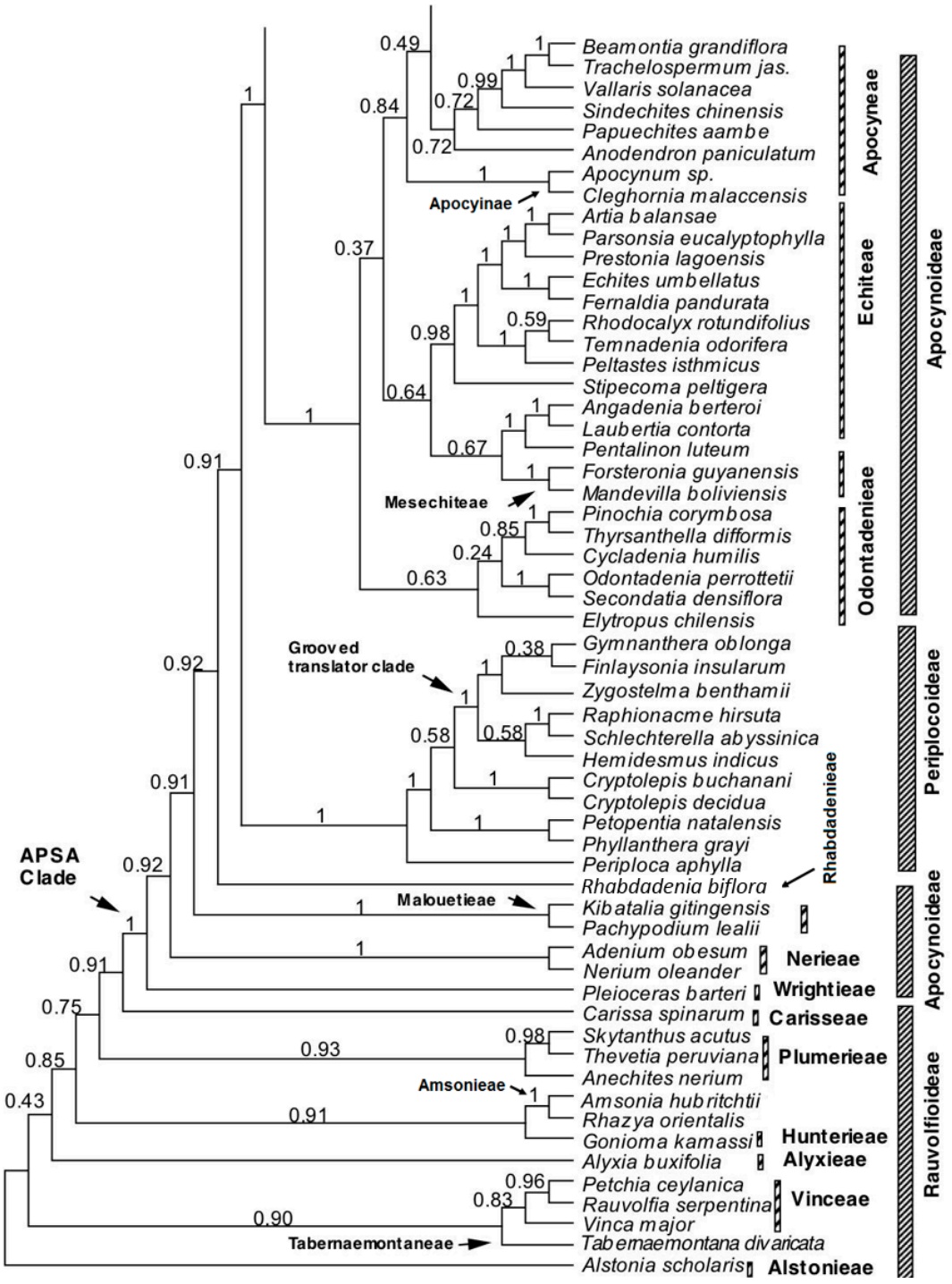

Fig. 2. (Continued).

basis of evidence from previous studies (Sennblad and Bremer 2002; Simões et al. 2004 and 2007), members of Alstonieae are sister to the rest of Apocynaceae. In our study, *Alstonia* was designated as the outgroup (Figures 1, 2). The separate position of *Amsonia* and *Rhazya* from the rest of Vinceae is in agreement with earlier DNA studies (Potgieter and Albert 2001; Endress et al. 2007b; Simões et al. 2007). However, a floral study conducted by Endress et al. (2007b) on *Amsonia* and *Rhazya* suggested that these two genera are more similar to *Catharanthus*

and *Vinca*, but our results place the former pair with Hunterieae. Endress and Bruyns (2000) treated *Rhazya* as a synonym of *Amsonia* on the basis of similar fruits, seeds and floral morphology (Pichon 1949; Nilsson 1986), and this relationship is also strongly supported in our study (BP 100; PP 1.0). As in Simões et al. (2007), monophyly of Plumerieae did not receive strong support in our analyses. Carisseae emerge as a sister group to the APSA clade, corresponding with the results of Civeyrel et al. (1998), Potgieter and Albert (2001), Simões et al. (2007) and Livshultz et al. (2007).

4.1 APSA clade

Wrightieae of subfamily Apocynoideae is sister to the rest of the APSA clade as was the case in other phylogenetic analyses of Apocynaceae (Sennblad and Bremer 1996 and 2002; Sennblad et al. 1998; Potgieter and Albert 2001; Livshultz et al. 2007; Livshultz 2010).

A strongly supported clade termed as the 'crown clade' by Livshultz et al. (2007) received less support in our Bayesian tree (PP 0.92) and is weakly supported in our MP analysis as compared to Livshultz et al. (2007) and Livshultz (2010). However the moderately supported (PP 0.91) sister-group relationship of Malouetieae with the crown clade, as illustrated in recent studies (Livshultz et al. 2007; Livshultz 2010), is also confirmed in our analyses. *Pachypodium* has traditionally been included in Echiteae (Pichon 1950), but Endress and Bruyns (2000) transferred this genus into Malouetieae, and this change was supported by Livshultz et al. (2007) and our study.

Old World Apocyneae form a well-supported clade with the New World tribes (Odontadenieae, Echiteae and Mesechiteae) of Apocynoideae in both analyses. In a recent phylogenetic analysis (Livshultz 2010), this clade received less support: BP 68 compared to BP 100/PP 1.0 here. Monophyly of Apocyneae is not supported by the MP analysis as compared to 100 BP in Livshultz (2010), but in the Bayesian tree they receive low support (PP 0.84). Our sampling of more taxa may be responsible for the shift in support observed in our results relative to those of Livshultz (2010). The topology in Apocyneae is somewhat inconsistent with that in Livshultz (2010), only by adding *Trachelospermum*, a basal clade (PP 0.72) emerges comprising of *Beaumontia*, *Trachelospermum*, *Vallaris*, *Sindechites*, *Papuechites* and *Anodendron*. In previous phylogenetic studies (Potgieter and Albert 2001; Sennblad and Bremer 2002; Simões et al. 2004 and 2007) *Beaumontia* and *Trachelospermum* form a clade with *Chonemorpha*, but here *Chonemorpha* from subtribe Chonemorphinae is sister to *Urceola* from subtribe Urceolinae (BP 100; PP 1.0; Figures 1, 2). In the present study, only two subtribes Apocyinae and Ichnocarpinae of the tribe Apocyneae described in updated classification of Apocynaceae (Endress et al., 2014) appeared monophyletic.

New World Apocynoideae (Echiteae, Mesechiteae and Odontadenieae) do not form a well-supported clade in our analyses as observed by Livshultz et al. (2007) and Livshultz (2010). In our analyses we did not add more taxa to the New World Apocynoideae group. Therefore intergeneric relationships of New World Apocynoideae are similar to those observed in the studies of Livshultz (2010) (Figures 1, 2). Endress et al. (2014) recently described subtribe Rhabdadenieae, which is sister to the crown clade (as a separate clade in the Bayesian analysis and with members of Malouetieae in MP) as observed by Livshultz (2010).

4.2 Baisseeae (African clade)

Endress et al. (2007a) defined a new tribe Baisseeae comprising three African genera – *Baissea*, *Oncinotis* and *Motandra* – and Livshultz et al. (2007) stated that Baisseeae are sister to the milkweeds rather than subfamily Periplocoideae. This relationship was originally suggested by Macfarlane (1933) on the basis of their geography (Livshultz et al. 2007). In previous phylogenetic analyses, this relationship has frequently been noted, but with weak support (Sennblad et al. 1998; Potgieter and Albert 2001; Sennblad and Bremer 2002) and more recently with stronger support (Lahaye et al. 2007; Livshultz et al. 2007; Simões et al. 2007). In our analysis, this sister relationship of Baisseeae receives strong support in the Bayesian analysis (PP 1.0) and comparatively weak bootstrap support (BP 78). In contrast, tetrad bearing Periplocoideae are most closely related to pollinium-bearing milkweeds, and Baisseae in the present study and previous molecular studies (Sennblad and Bremer, 2000; Livshultz et al. 2007) received strong support as sister to the pollinium-bearing milkweeds. In the classification of Endress and Bruyns (2000), *Baissea* and *Motandra* are grouped with *Prestonia* and *Cycladenia* on the basis of corona characters (particularly finger-like projections above the stamens).

In molecular phylogenetic analyses *Prestonia* forms a group with the 'core Echiteae', and *Baissea* and *Motandra* form a separate clade (Baisseeae; Livshultz 2010). Recently, Livshultz et al. (2007) identified these genera as having colleters on the adaxial surface of their petiole (rarely extending onto the base). However, this character is shared by *Farquharia* (Malouetieae), *Isonema* and *Nerium* (Nerieae). Therefore, morphologically, the African

clade still needs additional characters to justify its separate tribal identity as the sister group of the milkweeds.

4.3 Periplocoideae

In both these analyses (Bayesian and MP), the position of Periplocoideae in Apocynoideae differs from the analyses of Livshultz (2010). However, this result has been observed in other previous studies (Sennblad and Bremer 2000; Potgieter and Albert 2001; Livshultz et al. 2007; Livshultz 2010). On the basis of floral morphology (Table 3), the subfamily is regarded as an intermediate stage in a transition series between characters typical of Apocynoideae and those of milkweeds (Demeter 1922; Safwat 1962; Cronquist 1981; Rosatti 1989; Endress 1994, 2001 and 2004; Endress and Bruyns 2000; Wyatt et al. 2000). *Apocynum* has pollen in tetrads with simple translators, which is frequently considered to be the first stage in this series (Demeter 1922; Safwat 1962; Nilsson et al. 1993 and also cited by Livshultz et al. 2007). This is followed by pollen in tetrads with spoon-shaped translators in some Periplocoideae and then further aggregation leading to a pollinia in some Periplocoideae (Nilsson et al. 1993; Verhoeven and Venter 1998; Livshultz et al. 2007). Therefore, Periplocoideae as sister to the milkweeds is a common concept in the literature, but results of phylogenetic analyses have shown that Periplocoideae are more closely related to Apocynaceae sensu stricto; instead, Baisseeae are the sister of the milkweeds (Kunze 1996; Judd et al. 1994; Struwe et al. 1994; Sennblad and Bremer 1996; Endress 1997; Sennblad 1997; Potgieter and Albert 2001; Sennblad and Bremer 2002; Livshultz et al. 2007). Pollen in tetrads and pollinia have evolved in parallel in the APSA clade (Livshultz et al. 2007).

In this analysis, Periplocoideae are well supported (BP 100; PP 1.0) as observed in Livshultz et al. (2007) and Livshultz (2010). The grooved translator clade described by Ionta and Judd (2007) is also well supported in the Bayesian tree (PP 1.0) and receives relatively less support in the MP analysis (BP 70). These results show *Periploca* (the type genus of subfamily Periplocoideae) is sister to the rest of the subfamily, which can be contrasted with the findings of Ionta and Judd (2007), in which *Phyllanthera* is sister to the rest of Periplocoideae. Note that *Phyllanthera* is sister to *Petopentia* (BP 92; PP 1.0) with these data.

4.4 Asclepiadoideae-Secamonoideae (milkweed clade)

Secamonoideae have commonly been observed as sister of Asclepiadoideae (Sennblad and Bremer 1996, 2000 and 2002; Civeyrel et al. 1998; Civeyrel and Rowe

Table 3. Key morphological characters in subfamilies of family Apocynaceae.

Subfamily	Key Characters	Reference
Rauvolfioideae	Corolla with sinistrorse aestivation in bud; anthers free from style head; staminal filaments free; sclerified anther wings absent; pollen granular; stylar head secretions not differentiated; fruit a berry drupe or follicle; seeds lacking a coma	Sennblad (1997); Endress and Bruyns (2000)
Apocynoideae	Corolla with dextrorse aestivation in bud; anthers adnate to style head; staminal filaments free; sclerified anther wings absent; pollen granular; stylar head secretions not differentiated; fruit a follicle; seeds comose	Endress et al. (1996); Endress and Bruyns (2000)
Periplocoideae	Corolla with dextrorse to valvate aestivation in bud; anthers adnate to style head; staminal filaments free; sclerified anther wings absent; pollen in tetrads, sometimes clumped into pollinia lacking waxy coating; stylar head secretions forming spoonlike translators with sticky basal viscidium; pollinia if present 4 per translator; fruit a follicle; seeds comose	Verhoeven and Venter (1998); Endress and Bruyns (2000); Goyder et al. (2012)
Secamonoideae	Corolla with dextrorse or sinistrorse to valvate aestivation in bud; anthers and style head fused to form gynostegium; staminal filaments fused into a tube; sclerified anther wings present; pollen in tetrads clumped into pollinia lacking waxy coating; stylar head secretions differentiated into pale soft translator lacking clearly structured translator arms (pollinia fused directly to corpusculum or on short stalks); pollinarium with 4(-5) pollinia; fruit a follicle; seeds comose	Civeyral (1996); Verhoeven and Venter (1998); Endress and Bruyns (2000); Goyder et al. (2012)
Asclepiadoideae	Corolla with dextrorse to valvate aestivation in bud; anthers and style head fused to form gynostegium; staminal filaments fused into a tube; sclerified anther wings present; pollen in tetrads clumped into pollinia encased in waxy coating; stylar head secretions differentiated into dark hard translator with translator arms (pollinia (mostly) linked to corpusculum via variously structured translator arms); pollinarium with 2 pollinia; fruit a follicle; seeds comose	Klackenberg (1995b); Civeyral (1996); Endress and Bruyns (2000); Goyder et al. (2012)

2001; Fishbein 2001; Potgieter and Albert 2001; Lahaye et al. 2005 and 2007; Livshultz et al. 2007). In our study, this clade receives strong support (BP 100; PP 1.0). Although not broadly sampled here, the included taxa confirm monophyly of Secamonoideae with high support (BP 99; PP 1.0) *Secamone* is not recovered here as monophyletic, which is congruent with the results of Lahaye et al. (2007).

Asclepiadoideae, the largest subfamily of Apocynaceae, comprises ~3000 species distributed worldwide (Goyder, 2006). Currently, five tribes are recognized in the subfamily: Fockeeae, Ceropegieae, Marsdenieae,Asclepiadeae (Endress et al., 2007a) and Eustegieae (Endress et al., 2014). The position here for Fockeeae is consistent with previous analyses (Civeyrel et al. 1998; Fishbein 2001; Potgieter and Albert 2001; Rapini et al. 2003; Livshultz et al. 2007; Livshultz 2010). *Eustegia* is a monotypic genus with pendent pollinia, placed in to separate tribe of Asclepiadoideae (Goyder 2006), but phylogenetic studies based on plastid markers (Liede 2001; Rapini et al. 2003; Goyder et al. 2007) have placed *Eustegia* sister to the Marsdenieae-Ceropegieae clade, a result confirmed by our results

4.5 Ceropegieae-Marsdenieae clade

Meve and Liede (2004) recognized four subtribes in Ceropegieae based on anatomical characters: Anisotominae, Heterostemminae, Leptadeniinae and Stapeliinae. In our study Leptadeniinae are sister to the rest of Ceropegieae. Stapeliinae receive strong support (BP 100; PP 1.0), and Anisotominae are sister to Stapeliinae with strong support in the Bayesian analysis (PP 1.0) and moderate support in the parsimony analysis (BP 88).

Both subtribes have overlapping morphological features (Meve 1995; Meve and Liede 2001a, 2001b and 2004). The *Hoya*/*Dischidia* group forms a well-supported subclade in both analyses (BP 100; PP 1.0) and along with members of the genus *Marsdenia* they receive strong support in the Bayesian analysis (PP 1.0) and moderate MP support (BP 88). The association of *Hoya* and *Dischidia* has previously been supported by Potgieter and Albert (2001), Livshultz (2002 and 2003), Rapini et al. (2003), Meve and Liede (2004) and Wanntorp et al. (2006a and 2006b). There is little molecular phylogenetic data available for Marsdenieae; however, recently a few studies have focused on *Hoya* (Wanntorp and Forster 2007; Wanntorp and Kunz 2009; Wanntrop et al. 2011).

Another well-supported subclade (BP 97; PP 1.0) in Marsdenieae is comprised of *Dregea*, *Gymnema*, *Stephanotis* and *Wattakaka*. However, the position of *Rhyssolobium* seems unclear in both analyses. In the Bayesian analysis this genus is sister to the subclade that is sister to the rest, whereas with MP it is sister to other members of Marsdenieae; in both analyses, the position of this genus is poorly supported. This result is congruent with Meve and Liede (2004) and Wanntorp et al. (2006a).

Monophyly of Ceropegieae-Marsdenieae (which possess erect pollinia, regarded as a primitive condition in Asclepiadoideae; Kunz, 1993) is well supported in Bayesian analysis (PP 1.0). In earlier studies (Orbigny, 1843; Decaisne, 1844) Ceropegieae and Marsdenieae sensu Endress and Bruyns (2000) were considered a single entity.

However Endress and Bruyns (2000) treated Marsdenieae and Ceropegieae as two tribes, due to the lack of hyaline insertion crest on outer surface of pollinium and absence of an outer corona and milky latex in former (Bruyns and Forster 1991; Omlor 1998; Meve and Liede 2004). However, Swarupanandan et al. (1996) again united these two tribes, and this idea was later supported by molecular phylogenetic analyses (Potgieter and Albert 2001; Rapini et al. 2003; Meve and Liede 2004). Both tribes have also been observed to have the lowest level of polyploidy compared to other member of Asclepiadoideae (Albers and Meve, 2001).

4.6 Asclepiadeae

Asclepiadeae, the largest tribe of Asclepiadoideae having pendent pollinia (Table 3) and reduced chromosome number (x=10, x=9) from basic number (x=11) (Albers and Meve, 2001), are recovered here as monophyletic. The African genus *Eustegia* appearing as sister to the Ceropegieae-Marsdenieae clade is now recognized as separate tribe Eustegieae in Asclepiadoideae (Endress et al., 2014). Higher levels of intergeneric resolution in Asclepiadeae are recovered in the Bayesian analysis as compared to parsimony. In a broad overview of Apocynaceae conducted by Rapini et al. (2003), three main clades were defined — Astephaninae comprising of only three genera *Astephanus*, *Microloma* and *Oncinema* sensu Liede (2001), ACTG (Asclepiadinae, Cynanchinae, Tylophorinae and Glossonematinae) and MOG (Metastelmatinae, Oxypetalinae and Gonolobinae). In the present study, *Oncinema* and *Microloma* of Astephaninae are well supported as sister to the rest of Asclepiadeae, a result similar to previous molecular studies (Liede 2001; Rapini et al. 2003; Figures 1, 2). Of the other two clades recovered by Rapini et al. (2003), the MOG clade is resolved as monophyletic, whereas the ACT clade remains non-monophyletic with these data. *Oxystelma* is recovered here as sister to the Asclepiadine-

ae-Tylophorinae clade (AT clade) with strong support in the Bayesian analysis (PP 1.0). *Oxystelma* was among the *incertae sedis* of Asclepiadoideae (Liede and Taüber 2000; Endress et al. 2007a), and previously Liede (1997) included it in Metastelmatinae. In subsequent molecular phylogenetic analyses (e.g., Potgieter and Albert 2001; Liede and Taüber 2002; Liede et al. 2002; Rapini et al. 2003) the genus failed to a form a clade with members of Metastelmatinae. Instead, this genus occupied a position sister to the rest of the AT clade, as also observed here; however, in previous molecular phylogenetic analyses using plastid loci this close relationship was not well-supported. In the updated classification of Apocynaceae by Endress et al. (2014), *Oxystelma* was placed in subtribe Asclepiadineae. Cynanchineae here comprised of only Old World taxa (*Cynanchum viminale*, C. *jacquemontianum* and *C. obtusifolium*) appear as sister of the MOG clade (PP 1.0), which is comprised of members from the New World. However, these results can be contrasted with Rapini et al. (2003) where Cynanchinae are embedded in the ACT clade (but without support).

The MOG clade (New World) is recovered here with high support (PP 1.0) as observed in previous studies (Liede and Taüber 2000, 2002; Rapini et al. 2003; Liede-Schumann et al. 2005; Rapini et al. 2006). *Blepharodon lineare* and *Funastrum clausum* were resolved taxa in the study of Rapini et al. (2006) and appeared as sister to Metastelmatinae and Oxypetalinae, respectively. According to Liede (1997) *Funastrum clausum* was previously included in Metastelmatinae on the basis of morphological characters, but in the most recent classification (Endress et al. 2007a; Endress et al., 2014) and also various molecular studies (Rapini et al. 2006) it is placed in Oxypetalinae. However here in the Bayesian analysis the relationship between *Blepharodon lineare* and *Funastrum clausum* is unclear, but their sister-group position to the rest of Oxypetalinae is well supported (PP 1.0; Figure 2). The MP analysis fails to produce good resolution in the MOG clade. In the present study, *Oxypetalum* is sister to *Araujia-Philbertia*, similar to the result of Rapini et al. (2006). However, in earlier studies (with fewer data) a close relationship between *Philbertia* and *Blepharodon* (Liede and Taüber 2000) or *Philbertia* and *Funastrum* (Rapini et al. 2003) was observed. Gonolobineae receive strong support with these data (BP 97; PP 1.0).

Our study included a low-copy nuclear region and shows better resolution within some key clades in Apocynaceae when compared to previous studies, but the relationships recovered are not in particular markedly divergent from those obtained previously with just plastid data. The present analyses concluded that Rauvolfioideae, Apocynoideae and the traditional Asclepiadaceae are all non-monophyletic groups and that, in contrast, the APSA clade is well supported. The crown clade of Livshultz et al. (2007) and Livshultz (2010) received only moderate support here. Our studies confirm that Periplocoideae are nested within Apocynoideae, in a position comparable to that in Livshultz et al. (2007). Periplocoideae should be placed in Apocynoideae rather than thought of as the sister group of the milkweeds. The sister group relationship between Baisseeae and the milkweeds is also confirmed by our analyses. The ACT clade was not monophyletic, whereas the MOG clade was. Old World Cynanchineae forms a well-supported group within the New World MOG clade.

In the present study support for clades are comparatively better than in studies where plastid regions alone were sequenced. In the future, there is a need to sequence greater numbers of taxa of Apocynaceae to further refine the relationships in the family. There is also a need to be increased field collection of material so that high-quality DNA can be recovered from a wider range of Apocynaceae taxa.

ACKNOWLEDGEMENTS

We would like to acknowledge the Higher Education Commission of Pakistan and Prof. Vincent Savolainen (Imperial College, London) for facilitating the project. We would also like to thank Tatyana Livshultz for her studies on Apocynaceae and Edith Kapinos and Laszlo Czsiba of the Royal Botanic Gardens, Kew, for their assistance.

REFERENCES

Albers, F. & Meve, U. 2001. A karyological survey of Asclepiadoideae, Periplocoideae, and Secamonoideae, and evolutionary considerations within Apocynaceae s.l. Ann Missouri Bot Gard. 88:624–656.

Bruyns PV, Forster PI.1991. Recircumscription of the Stapelieae (Asclepiadaceae). Taxon 40:381–391.

Civeyrel L, LeThomas A, Ferguson K, Chase MW. 1998. Critical reexamination of palynological characters used to delimit Asclepiadaceae in comparison to the molecular phylogeny obtained from plastid *matK* sequences. Mol Phylogenet Evol. 9:517–127.

Civeyrel L, Rowe N. 2001. Phylogenetic relationships of Secamonoideae based on the plastid gene *matK*, morphology, and biomechanics. Ann Missouri Bot Gard. 88:583–602.

Cronquist A. 1981. An Integrated System of Classification of Flowering Plants. New York (NY): Columbia University Press.

Darlu, P, Lecointre G. (2002). When does the incongruence length difference test fail? Mol. Biol. Evol. 19:432–437.

Dave Y, Kuriachen PM. (1991). Comparative anatomical characters of *Periplocaceae* follicles and their taxonomic significance. Feddes Repert 102:63–68.

De Candolle AP, editor. 1844. *Asclepiadaceae*. Vol. 8. Prodromus Systematis Naturalis Regni Vegetabilis. Paris: Treuttel and Würtz.

Demeter K.1922. Vergleichende Asclepiadeenstudien. Flora. 115:130–176.

Doyle JJ, Doyle JL. 1987. A rapid DNA isolation procedure for small quantities of fresh leaf tissue. Phytochem Bull. 19:11–15.

Endress M. 2004. Apocynaceae: Brown and now. Telopea. 10:525–541.

Endress ME. 1997. Key characters at the interface of the apocynacs and the asclepiads. Amer J Bot. 84:180–190.

Endress ME, Bruyns P. 2000. A revised classification of the Apocynaceae sensu lato. Bot Rev. 66:1–56.

Endress ME, Liede-Schumann S, Meve U. 2007a. Advances in Apocynaceae: the enlightenment, an introduction. Ann Missouri Bot Gard. 94:259–267.

Endress ME, Liede-Schumann S, Meve U. 2014. An updated classification for Apocynaceae. Phytotaxa. 159:175–194.

Endress ME, Van der Ham RWJM, Nilsson S, Civeyrel L, Chase MW, Sennblad B, Potgieter K, Joseph J, Powell M, Lorence D, Zimmerman Y-M, Albert VA. 2007b. A phylogenetic analysis of Alyxieae (Apocynaceae) based on *rbcL*, *matK, trnL* intron, *trnL-F* spacer sequences, and morphological characters. Ann Missouri Bot Gard. 94:1–35.

Endress PK. 1994. Floral structure and evolution of primitive angiosperms: recent advances. Plant Syst Evol. 192:79–97.

Endress PK. 2001. The flowers in extant basal angiosperm and inferences on ancestral flowers. Int J Plant Sci. 162:1111–1140.

Farris JS, Källersjö M, Kluge AG, Bult C. (1994). Testing significance of congruence. Cladistics 10:315–319.

Fishbein M. 2001. Evolutionary innovation and diversification in the flowers of Asclepiadaceae. Ann Missouri Bot Gard. 88:603–623.

Fishbein M, Chuba D, Ellison C, Mason-Gamer RJ, Lynch SP. 2011. Phylogenetic relationships of *Asclepias* (Apocynaceae) inferred from non-coding chloroplast DNA. Syst Bot. 36:1008–1023.

Goyder D, Harris T, Masinde S, Meve U, Venter, J. 2012. Flora of Tropical East Africa Apocynaceae (Part 2), ed. H. J. Beentje. Royal Botanic Gardens, Kew. pp. 115–530.

Goyder DJ. 2006. An overview of asclepiad biogeography. In: Ghazanfar SA, Beentje H. editors. Taxonomy and Ecology of African Plants and their Conservation and Sustainable Use. London: Royal Botanic Gardens, Kew; p. 205–214.

Goyder DJ, Nicholas A, Liede-Schumann S. 2007. Phylogenetic relationships in subtribe Asclepiadinae (Apocynaceae: Asclepiadoideae). Ann Missouri Bot Gard. 94:423–434.

Huelsenbeck JP, Ronquist F. 2001. Mr. Bayes: Bayesian inference of phylogenetic trees. Bioinformatics. 17:754– 755.

Ionta GM, Judd WS. 2007. Phylogenetic relationships in Periplocoideae (Apocynaceae sensu lato) and insights into the origin of pollinia. Ann Missouri Bot Gard. 94:360–375.

Judd WR, Sanders RW, Donoghue MJ. 1994. Angiosperm family pairs: preliminary phylogenetic analyses. Harv Pap Bot. 1:1–51.

Kelchner SA. 2000. The evolution of noncoding chloroplast DNA its application in plant systematics. Ann Missouri Bot Gard. 87:482–498.

Kunze H. 1990. Morphology and evolution of the corona in Asclepiadaceae and related families. Trop Subtrop Pflanzenw. 76:1–51.

Kunze H. 1996. Morphology of the stamen in the Asclepiadaceae and its systematic relevance. Bot Jahrb Syst. 118:547–579.

Kunze H. 1993. Evolution of the translator in Periplocaceae and Asclepiadaceae. Plant Syst Evol. 185:99–122.

Kunze H, Meve U, Liede S. 1994. *Cibirhiza albersiana*, a new species of Asclepiadaceae, and establishment of the tribe *Fockeeae*. Taxon. 43:367–376.

Lahaye R, Civeyrel L, Speck T, Rowe N. 2005. Evolution of shrub-like growth forms in the lianoid subfamily Secamonoideae (Apocynaceae sensu lato) of Madagascar: Phylogeny, biomechanics, and development. Amer J Bot. 92:1381–1396.

Lahaye R, Klackenberg J, Kallersjo M, Van Campo E, Civeyrel L. 2007. Phylogenetic relationships between derived Apocynaceae sensu lato and within Secamonoideae based on chloroplast sequences. Ann Missouri Bot Gard. 94:376–391.

Liede S. 1997. Subtribes and genera of the tribe Asclepiadeae (Apocynaceae, Asclepiadoideae) – A synopsis. Taxon. 46:233–247.

Liede S. 2001. Molecular considerations on the subtribe Astephaninae Endl. ex Meisn. (Apocynaceae - Asclepiadoideae). Ann Missouri Bot Gard. 88:657–668.

Liede S, Kunze H. 1993. A descriptive system for corona analysis in the Asclepiadaceae. Plant Syst Evol. 185:99– 284.

Liede S, Taüber A. 2000. *Sarcostemma* R. Br. (Apocynaceae–Asclepiadoideae). A controversial generic circumscription reconsidered: Evidence from *trnL-trnF* spacers. Plant Syst Evol. 225:133–140.

Liede S, Taüber A. 2002. Circumscription of the genus *Cynanchum* (Apocynaceae-Asclepiadoideae). Syst Bot. 27:789–801.

Liede S, Taüber A, Schneidt J. 2002. Molecular considerations in the Tylophorinae K. Schum (Apocynaceae-Asclepiadoideae). Edinburgh J Bot. 59:377–403.

Liede-Schumann S, Rapini A, Goyder DJ, Chase MW. 2005. Phylogenetics of the New World subtribes of Asclepiadeae (Apocynaceae -Asclepiadoideae): Metastelmatinae, Oxypetalinae, and Gonolobinae. Syst Bot. 30:184–195.

Livshultz T. 2002. Systematics and evolution of ant-leaves in the genus *Dischidia* (Asclepiadaceae). Abstract, ASPT annual meeting, Portland.

Livshultz T. 2003. Lectotypification of *Dolichostegia Schlechter* (Asclepiadoideae, Apocynaceae) and a new combination, *Dischidia boholensis*. Taxon. 52:595–600.

Livshultz T. 2010. The phylogenetic position of milkweeds (Apocynaceae subfamilies Secamonoideae and Asclepiadoideae): Evidence from the nucleus and chloroplast. Taxon. 59:1016–1030.

Livshultz T, Middleton DJ, Endress ME, Williams J. 2007. Phylogeny of Apocynoideae and the APSA clade. Ann Missouri Bot Gard. 94:323–361.

Macfarlane JM. 1933. The Evolution and Distribution of Flowering Plants. Philadelphia (PA): Noel.

Meve U. 1995. *Neoschumannia* (including *Swynnertonia*), a primitive genus of the Asclepiadaceae-Stapelieae. Plant Syst Evol. 197:233–242.

Meve U, Liede S. 2001a. Inclusion of *Tenaris* and *Macropetalum* in *Brachystelma* (Apocynaceae-Asclepiadoideae-Ceropegieae) inferred from non-coding nuclear and chloroplast DNA sequences. Plant Syst Evol. 228:89–105.

Meve U, Liede S. 2001b. Reconsideration of the status of *Lavrania*, *Larryleachia* and *Notechidnopsis* (Asclepiadoideae-Ceropegieae). S Afr J Bot. 67:161–168.

Meve U, Liede S. 2004. Subtribal division of Ceropegieae (Apocynaceae- Asclepiadoideae). Taxon. 53:61–72. Nazar N, Mahmood T. 2010. Morphological and molecular characterization of selected *Artemisia* species from Rawalakot, Azad Jammu and Kashmir. Acta Physiol Plant. 33:625–633.

Nilsson S.1986. The significance of pollen morphology in the Apocynaceae. In: Blackmore S, Ferguson K, editors. Pollen and Spores: Form and Function. London: Academic Press; p. 359–374.

Nilsson S, Endress ME, Grafstrom E. 1993. On the relationships of the Apocynaceae and Periplocaceae. Grana. 32:3–20.

Omlor R. 1998. *Generische Revision der Marsdenieae* (*Asclepiadaceae*) [dissertation]. Germany: Universität Kaiserslautern.

Orbigny A. 1843. Dictionnaire Universel d'Histoire Naturelle, Vol. 3, Renard, Paris.

Pichon M. 1949. Classification des Apocynacees. IX. Rauvolfiées, Alstoniées, Allamandées et Tabernaémontanoidées. Mém Mus Natl Hist Nat. 27:153–251.

Pichon M. 1950. Classification des Apocynacées: XXVIII, Supplement aux Plumérioidées. Mém Mus Natl Hist Nat, Sér B Bot. 1:145–166.

Potgieter K, Albert VA. 2001. Phylogenetic relationships within Apocynaceae sensu lato based on trnL intron and trnL-F spacer sequences and propagule characters. Ann Missouri Bot Gard. 88:523–549.

Rapini A, Chase MW, Goyder DJ, Griffiths J. 2003. Asclepiadoideae classification: Evaluating the phylogenetic relationships of New World Asclepiadoideae (Apocynaceae). Taxon. 52:33–50.

Rapini A, Chase MW, Konno TUP. 2006. Phylogenetics of South American Asclepiadeae (Apocynaceae). Taxon. 55:119–124

Richard EJ. 1997. Preparation of plant DNA using CTAB. In: Ausubel F, Brent R, Kingston RE, Moore DD, Siedman JG, Smith JA, Struhl K, editors. Short Protocols in Molecular Biology. New York (NY): Wiley; p. 2.10–2.11.

Rosatti TJ. 1989. The genera of suborder Apocynineae (Apocynaceae and Asclepiadaceae) in the southeastern United States. J Arnold Arbor. 70:307–401.

Safwat FM. 1962. The floral morphology of *Secamone* and the evolution of the pollinating apparatus in Asclepiadaceae. Ann Missouri Bot Gard. 49:95–129.

Sennblad B. 1997. Phylogeny of the Apocynaceae sensu lato [dissertation]. Sweden: Uppsala University. Sennblad B, Bremer B. 1996. The familial and subfamilial relationships of Apocynaceae and Asclepiadaceae evaluated with *rbcL* data. Plant Syst Evol. 202:153–175.

Sennblad B, Bremer B. 2000. Is there a justification for differential a priori weighting in coding sequences? A case study from *rbcL* and Apocynaceae. Syst Biol. 49:101–113.

Sennblad B, Bremer B. 2002. Classification of Apocynaceae sensu lato according to a new approach combining Linnaean and phylogenetic taxonomy. Syst Biol. 51:389–409.

Sennblad B, Endress ME, Bremer B. 1998. Morphology and molecular data in phylogenetic fraternity the tribe Wrightieae (Apocynaceae) revisited. Amer J Bot. 85:1143–1158.

Simões AO, Endress ME, Van der Niet T, Conti E, Kinoshita LS. 2004. Tribal and intergeneric relationships of Mesechiteae (Apocynaceae, Apocynoideae): evidence from three noncoding plastid DNA regions and morphology. Amer J Bot. 91:1409–1418.

Simões AO, Livshultz T, Conti E, Endress ME. 2007. Phylogeny and systematics of the Rauvolfioideae (Apocynaceae) based on molecular and morphological evidence. Ann Missouri Bot Gard. 94:268–297.

Struwe L, Albert VA, Bremer B. 1994. Cladistics and family level classification of the Gentianales. Cladistics. 10: 175–206.

Swarupanandan K, Mangaly JK, Sonny TK, Kishorekumar K, Chand-Basha S. 1996. The subfamilial and tribal classification of the family Asclepiadaceae. Bot J Linn Soc. 120:327–369.

Swofford DL (2002). PAUP*. Phylogenetic Analysis Using Parsimony (and other methods), version 4.0 Beta 10. Sunderland, Massachusetts, Sinauer.

Venter HJT, Verhoeven R, Kotze JDS. 1990. The genus *Petopentia* (Periplocaceae). S Afr J Bot. 56:393–398.

Verhoeven RL, Liede S, Endress M. 2003. The tribal position of *Fockea* and *Cibirhiza* (Apocynaceae: Asclepiadoideae): evidence from the pollinium structure and cpDNA sequence data. Grana. 42: 70–81. Verhoeven RL, Venter HJT. 1998. Pollinium structure in Periplocoideae (Apocynaceae). Grana. 37:1–14.

Wanntorp L, Forster PI. 2007. Phylogenetic relationships between *Micholitzia* (Apocynaceae, Marsdenieae): Insights from flower morphology. Ann Missouri Bot Gard. 94:36–55.

Wanntorp L, Gotthardt K, Muellner AN. 2011. Revisiting the wax plants (*Hoya,* Marsdenieae, Apocynaceae): Phylogenetic analysis using the *matK* gene and *psbA-trnH* intergenic spacer. Taxon. 60:4–14.

Wanntorp L, Kocyan A, Renner SS. 2006b. Wax plants disentangled: A phylogeny of *Hoya* (Apocynaceae) using molecular markers. Mol. Phylogenet. Evol. 39:722–733.

Wanntorp L, Kocyan A, van Donkelaar R, Renner SS. 2006a. Towards a monophyletic *Hoya* (Marsdenieae, Apocynaceae): Inferences from the chloroplast *trnL* region and the *rbcL-atpB* spacer. Syst Bot. 31: 586–596.

Wanntorp L, Kunze H. 2009. Identifying synapomorphies in the flowers of *Hoya* and *Dischidia* – towards phylogenetic understanding. Int J Plant Sci. 170:331–342.

Wyatt R, Broyles SB, Lipow SR. 2000. Pollen-ovule ratios in milkweeds (Asclepiadaceae): an exception that probes the rule. Syst Bot. 25:171–180.

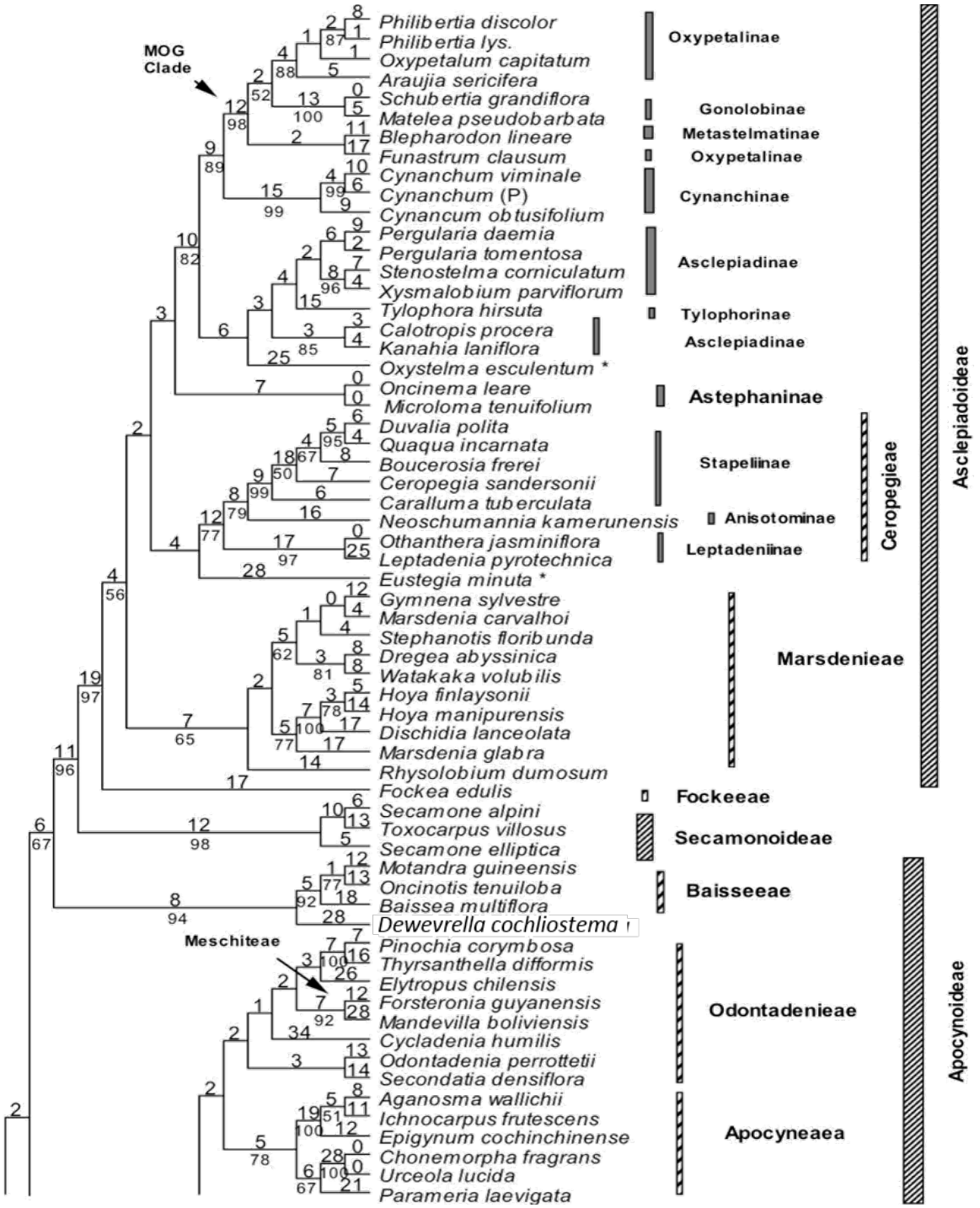

Fig. 1a. Parsimony analysis of only PHYA sequences from Apocynaceae. Bootstrap percentages > 50 and consistent with the strict consensus tree are indicated below branches. *Cynanchum* (P) = *Cynanchum jacquemontianum*.

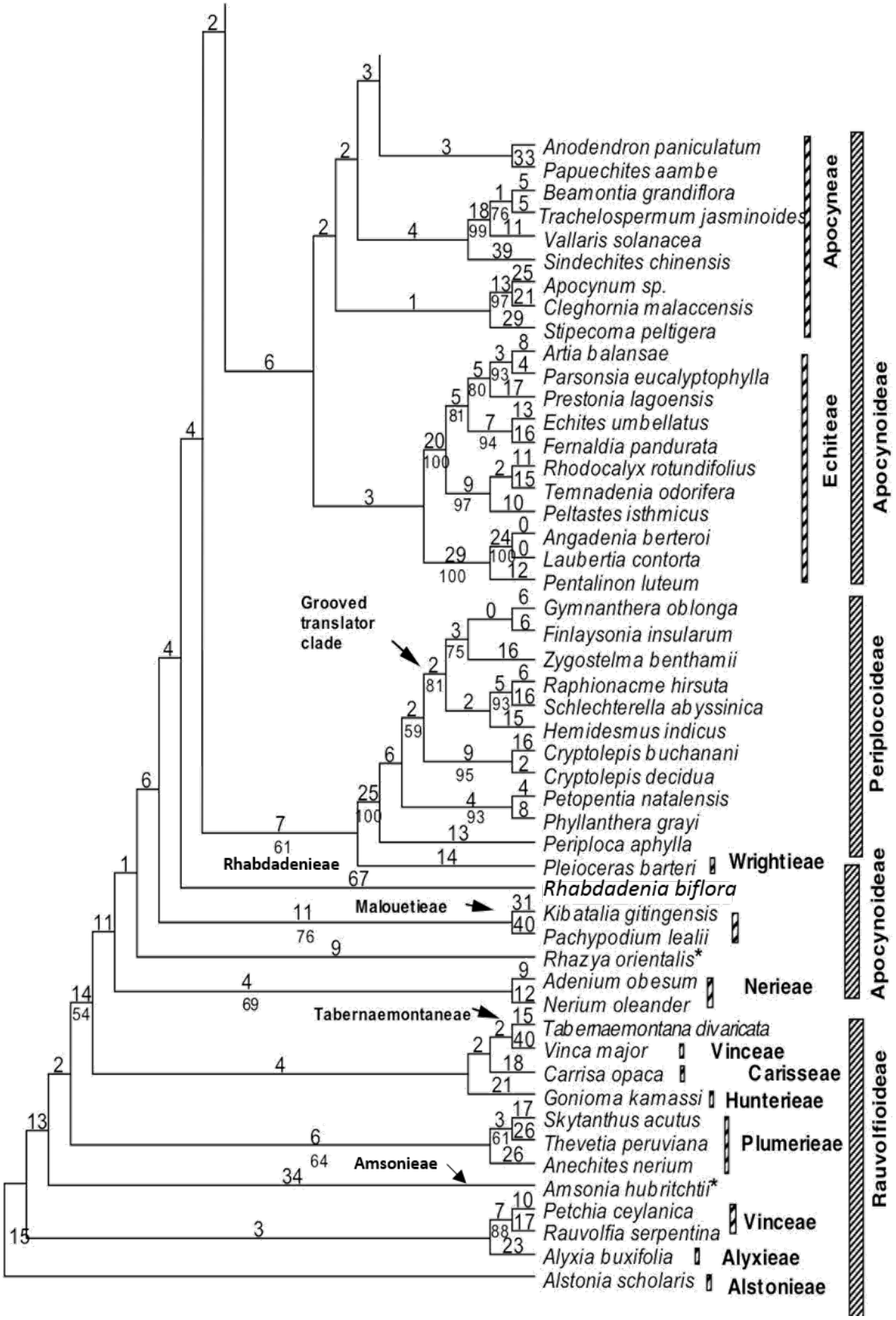

Fig. 1a. (Continued).

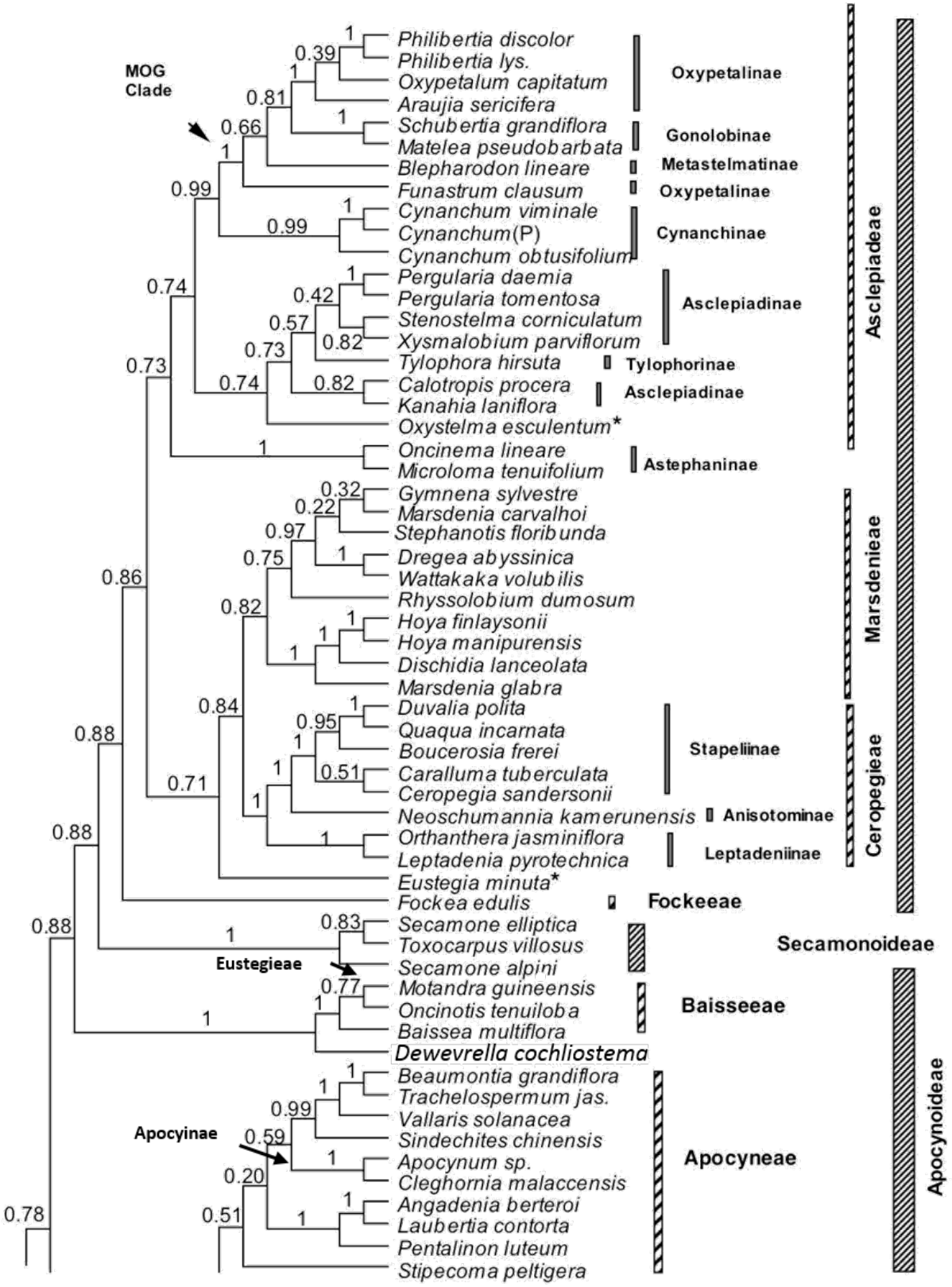

Fig. 1b. Bayesian tree based on only PHYA sequences. PP values are indicated above the branches. Values > 0.95 are considered as strong support. *Cynanchum* (P) = *Cynanchum jacquemontianum*.

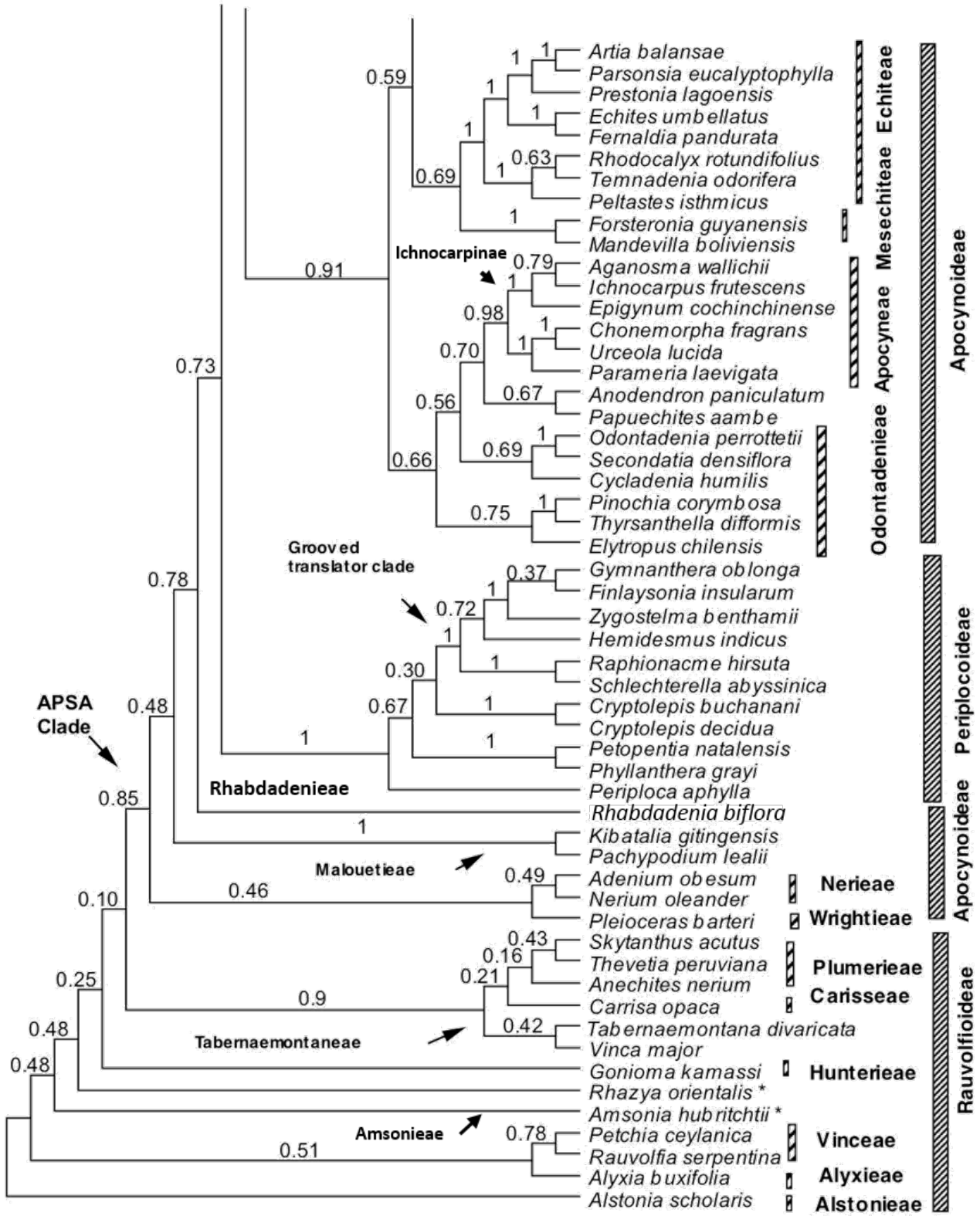

Fig. 1b. (Continued).

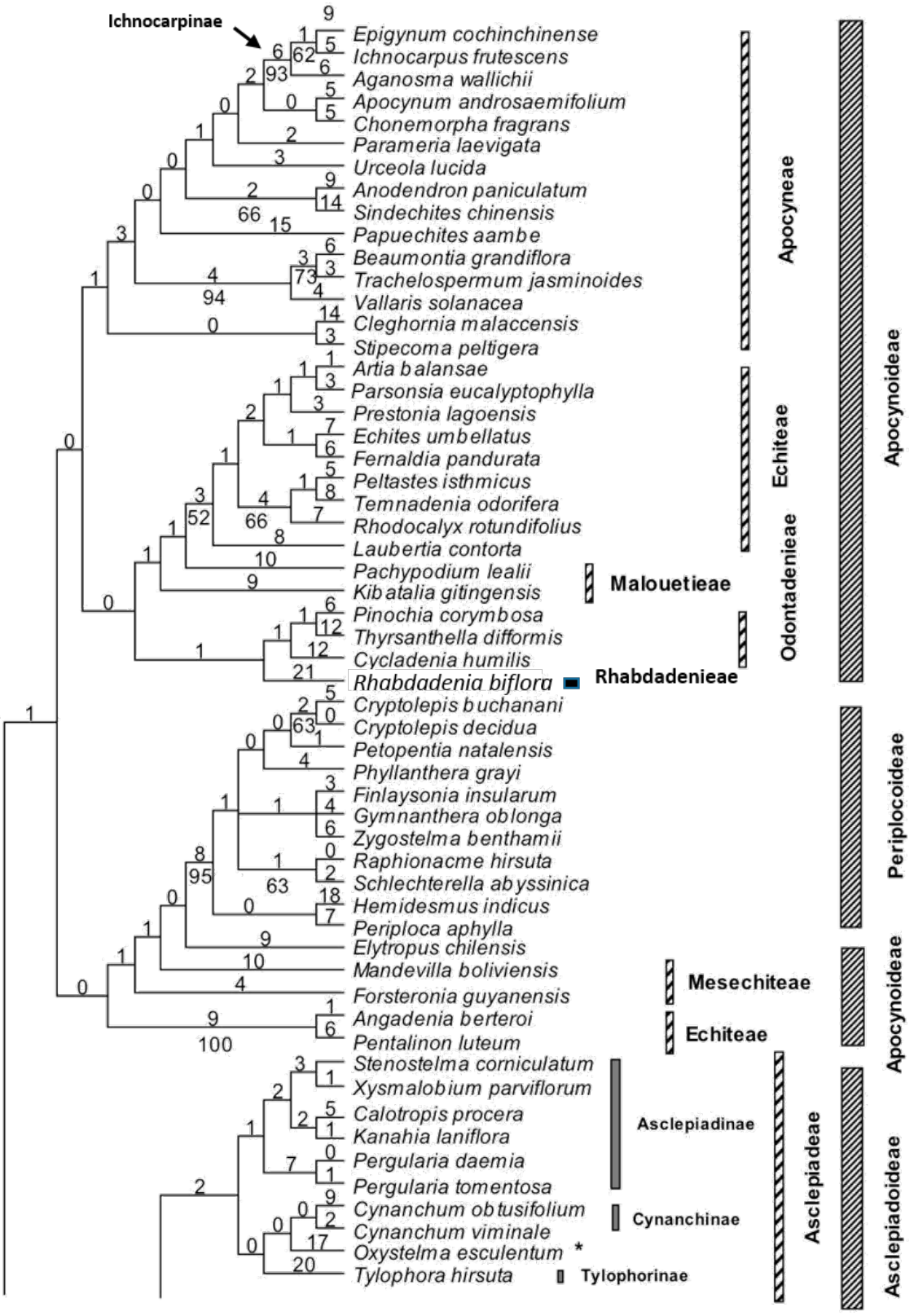

Fig. 2a. Parsimony analysis of *trnL-F* sequences of taxa present in combined analyses. Bootstrap percentages > 50 are indicated below branches. *Cynanchum* (P) = *Cynanchum jacquemontianum*.

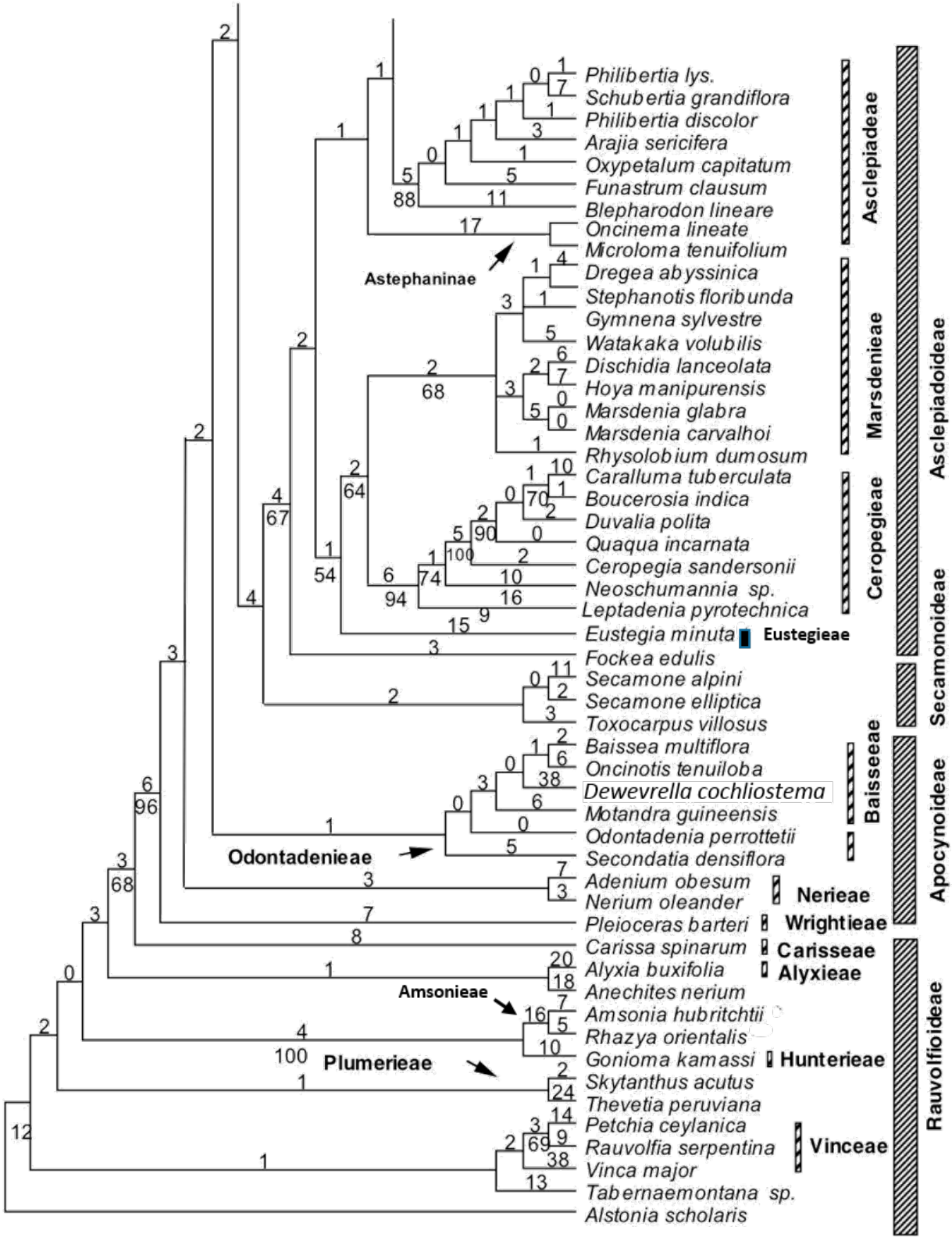

Fig. 2a. (Continued).

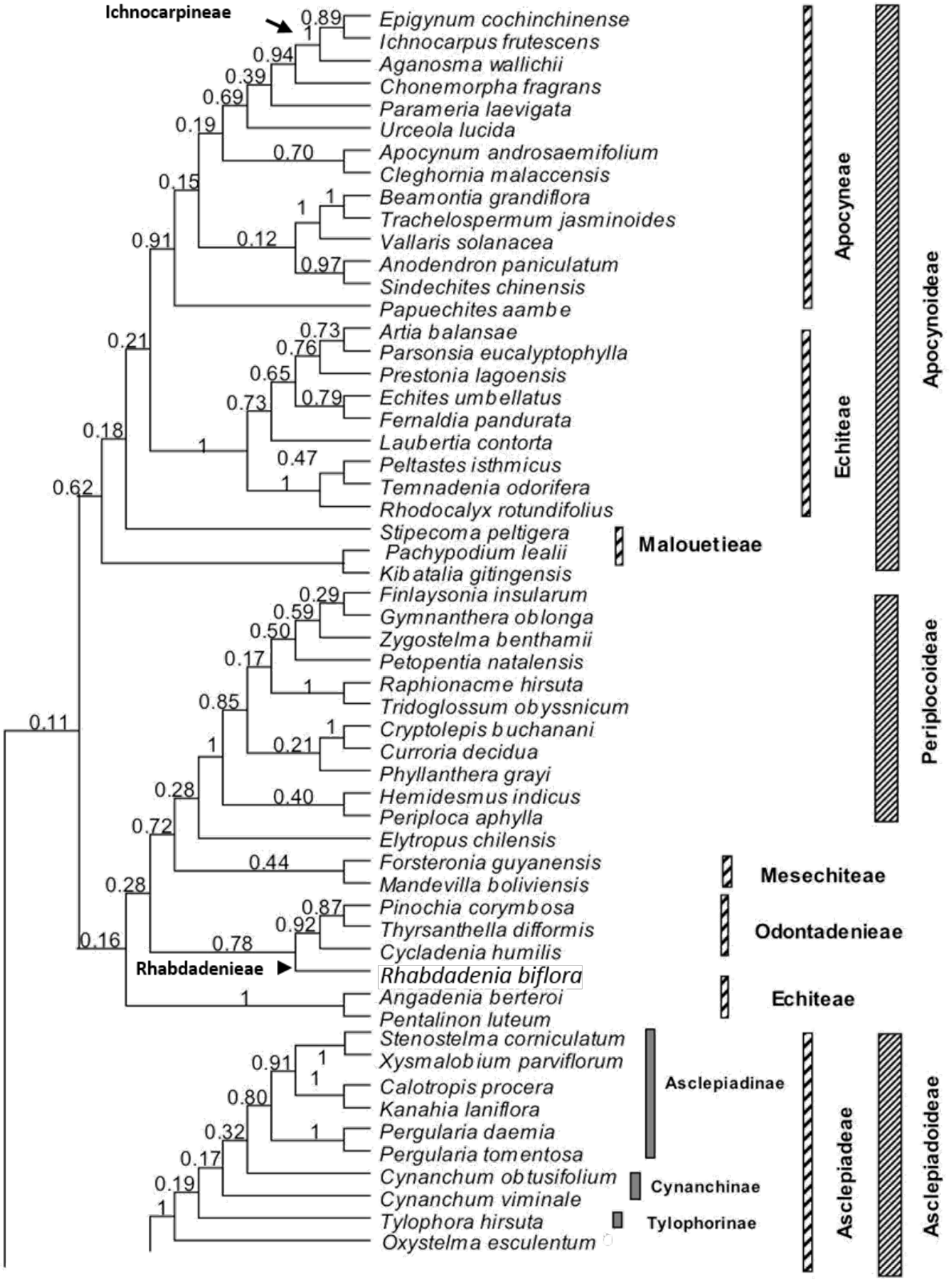

Fig. 2b. Bayesian analysis of *trnL-F* sequences of taxa included in combined analyses. Values > 0.95 are considered as strong support. *Cynanchum* (P) = *Cynanchum jacquemontianum*.

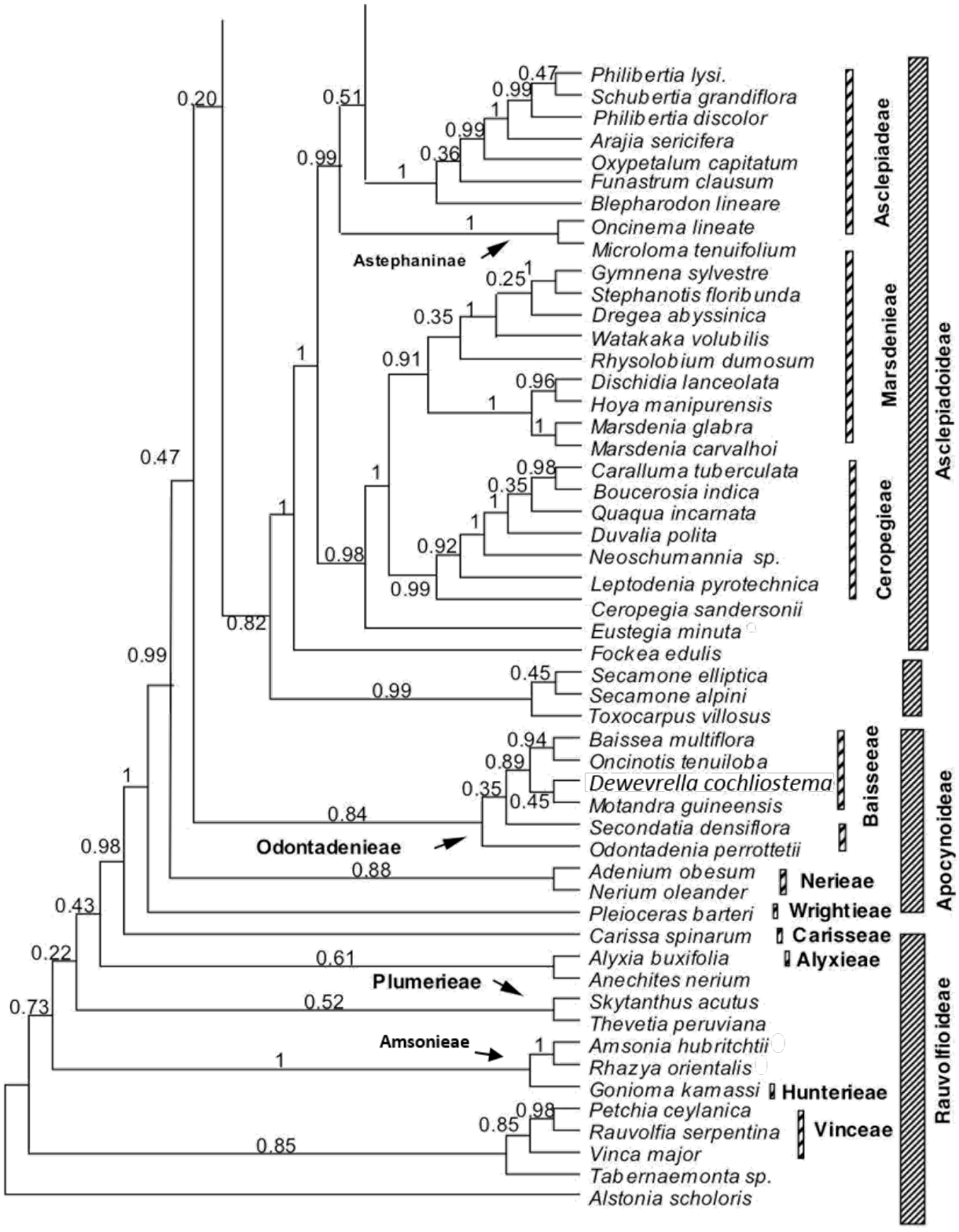

Fig. 2b. (Continued).

Finito di stampare da
Logo s.r.l. – Borgoricco (PD) – Italia

OPEN ACCESS POLICY

Caryologia provides immediate open access to its content. Our publisher, Firenze University Press at the University of Florence, complies with the Budapest Open Access Initiative definition of Open Access: By "open access" , we mean the free availability on the public internet, the permission for all users to read, download, copy, distribute, print, search, or link to the full text of the articles, crawl them for indexing, pass them as data to software, or use them for any other lawful purpose, without financial, legal, or technical barriers other than those inseparable from gaining access to the internet itself. The only constraint on reproduction and distribution, and the only role for copyright in this domain is to guarantee the original authors with control over the integrity of their work and the right to be properly acknowledged and cited. We support a greater global exchange of knowledge by making the research published in our journal open to the public and reusable under the terms of a Creative Commons Attribution 4.0 International Public License (CC-BY-4.0). Furthermore, we encourage authors to post their pre-publication manuscript in institutional repositories or on their websites prior to and during the submission process and to post the Publisher's final formatted PDF version after publication without embargo. These practices benefit authors with productive exchanges as well as earlier and greater citation of published work.

PUBLICATION FREQUENCY

Papers will be published online as soon as they are accepted, and tagged with a DOI code. The final full bibliographic record for each article (initial-final page) will be released with the hard copies of Caryologia. Manuscripts are accepted at any time through the online submission system.

COPYRIGHT NOTICE

Authors who publish with Caryologia agree to the following terms:

- Authors retain the copyright and grant the journal right of first publication with the work simultaneously licensed under a Creative Commons Attribution 4.0 International Public License (CC-BY-4.0) that allows others to share the work with an acknowledgment of the work's authorship and initial publication in Caryologia.
- Authors are able to enter into separate, additional contractual arrangements for the non-exclusive distribution of the journal's published version of the work (e.g., post it to an institutional repository or publish it in a book), with an acknowledgment of its initial publication in this journal.
- Authors are permitted and encouraged to post their work online (e.g., in institutional repositories or on their website) prior to and during the submission process, as it can lead to productive exchanges, as well as earlier and greater citation of published work (See The Effect of Open Access).

PUBLICATION FEES

Open access publishing is not without costs. Caryologia therefore levies an article-processing charge of € 150.00 for each article accepted for publication, plus VAT or local taxes where applicable.

We routinely waive charges for authors from low-income countries. For other countries, article-processing charge waivers or discounts are granted on a case-by-case basis to authors with insufficient funds. Authors can request a waiver or discount during the submission process.

PUBLICATION ETHICS

Responsibilities of Caryologia's editors, reviewers, and authors concerning publication ethics and publication malpractice are described in Caryologia's Guidelines on Publication Ethics.

CORRECTIONS AND RETRACTIONS

In accordance with the generally accepted standards of scholarly publishing, Caryologia does not alter articles after publication: "Articles that have been published should remain extant, exact and unaltered to the maximum extent possible".

In cases of serious errors or (suspected) misconduct Caryologia publishes corrections and retractions (expressions of concern).

Corrections

In cases of serious errors that affect or significantly impair the reader's understanding or evaluation of the article, Caryologia publishes a correction note that is linked to the published article. The published article will be left unchanged.

Retractions

In accordance with the "Retraction Guidelines" by the Committee on Publication Ethics (COPE) Caryologia will retract a published article if:

- there is clear evidence that the findings are unreliable, either as a result of misconduct (e.g. data fabrication) or honest error (e.g. miscalculation)
- the findings have previously been published elsewhere without proper crossreferencing, permission or justification (i.e. cases of redundant publication)
- it turns out to be an act of plagiarism
- it reports unethical research.

An article is retracted by publishing a retraction notice that is linked to or replaces the retracted article. Caryologia will make any effort to clearly identify a retracted article as such.

If an investigation is underway that might result in the retraction of an article Caryologia may choose to alert readers by publishing an expression of concern.

COMPLYNG WITH ETHICS OF EXPERIMENTATION

Please ensure that all research reported in submitted papers has been conducted in an ethical and responsible manner, and is in full compliance with all relevant codes of experimentation and legislation. All papers which report in vivo experiments or clinical trials on humans or animals must include a written statement in the Methods section. This should explain that all work was conducted with the formal approval of the local human subject or animal care committees (institutional and national), and that clinical trials have been registered as legislation requires. Authors who do not have formal ethics review committees should include a statement that their study follows the principles of the Declaration of Helsinki

ARCHIVING

Caryologia and Firenze University Press are experimenting a National legal deposition and long-term digital preservation service.

ARTICLE PROCESSING CHARGES

All articles published in Caryologia are open access and freely available online, immediately upon publication. This is made possible by an article-processing charge (APC) that covers the range of publishing services we provide. This includes provision of online tools for editors and authors, article production and hosting, liaison with abstracting and indexing services, and customer services. The APC, payable when your manuscript is editorially accepted and before publication, is charged to either you, or your funder, institution or employer.

Open access publishing is not without costs. Caryologia therefore levies an article-processing charge of € 150.00 for each article accepted for publication, plus VAT or local taxes where applicable.

FREQUENTLY-ASKED QUESTIONS (FAQ)

Who is responsible for making or arranging the payment?

As the corresponding author of the manuscript you are responsible for making or arranging the payment (for instance, via your institution) upon editorial acceptance of the manuscript.

At which stage is the amount I will need to pay fixed?

The APC payable for an article is agreed as part of the manuscript submission process. The agreed charge will not change, regardless of any change to the journal's APC.

When and how do I pay?

Upon editorial acceptance of an article, the corresponding author (you) will be notified that payment is due.

We advise prompt payment as we are unable to publish accepted articles until payment has been received. Payment can be made by Invoice. Payment is due within 30 days of the manuscript receiving editorial acceptance. Receipts are available on request.

No taxes are included in this charge. If you are resident in any European Union country you have to add Value-Added Tax (VAT) at the rate applicable in the respective country. Institutions that are not based in the EU and are paying your fee on your behalf can have the VAT charge recorded under the EU reverse charge method, this means VAT does not need to be added to the invoice. Such institutions are required to supply us with their VAT registration number. If you are resident in Japan you have to add Japanese Consumption Tax (JCT) at the rate set by the Japanese government.

Can charges be waived if I lack funds?

We consider individual waiver requests for articles in Caryologia on a case-by-case basis and they may be granted in cases of lack of funds. To apply for a waiver please request one during the submission process. A decision on the waiver will normally be made within two working days. Requests made during the review process or after acceptance will not be considered.

I am from a low-income country, do I have to pay an APC?

We will provide a waiver or discount if you are based in a country which is classified by the World Bank as a low-income or a lower-middle-income economy with a gross domestic product (GDP) of less than $200bn. Please request this waiver of discount during submission.

What funding sources are available?

Many funding agencies allow the use of grants to cover APCs. An increasing number of funders and agencies strongly encourage open access publication. For more detailed information and to learn about our support service for authors.

APC waivers for substantial critiques of articles published in OA journals

Where authors are submitting a manuscript that represents a substantial critique of an article previously published in the same fully open access journal, they may apply for a waiver of the article processing charge (APC).

In order to apply for an APC waiver on these grounds, please contact the journal editorial team at the point of submission. Requests will not be considered until a manuscript has been submitted, and will be awarded at the discretion of the editor. Contact details for the journal editorial offices may be found on the journal website.

What is your APC refund policy?

Firenze University Press will refund an article processing charge (APC) if an error on our part has resulted in a failure to publish an article under the open access terms selected by the authors. This may include the failure to make an article openly available on the journal platform, or publication of an article under a different Creative Commons licence from that selected by the author(s). A refund will only be offered if these errors have not been corrected within 30 days of publication.

2019
Vol. 72 – n. 1

Caryologia

International Journal of Cytology, Cytosystematics and Cytogenetics

Table of contents

€ 25,00